

Synthesis, Polymerisation and Characterisation of a Novel Olefin-Modified Acrylate Monomer, 1-Methyl-1-Propyl-Hexyl Acrylate

Dissertation presented for the Degree of Doctor of Philosophy

Ph.D. (Polymer Science)

At the

University of Stellenbosch

By

Siyabonga Mange



Supervisor:

Professor R.D. Sanderson

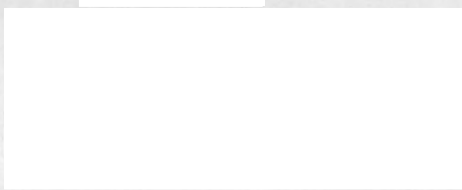
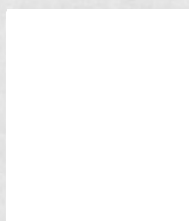
Co-Supervisor:

Dr. M. P. Tonge

Department of Chemistry and Polymer Science

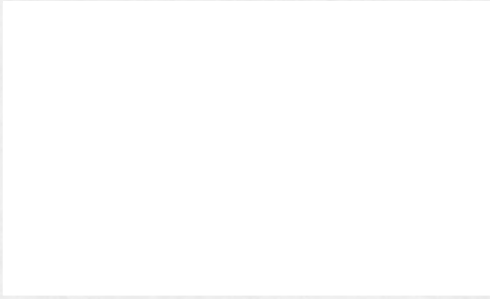
University of Stellenbosch

April 2005



Declaration

I, the undersigned, hereby declare that the work contained in this dissertation is my own original work and that I have not previously in its entirety or in part submitted it at any university for a degree.



“Our scientific power has outrun our spiritual power.

We have guided missiles and misguided men.”

Martin Luther King Jr. (1929 – 1968), *Strength to Love*, 1963

Abstract

Finding use for byproducts from the chemical industry holds many advantages for a country's economy. Synthesis of new monomers from such byproducts adds value to otherwise otherwise low-value material.

The synthesis of a new olefin-modified acrylate monomer, 1-methyl-1-propyl-hexyl acrylate (1-MPHA), derived from 1-pentene, is reported. Homopolymerisation of the monomer 1-MPHA was carried out in both benzene and in toluene. The products of full-conversion of the homopolymer poly-(1-MPHA) were characterised by GPC, NMR, TGA and DMA. Kinetic studies of the homopolymerisation process of 1-MPHA were also undertaken.

The monomer 1-methyl-1-propyl-hexyl acrylate (1-MPHA) was copolymerised with methyl methacrylate (MMA). Samples obtained from full conversion copolymerisations at various 1-MPHA/MMA feed ratios were characterised by GPC, NMR, TGA and DMA. Reactivity ratios of the two monomers were obtained from *in situ* ^1H NMR kinetic studies. 1-MPHA was also copolymerised with vinyl acetate (VAc). Samples obtained from full conversion copolymerisation with a 1-MPHA content ranging from 2 to 16 wt% were characterised by GPC, NMR, TGA and DMA. The solubility parameter and the hydrophobicity of the VAc/1-MPHA copolymers were also determined. Reactivity ratios of the two monomers were obtained from *in situ* ^1H NMR kinetic studies.

Further copolymerisation studies with styrene and glycidyl methacrylate as comonomers were undertaken. The chemical analysis and thermogravimetric analysis of the copolymers are reported.

In conclusion, the use of 1-methyl-1-propyl-hexyl acrylate as a comonomer results in a reduction in the glass transition temperature, better thermal stability, increased hydrophobicity with an insignificant loss in stiffness of the copolymers. These properties are due to the long and branched chain structure of the 1-MPHA monomer.

Opsomming

Gebruik van byprodukte van die chemiese nywerheid hou groot voordele in vir die land se ekonomie. Sintese van nuwe monomere vanuit sulke byprodukte dra by tot waardetoevoeging tot andersins lae-waarde byprodukte.

Die sintese van 'n nuwe olefien-gewysigde akrylaatmonomeer afkomstig van 1-penteen, naamlik 1-metiel-1-propiel-heksielakrylaat (1-MPHA), word hier beskryf. Homopolimerisasie van die monomeer 1-MPHA is uitgevoer in beide benseen en toluen. Die produkte van die volledige omskakeling van die homopolimeer is met behulp van GPC, KMR, TGA en DMA gekarakteriseer. Die reaksiekinetika van die homopolimerisasie van 1-MPHA is ook ondersoek.

Die monomeer 1-MPHA is met metielmetakrylaat (MMA) gekopolimeriseer. Monsters van die volledig omgeskakelde kopolimere met verskeie 1-MPHA/MMA voerverhoudings is m.b.v. GPC, KMR, TGA en DMA gekarakteriseer. Die reaktiwiteitsverhoudings van die twee monomere is vanaf ^1H KMR-studies bepaal.

1-MPHA is ook met vinielasetaat (VAc) gekopolimeriseer. Monsters van die produk van die volledige kopolimerisasie met 1-MPHA, met 'n inhoud van 2–16 massa %, is ook m.b.v. GPC, KMR, TGA en DMA gekarakteriseer. Die 1-MPHA het die hidrofobisiteit van VAc/1-MPHA aansienlik verhoog. Die reaktiwiteitsverhoudings van die twee monomere is vanaf *in situ* ^1H KMR-studies bepaal.

Verdere kopolimerisasiestudies met stireen en glisidietakrylaat as komonomere is onderneem. Chemiese- en termogravimetriese analyses van die kopolimere is gedoen en gerapporteer.

Ter afsluiting, die gebruik van 1-metiel-1-propiel-heksielakrylaat as komonomere het 'n verlaging in die glasoorgangstemperatuur, verhoogde termiese stabiliteit, verhoogde hidrofobisiteit, en 'n klein verlies in die stewigheid (Eng. stiffness) van die kopolimeer tot gevolg. Hierdie eienskappe

is as gevolg van die lang, vertakte kettingstruktuur van die 1-MPHA monomeer.

Acknowledgements

Let me start by expressing my gratitude to everyone who has contributed directly and indirectly to the success of this project, especially those people that I will not be able to mention by names. It is not because your contribution was insignificant but this has been a long process and some names have unfortunately been forgotten. I will always be indebted to you.

I would like to thank the University of Stellenbosch for allowing me to study at this world class University. I am also grateful for the financial support that I have received from the National Research Foundation (NRF), the Department of Labour (DoL), the University of Stellenbosch and Professor Sanderson.

I would like to thank Professor Sanderson for affording me the opportunity to join his world class establishment and entrust me with a novel idea that has the potential to go far. I am grateful for the guidance and support that he has given me over the years.

All the staff members, academic and support, at the Institute, past and present are greatly acknowledged for their contribution in making this project a reality. Special mention goes to Matthew, Valerie, Rotimi and Margie for their input in the interpretation of the results and the compilation of this document. The people who went out of their way to make the NMR kinetic work possible, James, Jean and Elsa are greatly acknowledged. I would also like to thank Methuli for the DMA work and Calvin for bending the rules when the need arises. I would also like to thank all the students who had to put up with me over the past four and half years, Nyambeni I miss those lunch time beaks.

I would like also like to thank my parents, MaCele and Jwarha for allowing me to make my own decisions and for supporting those decisions. To my brothers and sister, thank you for all your support. To Magamase, thank you

for putting your interests aside and give me undivided support, you are one of a kind.

And last but not least I would like to thank God for giving me the wisdom and the heart to go on and blessing me with the people and means needed to make this a success.

Table of Contents

Table of Contents	i
List of Abbreviations	iii
List of Symbols	v
List of Figures	vii
List of Schemes	xi
List of Tables	xi
CHAPTER 1	1
INTRODUCTION AND OBJECTIVES	1
1.1 Introduction	1
1.2 Aims and objectives of the study	3
1.3 Layout	3
1.4 References	4
CHAPTER 2	7
LITERATURE REVIEW AND HISTORICAL BACKGROUND	7
2.1 Introduction	7
2.2 Olefins	7
2.2.1 Thermal and catalytic cracking of paraffins	8
2.2.2 Oligomerisation of ethylene	10
2.3 Oligomerisation of olefins	12
2.4 Hydration of olefins	16
2.4.1 Hydroboration-oxidation of olefins	16
2.4.2 Oxymercuration-demercuration of olefins	18
2.5 Esterification of alcohols	19
2.6 Free radical polymerisation	20
2.6.1 Initiation	21
2.6.2 Propagation	21
2.6.3 Termination	21
2.6.4 Homopolymerisation	22
2.6.5 Copolymerisation	22
2.6.6 Copolymerisation models	23
2.6.7 Compositional drift	29
2.6.8 Estimation of reactivity ratios	31
2.6.9 Types of copolymerisation behaviour	34
2.7 Acrylate copolymers	37
2.8 References	38
CHAPTER 3	42
SYNTHESIS AND HOMOPOLYMERISATION OF THE OLEFIN-MODIFIED ACRYLIC MONOMER, 1-METHYL-1-PROPYL-HEXYL ACRYLATE	42
3.1 Introduction	42
3.2 Experimental	42
3.2.1 Reagents used	42
3.2.2 Analyses	43
3.3 Synthesis of 1-methyl-1-propyl-hexyl acrylate	44
3.3.1 Oligomerisation of 1-pentene	45
3.3.2 Hydration of 2-propyl-heptene	47
3.3.3 Esterification of 4-methyl-nonan-4-ol	48
3.4 Homopolymerisation of 1-methyl-1-propyl-hexyl acrylate	49
3.5 Kinetics of the homopolymerisation of 1-methyl-1-propyl-hexyl acrylate	54
3.6 Thermal properties of poly-(1-methyl-1-propyl-hexyl acrylate)	63
3.7 Conclusions	65
3.8 References	66

CHAPTER 4.....	67
COPOLYMERISATION OF 1-METHYL-1-PROPYL-HEXYL ACRYLATE WITH METHYL METHACRYLATE.....	67
4.1 Introduction	67
4.2 Experimental	68
4.2.1 Reagents used	68
4.2.2 Copolymerisation of 1-MPHA with MMA	68
4.2.3 Analyses	69
4.2.4 Determination of the kinetics of the copolymerisation of 1-MPHA with MMA	70
4.3 Results and discussion	74
4.3.1 Chemical analyses	75
4.3.2 Thermal analyses	77
4.3.3 Kinetics of the copolymerisation of 1-MPHA with MMA	85
4.4 Conclusions	89
4.5 References	90
CHAPTER 5.....	92
COPOLYMERISATION OF 1-METHYL-1-PROPYL-HEXYL ACRYLATE WITH VINYL ACETATE.....	92
5.1 Introduction	92
5.2 Experimental	93
5.2.1 Reagents used	93
5.2.2 Copolymerisation of VAc with 1-MPHA	93
5.2.3 Analyses	94
5.2.4 Determination of the kinetics of copolymerisation of VAc with 1-MPHA	95
5.3 Results and Discussion	96
5.3.1 Chemical analyses	96
5.3.2 Thermal analyses	98
5.3.3 Physical analysis	102
5.3.4 Kinetics of the copolymerisation of 1-MPHA with VAc	106
5.4 Conclusions	111
5.5 References	111
CHAPTER 6.....	113
CONCLUSIONS AND RECOMMENDATIONS.....	113
6.1 Conclusions	113
6.2 Future work and recommendations	115
APPENDIX A.....	116
APPENDIX B.....	121
APPENDIX C.....	123
APPENDIX D.....	125
APPENDIX E.....	127
APPENDIX F.....	132
APPENDIX G.....	135
APPENDIX H.....	138

List of Abbreviations

Abbreviation	Meaning
$(\text{CH}_3\text{CH}_2)_3\text{N}$	triethylamine
$(\text{CH}_3\text{CH}_2)_2\text{O}$	diethyl ether
$\beta\text{-H}$	beta-hydride
1-MPHA	1-methyl-1-propyl-hexyl acrylate
2-PH	2-propyl-heptene
4-MNOL	4-methyl-nonan-4-ol
AIBN	azobis-(isobutyronitrile)
Al	aluminium
AR	analytical reagent grade
ATRP	atom transfer radical polymerisation
B-C	boron-carbon bond
C_2H_4	ethylene
C_2H_6	ethane
C_3H_6	propene
C_3H_8	propane
C-C	carbon-carbon bond
CDCl_3	deuterated chloroform
CH_2	methylene group
CH_2CHCOCl	acryloyl chloride
CH_2Cl_2	dichloromethane
CH_4	methane
CO	carbon monoxide
C-O	carbon-oxygen bond
CO_2	carbon dioxide
$\text{Cp}_2^*\text{ZrCl}_2$	pentamethyl-cyclopentadienyl zirconocene dichloride
Cp_2ZrCl_2	cyclopentadienyl zirconocene dichloride
DCC	dicylohexylcarbodiimide
DMA	dynamic mechanical analysis
DMAP	dimethylaminopyridine
FT	Fischer-Tropsch
FTIR	fourier transform infra red spectroscopy
g	gram
GC	gas chromatography
GMA	glycidyl methacrylate
GPC	gel permeation chromatography
H_2	hydrogen
H_2O	water
$\text{Hg}(\text{OAc})_2$	mercuric acetate
Hg-C	mercury-carbon bond
HPLC	high performance liquid chromatography
LiAlH_4	lithium aluminium hydride
MAO	methylaluminumoxane
mL	milliliter
MMA	methyl methacrylate
mmol	millimole

MPa	megapascals
NaBH ₄	sodium borohydride
NaCl	sodium chloride
NaOH	sodium hydroxide
NMR	nuclear magnetic resonance
P-(1-MPHA)	poly-(1-methyl-1-propyl-hexyl acrylate)
PDI	polydispersity index
PMMA	polymethyl methacrylate
PVAc	polyvinyl acetate
R'OH	alcohol
R ₂ C=CHR	trisubstituted olefins
RAFT	reversible addition-fragmentation chain transfer
RCH=CH ₂	terminal olefin
RCH=CHR'	dialkyl ethenes
RCOOH	carboxylic acid
RCOOR'	carboxylic ester
SFRP	stable free radical polymerisation
SHOP	Shell Higher Olefins Process
TGA	thermogravimetric analysis
THF	tetrahydrofuran
TMA	trimethylaluminium
VAc	vinyl acetate
VEOVA	highly branched vinyl ester of versatic acid
Zr	zirconium
Zr-C	zirconium carbon
Zr-H	zirconium-hydride

List of Symbols

Symbol	Meaning
δ	solubility parameter
C_0	initial monomer concentration
C_{1-MPHA}	concentration of 1-MPHA
$C_{1-MPHA,0}$	initial concentration of 1-MPHA
$C_{MMA,0}$	initial concentration of MMA
C_{VAc}	concentration of vinyl acetate
$C_{VAc,0}$	initial concentration of vinyl acetate
E_{COH}	cohesive energy
f_1	mole fraction of monomer 1 in feed
$f_{1,0}$	initial mole fraction of monomer 1 in feed
f_2	mole fraction of monomer 2 in feed
$f_{2,0}$	initial mole fraction of monomer 2 in feed
F	molar attraction constant
F_1	mole fraction of monomer 1 in copolymer
F_2	mole fraction of monomer 2 in copolymer
f'_{MMA}	upper limit of the mole fraction of MMA in initial feed
f''_{MMA}	lower limit of the mole fraction of MMA in initial feed
H	drop height
H_x	integrated peak intensity of the double bond proton x
I	initiator
I_{CH_3}	integrated peak intensity of MMA methoxy protons
I_T	integrated peak intensity of total protons
k_{add}	rate coefficient for addition
k_d	rate coefficient for dissociation
k_i	rate coefficient for initiation
k_p	rate coefficient for propagation
k_{ic}	rate coefficient for chain termination by combination
k_{id}	chain termination rate coefficient by dissociation
k_{xx}	rate coefficient for homo-propagation
k_{xxx}	rate coefficient for homo-propagation
k_{xy}	rate coefficient for cross-propagation
k_{xxy}	rate coefficient for cross-propagation
k_{xyx}	rate coefficient for cross-propagation
$\sim M_x^\bullet$	propagating chain radical of monomer x
$\sim M_x M_x M_x^\bullet$	propagating chain after addition of monomer unit similar to both penultimate and terminal units

$\sim M_x M_y$	dead polymer chain ending in x and y monomers
$\sim M_x M_x M_y^\bullet$	propagating chain after addition of monomer unit different to both penultimate and terminal units
$\sim M_x M_y M_x^\bullet$	propagating chain after addition of monomer unit similar to penultimate unit but different to terminal unit
$[M]$	instantaneous monomer concentration
$[M]_0$	initial total monomer concentration
$[M_1]$	instantaneous concentration of monomer 1
$[M_2]$	instantaneous concentration of monomer 2
M_m	dead polymer chain containing m units
M_n	dead polymer chain containing n units
\overline{M}_n	number average molar mass
\overline{M}_w	weight average molar mass
M_{n+1}^\bullet	chain initiating species M_1^\bullet after adding n monomer units
M_1^\bullet	chain initiating species (monomer 1)
M_m^\bullet	chain initiating species (monomer m)
M_n^\bullet	chain initiating species (monomer n)
M_{n+m}	chain termination product by combination of M_n^\bullet and M_m^\bullet
m_1	mole fraction of monomer 1 in feed
m_2	mole fraction of monomer 2 in feed
M	monomer
n	number of data points
p	number of parameters
r_1	reactivity ratio for monomer 1
r_2	reactivity ratio for monomer 2
r_1'	reactivity ratio of monomer 1 with different penultimate and terminal units
r_2'	reactivity ratio of monomer 2 with different penultimate and terminal units
r_{1-MPHA}	reactivity ratio of 1-MPHA
r_{MMA}	reactivity ratio of MMA
R^\bullet	initiator radical
R	integrated peak intensity of the reference standard
S	contour enclosing the uncertainty region
S_R	sum of squares of residuals
T_g	glass transition temperature
V	molar volume at room temperature
W	drop width
Wt%	weight percentage
X	experimental monomer conversion

List of Figures

- Figure 2.1: The step-wise growth process in the conversion of syngas to olefin in the Fischer-Tropsch process^[1], d stands for desorbed species, α is the probability of chain growth and the chain represents an adsorbed species to the catalyst surface. 9
- Figure 2.2: Shell Higher Olefins Process for the oligomerisation of ethylene^[3, 6]. 12
- Figure 2.3: Some of the suggested uses for the derivatives of olefin oligomers^[13]. 14
- Figure 2.4: The mechanism and catalytic cycle for the formation of the dimer oligomer from the α -olefin^[14]. 15
- Figure 2.5: General mechanism for the hydroboration-oxidation of olefins^[20]. 18
- Figure 2.6: General mechanism for the oxymercuration-demercuration hydration of alkenes leading to the Markovnikov addition of water across the double bond. 19
- Figure 2.7: General mechanism for the esterification of alcohols with acid chlorides^[23]. 20
- Figure 2.8: A graphical presentation of the dependence of the types of copolymerisations on reactivity ratios. 37
- Figure 3.1: ¹H NMR spectra for the homopolymerisation of 1-MPHA in (a) benzene and (b) toluene, at 50 wt% solution, 2 wt% AIBN and 70 °C over three days. 51
- Figure 3.2: ¹H NMR spectra for (a) the monomer and (b) the homopolymer of 1-MPHA showing the disappearance of the double peaks between 5.6 to 6.4 ppm and the appearance of a new backbone peak at about 2.25 ppm in the homopolymer. 53
- Figure 3.3: FTIR spectra of the 1-MPHA monomer (bold line) showing the disappearance of the homopolymer of 1-MPHA (normal line). 54
- Figure 3.4: The homopolymerisation process of 1-MPHA showing ¹H NMR spectra drawn from the reaction mixture at the time intervals indicated. The reaction conditions were: 50 wt% monomer solution in toluene, 2 wt% AIBN and conducted at 70 °C. 55
- Figure 3.5: ¹H NMR spectra of the polymerisation of 1-MPHA with 5 wt% MMA at different reaction times, showing the vinyl peaks of the monomer and DMAP (the internal standard). 57
- Figure 3.6: A graphical representation of the homopolymerisation results, conversion vs reaction time, as monitored by ¹H NMR, for the 1-MPHA reaction "activated" with MMA and the reaction of pure 1-MPHA. 58
- Figure 3.7: The ¹H NMR spectrum of the peaks used to monitor reaction progress for the polymerisation of 1-MPHA at 50 wt% solution in deuterated toluene and 10 wt% AIBN at 70 °C *in situ* an NMR apparatus. 59
- Figure 3.8: Conversion data for the homopolymerisation of 1-MPHA of various purity levels: 100% purified by 3 columns, 99.8% purified by 2 columns and 96.8% purified by 1 column. The reaction conditions were 50 wt% monomer solutions in deuterated toluene, 10 wt% AIBN as initiator and run at a temperature of 70 °C. 60
- Figure 3.9: Plots of the ¹H NMR signal for the three double bond proton peaks (H₁, H₂ and H₃) of 1-MPHA as a function of time illustrating the effect of an extra radical scavenging species, the impurity, on reaction progress. In (a) the induction period is 110 minutes and in (b) after further purification the induction period decreased to 25 minutes. The reaction conditions for both

experiments were 50 wt% 1-MPHA solution in deuterated toluene, 10 wt% AIBN and were conducted at 70 °C.	61
Figure 3.10: TGA traces for the homopolymers of PMMA and poly-(1-MPHA).	63
Figure 3.11: DMA results for the homopolymer of 1-MPHA.	65
Figure 4.1: ¹ H NMR peaks monitored for the monomer consumption determination in the <i>in situ</i> copolymerisation of 1-MPHA with MMA.	72
Figure 4.2: ¹ H NMR spectra of poly-(1-MPHA-co-MMA) with (a) 25 mole% 1-MPHA and (b) 7 mole% 1-MPHA in copolymer precipitated in methanol after 18 hours at 70 °C.	76
Figure 4.3: A plot of the TGA data for the homopolymers and copolymers of 1-MPHA and MMA.	78
Figure 4.4: A plot of the temperatures at which 0, 50% and maximum weight loss occurs during the degradation of the poly-(1-MPHA-co-MMA) polymers.	80
Figure 4.5: DMA data for (a) DM19 containing 7 mole% 1-MPHA and (b) DM91 containing 25 mole% 1-MPHA.	82
Figure 4.6: A plot of tan delta as a function of temperature for poly-(1-MPHA-co-MMA) polymers.	83
Figure 4.7: A plot of the glass transition temperature for the poly-(1-MPHA-co-MMA) polymers as a function of amount of 1-MPHA in the copolymers.	84
Figure 4.8: ¹ H NMR signal versus time for the <i>in situ</i> ¹ H NMR copolymerisation of 1-MPHA with MMA. The solid symbols represent MMA and the open symbols represent 1-MPHA.	85
Figure 4.9: Rate of monomer consumption as a function of time for the <i>in situ</i> kinetic reactions in the copolymerisation of 1-MPHA with MMA. The solid symbols are MMA and the open symbols are for 1-MPHA.	86
Figure 4.10: Mole fraction MMA in feed as a function of experimental and calculated conversion from <i>in situ</i> NMR studies by monitoring double bond signals with time (solid markers – experimental conversion: Equation 4.9 and open markers – calculated conversion: Equation 4.8).	87
Figure 4.11: A plot of the confidence regions for the reactivity ratios of the MMA/1-MPHA copolymer system.	89
Figure 5.1: ¹ H NMR spectrum showing the peaks used to monitor monomer consumption in the <i>in situ</i> NMR copolymerisation of 1-MPHA with VAc.	96
Figure 5.2: ¹ H NMR spectra for the poly-(1-MPHA-co-VAc) polymers with copolymer compositions (a) 8 and (b) 2 mole% 1-MPHA.	97
Figure 5.3: Plots of the TGA data for the poly-(1-MPHA-co-VAc) polymers (a) over the whole temperature range and (b) showing the early decomposition in samples containing high 1-MPHA content.	100
Figure 5.4: Storage modulus as a function of temperature for the poly-(1-MPHA-co-VAc) polymers.	101
Figure 5.5: A plot of tan delta as a function of temperature for the poly-(1-MPHA-co-VAc) polymers.	102
Figure 5.6: Distilled water droplets on (a) polyvinyl acetate and (b) on a poly-(1-MPHA-co-VAc) polymer sample containing 8 mole% 1-MPHA spin-coated on a glass substrate.	105

- Figure 5.7: A plot of monomer consumption for both monomers as a function of time in the copolymerisation of 1-MPHA with VAc. The reactions were run at 70 °C *in situ* in an NMR instrument at 50 wt% solution in deuterated toluene with 2 wt% AIBN as initiator. 107
- Figure 5.8: Reaction rate comparison for three 1-MPHA/VAc copolymerisation reactions carried out *in situ* an NMR instrument. 108
- Figure 5.9: Plots of 1-MPHA ratio in the monomer feed as a function of theoretical and experimental conversion data for three starting feed compositions. The data was obtained from *in situ* ¹H NMR studies of the copolymerisation of 1-MPHA with vinyl acetate. The reactions were conducted at 70 °C in deuterated toluene at 50 wt% solution with 2 wt% AIBN as initiator. 110
- Figure A.1: A GC trace for the reaction product mixture of the oligomerisation of 1-pentene at 100:1 Al:Zr ratio. 116
- Figure A.2: ¹H NMR for the dimer oligomer of 1-pentene, 2-propyl-heptene. 116
- Figure A.3: ¹³C NMR spectrum of 2-propyl-heptene with carbon atom assignment. 117
- Figure A.4: ¹H NMR spectrum of 2-propyl-heptene (1) and 4-methyl-nonan-4-ol (2) showing the hydration of the oligomer. 117
- Figure A.5: ¹³C NMR spectrum of 4-methyl-nonan-4-ol with assignment of the carbon atoms. 118
- Figure A.6: FTIR spectrum of 4-methyl-nonan-4-ol showing the hydroxyl group around 3400 cm⁻¹ from the hydration of 2-propyl-heptene. 118
- Figure A.7: ¹H NMR spectra of the reaction product of the esterification of 4-methyl-nonan-4-ol with acryloyl chloride to 1-MPHA. 119
- Figure A.8: ¹³C NMR spectrum of 1-MPHA showing the assignment of the carbon atoms. The spectrum was run in CDCl₃ at 25 °C. 119
- Figure A.9: FTIR spectrum of 1-MPHA showing new functional groups, -C=O at 1720 and -C=C at 1619 cm⁻¹. 120
- Figure E.1: ¹H NMR spectrum for the trimer oligomer of 1-pentene. **Error! Bookmark not defined.**
- Figure E.2: ¹³C NMR spectrum for the trimer of 1-pentene, (a) the full range of the spectrum and (b) the expanded region showing the overlapping peaks. **Error! Bookmark not defined.**
- Figure E.3: ¹H NMR spectrum of the trimer alcohol. **Error! Bookmark not defined.**
- Figure E.4: ¹³C NMR spectrum for the trimer alcohol showing the assignment of the carbon peaks. **Error! Bookmark not defined.**
- Figure E.5: FTIR spectrum for the 1-pentene trimer alcohol showing the hydroxyl group around 3400 cm⁻¹. **Error! Bookmark not defined.**
- Figure F.1: ¹H NMR spectrum for the 1-pentene tetramer oligomer. 132
- Figure F.2: ¹³C NMR spectrum for the 1-pentene tetramer oligomer. 133
- Figure F.3: ¹H NMR spectrum for the 1-pentene tetramer alcohol. 134
- Figure F.4: ¹³C NMR spectrum for the 1-pentene tetramer alcohol. 134
- Figure G.1: ¹H NMR spectrum for the copolymers of poly-(1-MPHA-co-GMA) containing (a) 43 and (b) 5 mole% 1-MPHA. 135

- Figure G.2: TGA traces for the poly-(1-MPHA-co-GMA) copolymers. 137
- Figure H.1: ^1H NMR spectra for the poly-(1-MPHA-co-styrene) copolymers containing, (a) 75 and (b) 6 mole% 1-MPHA. 138
- Figure H.2: TGA traces for the poly-(1-MPHA-co-styrene) copolymers. 140

List of Schemes

- Scheme 3.1: Reaction scheme used for the preparation of 1-methyl-1-propyl-hexyl acrylate from 1-pentene. 45
- Scheme 3.2: Scheme for the homopolymerisation of 1-MPHA with 2 wt% AIBN at 70 °C. 50
- Scheme 3.3: Free radical termination by combination and disproportionation of poly-(1-MPHA) radicals. 65
- Scheme 4.1: Schematic representation for the copolymerisation of 1-MPHA with MMA. (NB – structure not intended to represent a block copolymer). 70
- Scheme 5.1: Schematic representation of the copolymerisation of 1-MPHA with VAc. 95
- Scheme 5.2: A schematic of poly-(1-MPHA) showing the various groups that contribute to the solubility parameter. 104

List of Tables

Table 3.1: Molecular weight data for the products of homopolymerisation of 1-MPHA at various monomer concentrations	52
Table 4.1: Concentration of the reagents used in the copolymerisation of 1-MPHA with MMA	71
Table 4.2: Chemical analysis results of the poly-(1-MPHA-co-MMA) polymers	77
Table 4.3: TGA results of the poly-(1-MPHA-co-MMA) polymers	79
Table 4.4: Results of the reactivity ratio determination	88
Table 5.1: Chemical analysis data for poly-(1-MPHA-co-VAc) polymers	98
Table 5.2: Summary of the DMA results for the poly-(1-MPHA-co-VAc) polymers and poly-(1-MPHA).	102
Table 5.3: Group contributions to the solubility parameter of poly-(1-MPHA)	104
Table 5.4: Contact angle measurements for the poly-(1-MPHA-co-VAc) copolymers	106
Table 5.5: Reactivity ratio results for the VAc/1-MPHA system obtained from <i>in situ</i> ^1H NMR studies at 70 °C in deuterated toluene at 50 wt% solution with 2 wt% AIBN as initiator	110
Table B.1: Normalised concentration as a function of time for the <i>in situ</i> homopolymerisation of 1-MPHA at different purity levels	121
Table C.1: Raw data for the <i>in situ</i> kinetics of the copolymerisation of 1-MPHA with MMA at three different initial monomer feed ratios	123
Table D.1: Raw data for the <i>in situ</i> kinetics of the copolymerisation of 1-MPHA with VAc at three different initial monomer feed ratios	125
Table G.1: Chemical analysis data for the poly-(1-MPHA-co-GMA) copolymers	136
Table G.2: Thermal decomposition data for the poly-(1-MPHA-co-GMA) polymers	137
Table H.1: Chemical analysis data for the poly-(1-MPHA-co-styrene) copolymers	139
Table H.2: Thermal decomposition data for the poly-(1-MPHA-co-styrene) polymers	140

CHAPTER 1

INTRODUCTION AND OBJECTIVES

1.1 Introduction

Despite the recent advances in polymerisation techniques, there has been little reported on new monomers. Development of new monomers could bring down the price of monomers as there will be a wider range of monomers to choose from. This can also lead to the introduction of new ranges of products with properties that can be determined during the design process, for instance a functionality that is required in the end product can be introduced during the synthetic stages. In order for the South African economy to sustain its development, optimal exploitation of its unique raw materials situation is necessary.

When compared with conventional Ziegler-Natta catalysis, metallocene catalysis allows better control of polymer chain length, molar mass distribution, degree of branching and comonomer incorporation as a function of the metallocene structure^[1, 2]. This is possible because the metallocene catalysts are homogeneous and provide uniform reaction sites, which are known as single sites. The Ziegler-Natta catalysts are heterogeneous and result in non-uniform reaction sites.

Also, recent developments in the field of free radical polymerisation such as the controlled free radical techniques mean that now there are new tools to create new products from existing monomers with superior end-properties. Conventional free radical copolymerisation generally results in copolymers with a high polydispersity index and no control over the molecular and chain structure. In order to obtain products with low polydispersity, accurate control of molecular weight and chain ends, anionic^[3], cationic^[4] and group transfer^[5] procedures have been used. The above methods are however not well suited for the preparation of well-defined statistical copolymers from vinyl monomers such as styrenics and acrylates^[6]. These processes also require very rigorous conditions and are thus difficult and expensive.

Methods such as stable free-radical polymerisation (SFRP)^[7, 8], atom transfer radical polymerisation (ATRP)^[9-11] and reversible addition-fragmentation chain transfer (RAFT)^[12-14] were developed to achieve control of the radical copolymerisation process. By means of these methods the molecular weight of a polymer increases linearly with conversion and the polydispersity is low.

The advantages offered by metallocene catalysis and controlled free radical polymerisation reactions have thus contributed significantly towards attaining a wider and better range of product properties over what is possible by means of conventional techniques. The control of chain architecture and length leads to materials with desirable properties.

Materials with desirable properties can be made through creation of new monomers. This can be achieved by selecting specific desired functionalities, as the monomer can be designed to impart specific properties to the product.

1-Pentene, a by-product of the Fischer-Tropsch process used by Sasol to convert coal to fuel via syngas, is an odd-numbered α -olefin which has been available in commercial quantities for over a decade^[15]. To date, 1-pentene is mainly used as a comonomer with propene^[16]. South Africa occupies a unique position in the world's olefin market. The Fischer-Tropsch process produces, as by-products, α -olefins containing both odd- and even- numbered carbon chains. The bulk production of odd-numbered α -olefins is unique to the Sasol process; the rest of the world obtains its α -olefins from the Shell Higher Olefins Process (SHOP)^[17], which oligomerises ethylene to higher even-numbered α -olefins.

The odd numbered α -olefins obtained by the Sasol process constitute a new range of low cost reagents. Recent studies have demonstrated that metallocene catalysis can be used to convert 1-pentene to low molar mass oligomers^[18, 19]. The product composition can range from dimers to polymers, depending on the ratio of co-catalyst-to-catalyst used. Metallocene catalysts produce oligomers that show a high regioselectivity and also high specificity in their chain-termination reactions^[20].

1.2 Aims and objectives of the study

The abundance of the odd-numbered α -olefins, the lack of down stream application of their derivatives, the ability to control oligomerisation with metallocene catalysis and the versatility of free radical polymerisation, all contribute to presenting an opportunity to add value to the α -olefins produced by Sasol. Basic research into the synthesis of a novel monomer from 1-pentene was conducted in this study.

Thus, the objectives of this study were to:

- synthesise 1-pentene oligomers in bulk, with special attention to the dimeric product,
- convert the dimer oligomer to an alcohol,
- convert the alcohol to a polymerisable acrylate ester,
- investigate the homopolymerisation of the new acrylate monomer,
- investigate thoroughly the copolymerisation of the new monomer with methyl methacrylate and vinyl acetate. Copolymerisation with glycidyl methacrylate and styrene was also investigated,
- characterise the new copolymers, and
- study the kinetics of both the homopolymerisation of 1-MPHA and its copolymerisation with MMA and VAc.

1.3 Layout

The dissertation comprises six chapters. The first two chapters are introductory chapters. Chapter 1 gives an overall introduction to the field and research and Chapter 2 is an overview of the relevant historical and theoretical background.

The next three chapters are written in publication format; Chapter 3 describes the synthesis, purification and homopolymerisation of the new monomer, 1-methyl-1-propyl-hexyl acrylate (1-MPHA). Chapter 4 describes the copolymerisation of 1-MPHA with methyl methacrylate (MMA). Characterisation of the copolymers and the

kinetics of the copolymerisation reactions are described. Chapter 5 describes the copolymerisation of 1-MPHA with vinyl acetate (VAc). Characterisation of the copolymers and the kinetics of the copolymerisation reactions are described.

Chapter 6 summarises the overall conclusions of the work and recommendations for future work are made.

Appendix A contains additional information in the synthesis and polymerisation of 1-methyl-1-propyl-hexyl acrylate.

Appendix B contains the kinetic data of the *in situ* homopolymerisation of 1-MPHA.

Appendix C contains the kinetic data of the *in situ* copolymerisation of 1-MPHA with methyl methacrylate.

Appendix D contains the kinetic data of the *in situ* copolymerisation of 1-MPHA with vinyl acetate.

Appendix E contains the results for the 1-pentene trimer oligomer and its hydration.

Appendix F contains the results for the 1-pentene tetramer oligomer and its hydration.

Appendix G contains the results for the copolymerisation of 1-MPHA with glycidyl methacrylate.

Appendix H contains the results for the copolymerisation of 1-MPHA with styrene.

1.4 References

1. Jungling, S., Mulhaupt, R., Stehling, U., Brintzinger, H. H., Fischer, D., and Langhauser, F., *J. Polym. Sci. Part A: Polym. Chem.*, 1995. **33**: p. 1305 - 1317.
2. Brintzinger, H. H., Fischer, D., Mulhaupt, R., Rieger, B., and Waymouth, R. M., *Angew. Chem. Internat. Edit. Engl.*, 1995. **34**: p. 1143 - 1170.
3. Quirk, R. P. and Lynch, T., *Macromolecules*, 1993. **26**: p. 1206 - 1212.
4. Sawamoto, M., *Prog. Polym. Sci.*, 1991. **16**: p. 111 - 172.
5. Sogah, D. Y., Hertler, W. R., Webster, O. W., and Cohen, G. M., *Macromolecules*, 1987. **20**: p. 1473 - 1488.
6. Madruga, E. L., *Prog. Polym. Sci.*, 2002. **27**: p. 1879 - 1924.
7. Georges, M. K., Veregin, R. P. N., Kazmaier, P. M., and Hamer, G. K., *Macromolecules*, 1993. **26**: p. 2987 - 2988.
8. Hawker, C. J., *J. Am. Chem. Soc.*, 1994. **116**: p. 11185 - 11186.
9. Wang, J.-S. and Matyjaszewski, K., *Macromolecules*, 1995. **28**: p. 7572 - 7573.
10. Kato, M., Kamigaito, M., Sawamoto, M., and Higashimura, T., *Macromolecules*, 1995. **28**: p. 1721 - 1723.
11. von Werne, T. and Patten, T. E., *J. Am. Chem. Soc.*, 2001. **123**: p. 7497 - 7505.
12. Chong, Y. K., Le, T. P. T., Moad, G., Rizzardo, E., and Thang, S. H., *Macromolecules*, 1999. **32**: p. 2071 - 2074.
13. Chiefari, J., Chong, Y. K., Ercole, F., Krstina, J., Ferrery, J., Le, T. P. T., Mayadunne, R. T. A., Meijs, G. F., Moad, C. L., Moad, G., Rizzardo, E., and Thang, S. H., *Macromolecules*, 1998. **31**: p. 5559 - 5562.
14. De Brouwer, H., Schellekens, M. A. J., Klumperman, B., Monteiro, M. J., and German, A. L., *J. Polym. Sci. Part A: Polym. Chem.*, 2000. **38**: p. 3596 - 3603.
15. Waddacor, M., *Chemical Processing SA*, 1994. **1**: p. 2.
16. Sacchi, M. C., Forlini, F., Losio, S., Tritto, I., Wahner, U. M., Tincul, I., Joubert, D. J., and Sadiku, E. R., *Macromol. Chem. Phys.*, 2003. **204**(13): p. 1643 - 1652.
17. Skupinska, J., *Chem. Rev.*, 1991. **91**(4): p. 613 - 648.
18. Wahner, U. M., Brull, R., Pasch, H., Raubenheimer, H. G., and Sanderson, R. D., *Angew. Makromol. Chem.*, 1999. **270**: p. 49 - 55.

19. Christoffers, J. and Bergman, R. G., *J. Am. Chem. Soc.*, 1996. **118**: p. 4715 - 4716.
20. Resconi, L., Piemontesi, F., Franciscano, G., Abis, L., and Fiorani, T., *J. Am. Chem. Soc.*, 1992. **114**: p. 1025 - 1032.

CHAPTER 2

LITERATURE REVIEW AND HISTORICAL BACKGROUND

2.1 Introduction

The importance of Sasol's Fischer-Tropsch process in α -olefins has already been discussed in Section 1.1. The presently known reserves of methane and of coal exceed that of crude oil by factors of about 1.5 and 2.5 respectively^[1]. This places the Sasol process that is coal-based in a very favourable position.

This chapter includes a brief background on olefins, their sources, ways in which value can be added to the olefins and their derivatives through hydration to alcohols and esterification of alcohols to polymerisable compounds, monomers. A brief background to the kinetics of polymerisation and general polymer characterisation techniques used is also given.

2.2 Olefins

Olefins are aliphatic hydrocarbons containing at least one carbon-carbon double bond. The name olefin is derived from the oily liquid-forming property on reaction of these compounds with halogens, (gaz olefiant – oil-forming gas)^[2]. Olefins form the main building blocks for the chemical industry^[3]. Olefins such as ethylene, propylene and butene form the bulk of production of the polymer industry.

α -Olefins have the reactive double bond at the end of the carbon chain. They are generally obtained by^[4]:

- thermal and catalytic cracking of paraffins,

- oligomerisation of ethylene,
- dehydrogenation of paraffins,
- dimerisation and metathesis of olefins,
- dehydration of alcohols and
- electrolysis of $C_3 - C_{30}$ straight chain carboxylic acids.

The thermal and catalytic cracking of paraffins and oligomerisation of ethylene are bulk industrial production processes for the formation of α -olefins. These are explained further below.

2.2.1 Thermal and catalytic cracking of paraffins

Coal, natural gas and petroleum are sources of fossil fuel that can be converted to syngas. Syngas ($CO + H_2$) obtained from these fossil fuels, is catalytically converted via the Fischer-Tropsch (FT) process^[1] into a wide range of olefins, paraffins and other oxygenates (alcohols, aldehydes, acids and ketones). The product composition is controlled by variables such as temperature, feed gas composition, pressure, catalyst type and promoters. The growth of chains on the catalyst surface is stepwise, as is illustrated in Figure 2.1.

In the initiation step, the adsorbed CO is hydrogenated to form adsorbed CH_2 and H_2O . During the chain growth and termination steps,

- H_2 is added to the adsorbed CH_2 to form CH_4
- CH_2 adds (α - being the probability for chain growth) to the adsorbed CH_2 to form adsorbed C_2H_4 which can either be desorbed as C_2H_4 or add another H_2 to be desorbed as C_2H_6
- CH_2 further adds to the adsorbed C_2H_4 to form adsorbed C_3H_6 which can be desorbed as C_3H_6 or add another H_2 and be desorbed as C_3H_8 . Further repetition of these steps results in longer chains of both the saturated and unsaturated hydrocarbons.

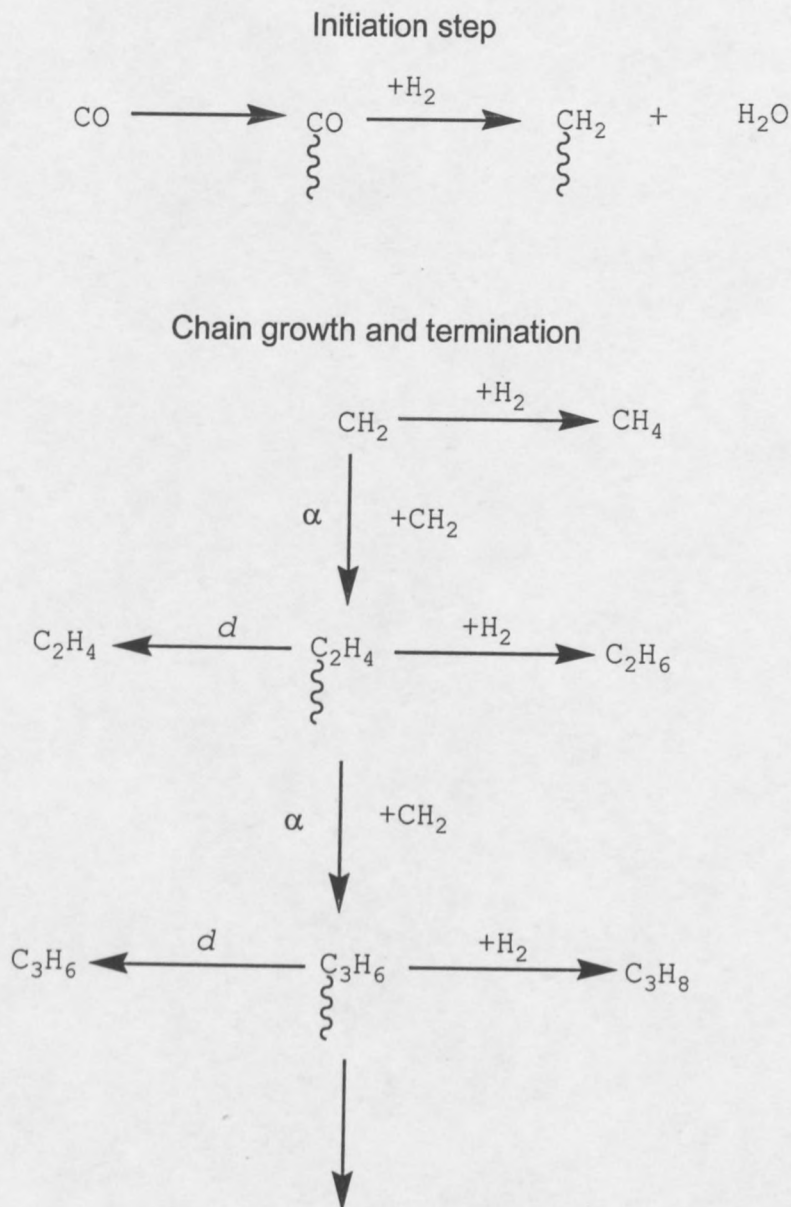


Figure 2.1: The step-wise growth process in the conversion of syngas to olefin in the Fischer-Tropsch process^[1], *d* stands for desorbed species, α is the probability of chain growth and the chain represents an adsorbed species to the catalyst surface.

Moreover, the chain growth process in FT can generally be regarded as a repeated reaction sequence, in which the hydrogen atoms are added to the carbon and oxygen with the splitting of the C-O bond and formation of a new C-C bond. In order to form one CH₂ group, at least 10 reactions are necessary^[5]:

- associative adsorption of CO
- splitting of the C-O bond
- dissociative adsorption of 2H₂

- transfer of 2H to the oxygen to yield H₂O
- desorption of H₂O
- transfer of 2H to the carbon to yield CH₂
- formation of a new C-C bond.

The following two steps yield the products:

- either the hydrogen is added to adsorbed CO first and thereby forms oxygen containing intermediates
- or the C-O bond splits first to give hydrocarbon intermediates.

In a Fischer-Tropsch process, the production of purified syngas typically accounts for 60 - 70% of the capital and running costs^[1]. The capital cost of the methane conversion plant is about 30% lower and is more efficient than the coal one. About 20% carbon is converted to CO₂ in methane conversion, compared to the 50% conversion to CO₂ during coal gasification. The complexity of the syngas production from coal accounts for the higher production cost relative to syngas from methane. The high cost of the coal process is a difficulty that can be offset by better use of the by-products.

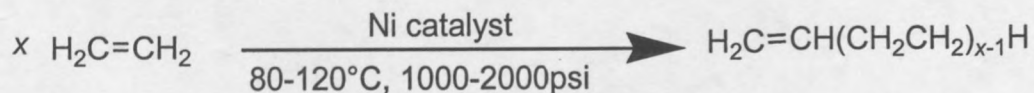
2.2.2 Oligomerisation of ethylene

The Shell Higher Olefins Process (SHOP) is the most modern method for oligomerisation of ethylene^[4]. The process consists of four steps: ethylene oligomerisation, isomerisation of oligomers, metathesis and hydroformylation. These steps depicted in Figure 2.2 are explained below^[3, 4, 6].

2.2.2.1 Oligomerisation

Ethylene which is obtained from the steam cracking of hydrocarbons is oligomerised with a homogeneous catalyst consisting of nickel chloride and the potassium salt of

o-diphenylphosphinobenzoic acid in 1,4-butanediol. The oligomers are α -olefins with an even number of carbon atoms ranging from C₄–C₄₀.



In the distillation column, these are distilled into three fractions, viz.: a light C₄–C₈ fraction, a C₁₀–C₁₄ fraction and a heavy C₁₆–C₄₀ fraction.

2.2.2.2 Hydroformylation

The intermediate fraction C₁₀–C₁₄ is fed to a hydroformylation reactor where it is converted into straight chain aldehydes and finally to the corresponding alcohols.

2.2.2.3 Isomerisation

The light and heavy fraction α -olefins are fed to an isomerisation reactor and isomerised to form internal olefins with the double bond situated within the oligomer chain.

2.2.2.4 Metathesis

The internal olefins are fed to the metathesis reactor where the short and long chain internal olefins disproportionate. For example, C₄ and C₂₀ olefins give two C₁₂ internal olefin molecules.

The internal olefins from the metathesis step are fed into the distillation column and the C₁₀ – C₁₄ internal olefins fraction is separated and fed to the hydroformylation reactor.

In the hydroformylation reactor a rhodium catalyst is used to convert the internal olefins into α -olefins. Figure 2.2 is a schematic of the oligomerisation of ethylene by the Shell Higher Olefins Process.

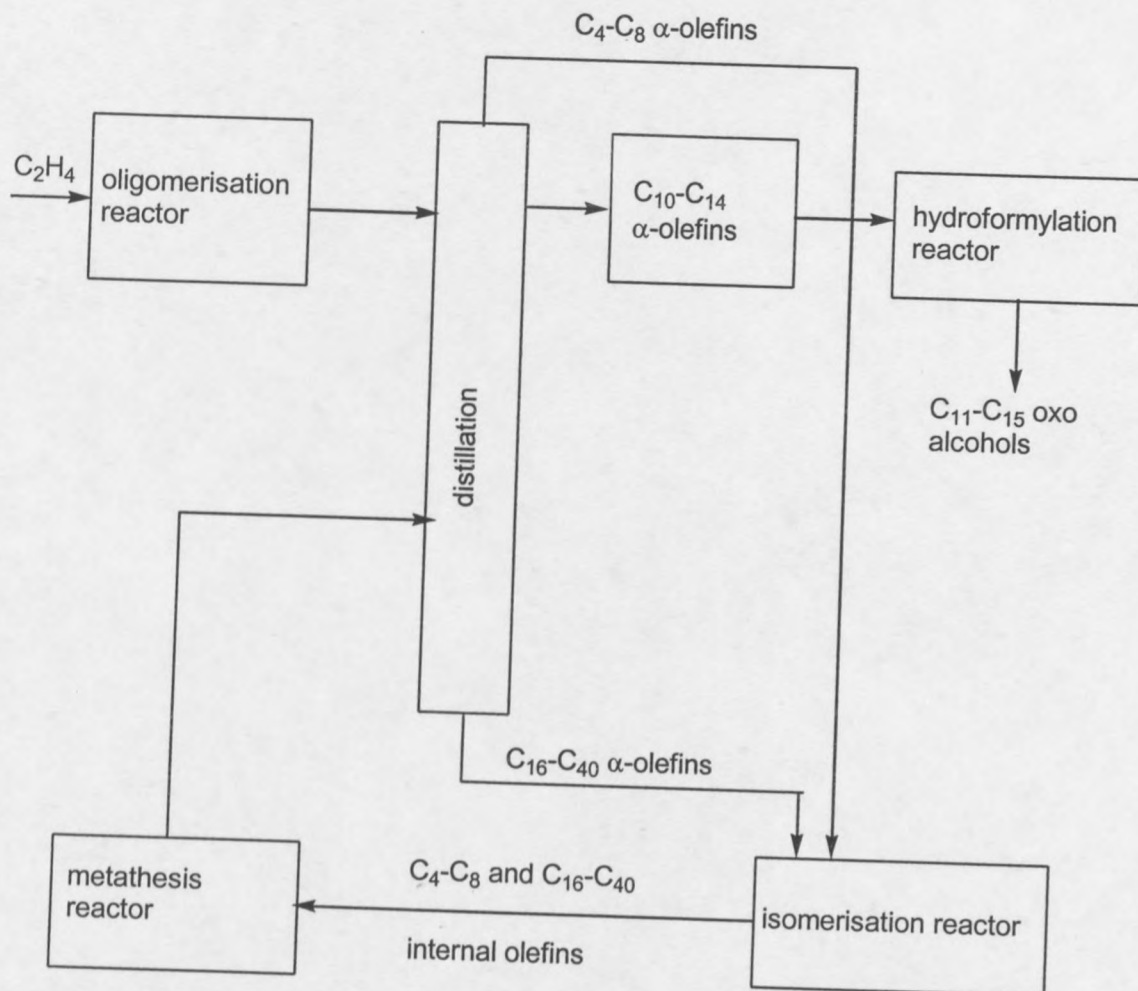


Figure 2.2: Shell Higher Olefins Process for the oligomerisation of ethylene^[3, 6].

2.3 Oligomerisation of olefins

Metallocene catalysts are traditionally catalysts based on a group IV central metal with ligands that determine the stereoregularity of the polymerisation product. These catalysts are homogeneous and are usually activated by co-catalysts such as methylaluminoxane (MAO). Methylaluminoxane is a partial hydrolysis product of trimethylaluminium (TMA), is oligomeric in nature, and has a molecular weight in the

range of 800 – 1500^[7]. The exact structure is not known but it possesses –Al(Me)-O-repeat units, with tetra-coordinated Al. MAO is always associated with some amount of unhydrolysed TMA. Metallocene catalysts offer better control of polymer structure, molecular weight and molecular weight distribution, compared to Ziegler Natta catalysts, as they have a well-defined single type of metal centre with a defined coordination environment^[8].

Varying the ratio between the catalyst and co-catalyst makes it possible to tailor-make the subsequent products to be either low molecular weight oligomers or high molecular weight polymers. Polymerisation occurs when a large excess of methylaluminoxane relative to catalyst is used in the reactions^[9]. A low co-catalyst-to-catalyst ratio (Al/Zr ca. 1:1) gave analytically pure dimers^[10]. 1-Pentene was oligomerised using a number of catalysts activated by MAO; Cp₂ZrCl₂ was the only catalyst capable of producing low molar mass oligomers^[11].

The chain termination reaction yields oligomers with double-bond functional groups, which are predominantly of the vinylidene type when the catalyst is the unsubstituted Cp₂ZrCl₂, and when the bulkier substituted Cp₂*ZrCl₂ is used (Cp₂* is pentamethyl-cyclopentadienyl) then the double bond is of the vinyl type^[12]. The oligomers can be used as intermediates in the preparation of some industrially important compounds, see Figure 2.3^[13].

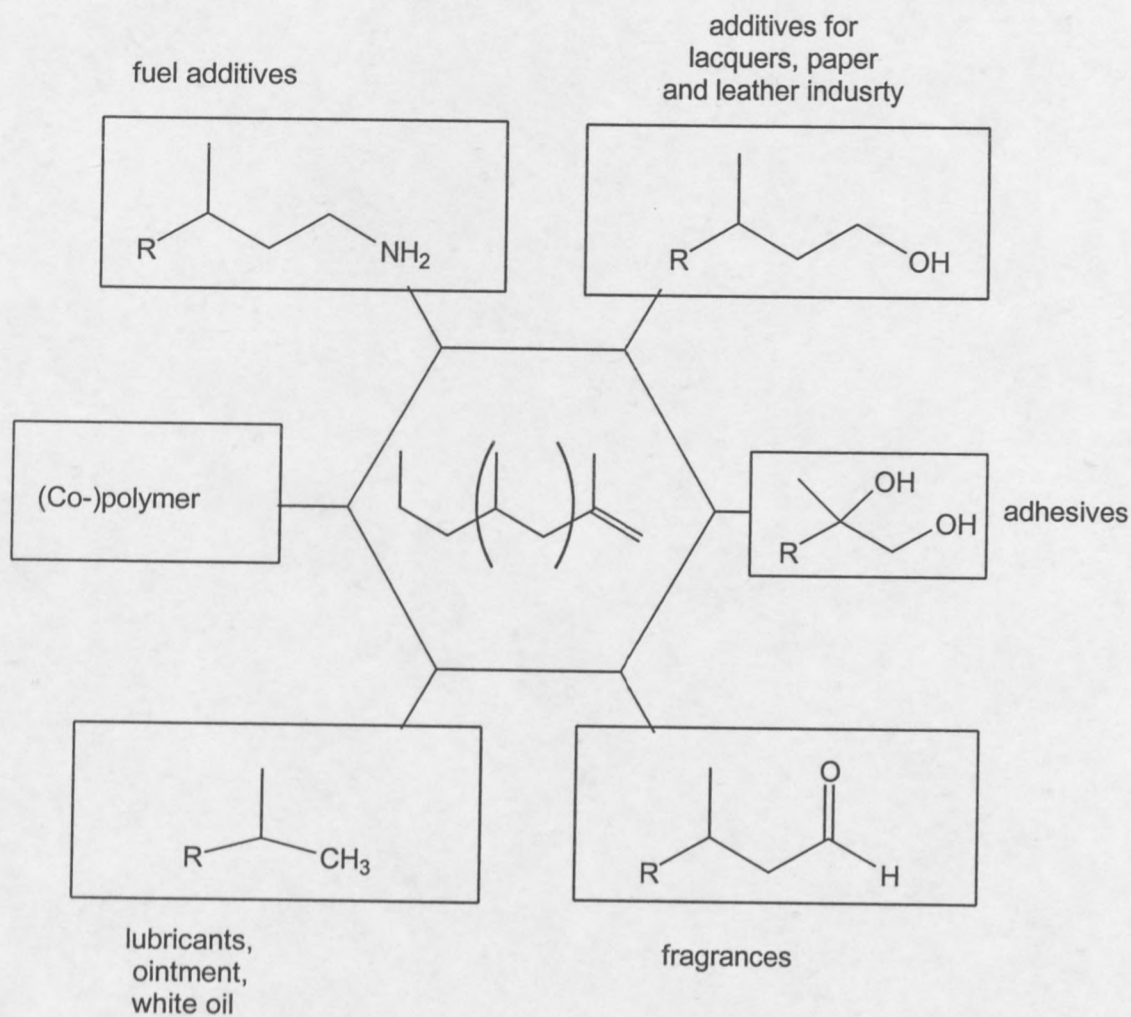


Figure 2.3: Some of the suggested uses for the derivatives of olefin oligomers^[13].

The mechanism for the dimerisation process, as proposed by Christoffers *et al*^[14] is shown in Figure 2.4.

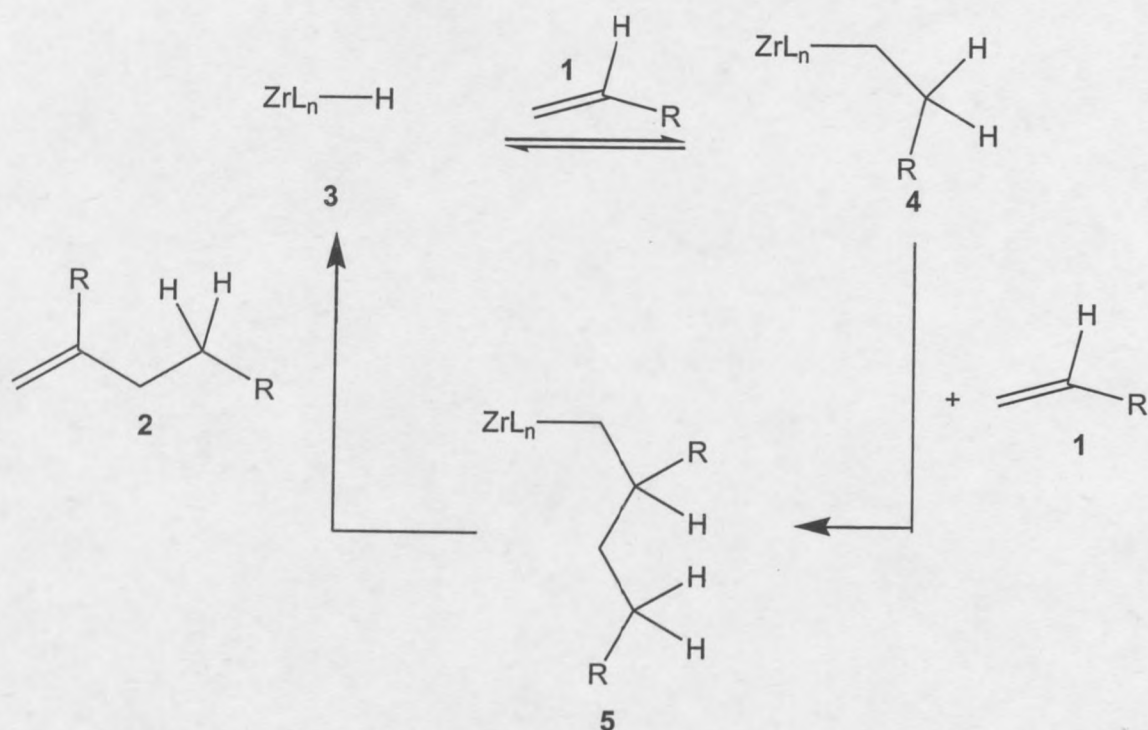


Figure 2.4: The mechanism and catalytic cycle for the formation of the dimer oligomer from the α -olefin^[14].

Alkene 1 is inserted into the Zr-H bond of the zirconocene catalyst 3, to give a Zr-alkyl complex 4 which is in equilibrium with 3, which can either regenerate alkene 1 and catalyst 3 via a β -H elimination reaction, or undergo further insertion of another alkene 1 into the Zr-C bond of complex 4, to give the new, longer, Zr-alkyl species 5. The dimeric alkene 2, and the Zr-H complex 3, are obtained from the β -H elimination from complex 5. The presence of a chloro-ligand in the coordination sphere of Zr makes the β -elimination process more favourable than further insertion steps, and thus is the cause of selective dimer formation, rather than higher oligomers or polymers^[14].

Metallocene catalysts give oligomers with high regioselectivity and high specificity in chain termination. This phenomenon ensures uniform reactivity of the oligomers in subsequent reactions. These reactive oligomers can further be functionalised into alcohols, esters, anhydrides, and thiols, which are important industrially^[4]. The oligomers also find use in the synthesis of biodegradable detergents and plasticisers.

2.4 Hydration of olefins

Conversion of the olefins into the alcohols is known as hydration, as a water molecule is added across the double bond. The addition of the hydroxyl group on an unsymmetrical double bond can be to the carbon atom with either the least or the most substituted protons. Addition of the hydroxyl group on the carbon atom with the least substituted protons is known as the anti-Markovnikov addition (by, for example, hydroboration-oxidation), whereas addition to the most substituted carbon atom is known as Markovnikov addition (by, for example, oxymercuration-demercuration).

In both hydroboration and oxymercuration, alkyl substitution retards the reaction rate, except in cases in which the alkyl group is placed beta to the site of carbon-boron or carbon-mercury bond formation^[15]. The authors of [15] observed that steric effects retard hydroboration more than oxymercuration, presumably because of the shorter B-C distance relative to the Hg-C distance in the transition state structures.

2.4.1 Hydroboration-oxidation of olefins

The hydroboration of olefins involves the addition of a boron-hydrogen bond to the carbon-carbon multiple bond^[16-19]. The corresponding organoboranes are readily available as intermediates in organic synthesis, e.g. oxidation with alkaline peroxides to give alcohols.

The hydroboration of olefins involves a *cis* addition of the boron-hydrogen bond with the boron atom attached to the less substituted of the two olefinic carbon atoms of the double bond^[20]. The formation of products in hydroboration occurs via a one-step concerted reaction. The borane forms carbon-hydrogen and carbon-boron bonds simultaneously on the same face of the olefin to form a four-membered ring transition state. The borane acts as an electrophile and interacts with the nucleophilic olefin with a partial transfer of electrons from the olefin to the boron. The boron then carries a partial negative charge whereas the olefin carries a partial positive charge.

In an unsymmetrical olefin the partial positive charge is better stabilised on the carbon atom with more substituents because of the electron donating effect of the alkyl substituents. Also, the addition of the boron to the less substituted olefin carbon atom is less sterically hindered. Both the electronic and steric factors explain why the addition of water to unsymmetric olefins occurs in an anti-Markovnikov nature.

Oxidation of the complex with aqueous hydrogen peroxide breaks the carbon-boron bond and a new hydroxyl-carbon bond forms. The reaction occurs with the retention of configuration, with the hydroxyl group at the position occupied by the boron atom in the initial organoborane. The general mechanism for the hydroboration-oxidation of alkenes is depicted in Figure 2.5.

Terminal olefins, $RCH=CH_2$, on hydroboration-oxidation, give predominantly products with the hydroxyl group added to the terminal olefinic carbon atom. Dialkyl ethenes, $RCH=CHR'$ give almost equal amounts with the hydroxyl group added at both of the two olefinic carbon atoms. Trisubstituted olefins, $R_2C=CHR$, add the hydroxyl group predominantly at the less substituted olefinic carbon atom^[21, 22].

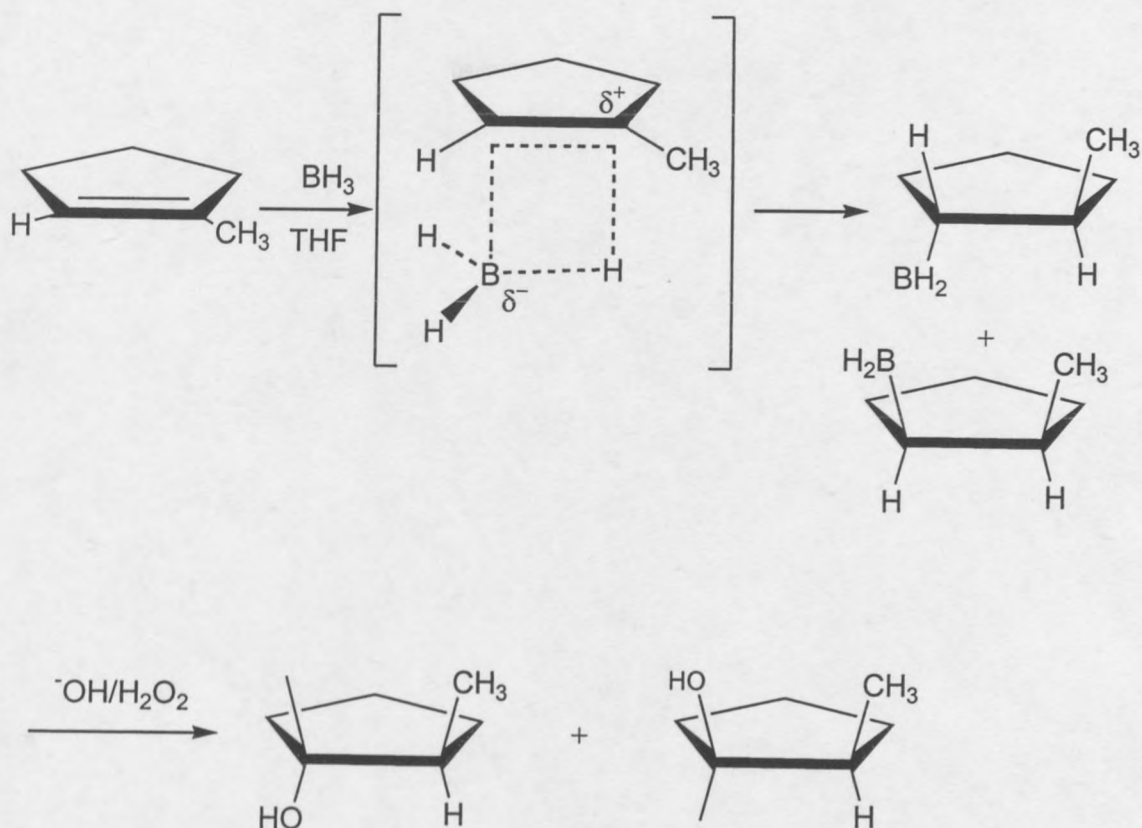


Figure 2.5: General mechanism for the hydroboration-oxidation of olefins^[20].

2.4.2 Oxymercuration-demercuration of olefins

The oxymercuration reaction is the addition of a mercuric salt to an olefinic bond. Reduction of the carbon-mercury bond (demercuration) gives the corresponding alcohol.

The general mechanism for the oxymercuration-demercuration of olefins is depicted in Figure 2.6^[23]. The olefin oxymercuration is initiated by addition of mercuric ion to the olefin to give an intermediate mercurinium ion. Water acts as a nucleophile and attacks the mercurinium ion resulting in a loss of a proton. This results in the formation of a stable organomercury addition product. Reaction of the organomercury product with sodium borohydride reduces the mercury ion to metal mercury. The hydroxyl group gets added to the more highly substituted carbon atom. This addition is better known as the Markovnikov addition.

Brown et al^[24] observed that mono-, di-, tri-, and tetra-alkyl as well as phenyl substituted olefins undergo hydration readily by oxymercuration-demercuration to give high yields of the Markovnikov alcohol.

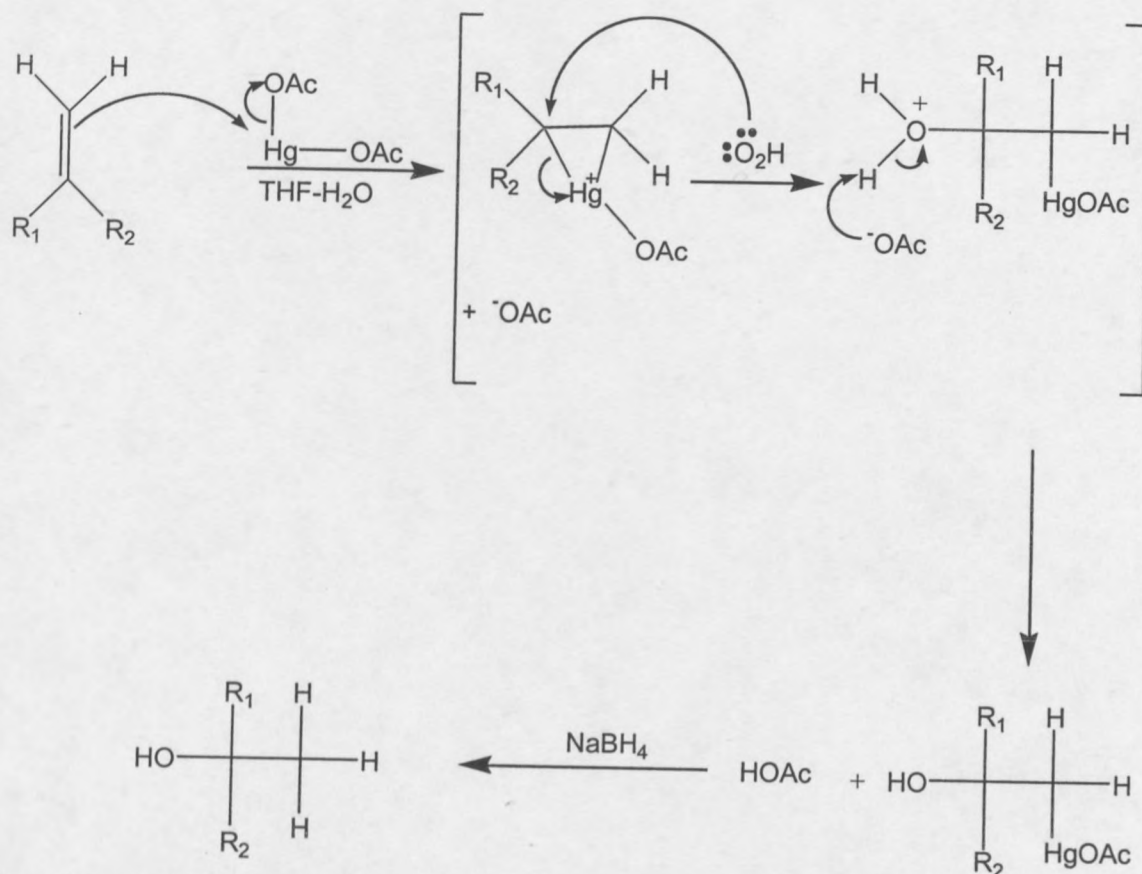
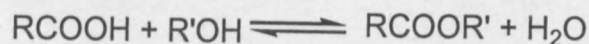


Figure 2.6: General mechanism for the oxymercuration-demercuration hydration of alkenes leading to the Markovnikov addition of water across the double bond.

2.5 Esterification of alcohols

The general equation for esterification of alcohols with carboxylic acids is^[25]:



Esterification of alcohols with carboxylic acids can be accomplished only if a means is available to drive the equilibrium to the right. Some of the ways of doing this are:

(i) addition of an excess of one of the reactants, usually the alcohol; (ii) removal of

the water or the ester by distillation; (iii) removal of water by azeotropic distillation; and (iv) removal of water by use of a dehydrating agent, such as silica gel or a molecular sieve. Various dehydrating agents are used, such as dicyclohexylcarbodiimide (DCC) and dimethylaminopyridine (DMAP).

Acid chlorides overcome the need to eliminate the water, by releasing an acid that can be neutralised *in situ* with a base, or allowed to escape as gas. Acryloyl chloride is widely used in the esterification of alcohols, leading to a number of new monomers^[26-31]. Figure 2.7 shows the general mechanism for the esterification of alcohols with acid chlorides. The mechanism is explained below^[23]:

The reaction of acid chlorides with alcohols occurs via a nucleophilic substitution reaction. The carbonyl group of the acid chloride reacts with the hydroxyl group of the alcohol; the nucleophile which subsequently adds to the acid chloride with the formation of a tetrahedral intermediate. The chloride, which is a good leaving group, is expelled and the ester is obtained as the new compound.

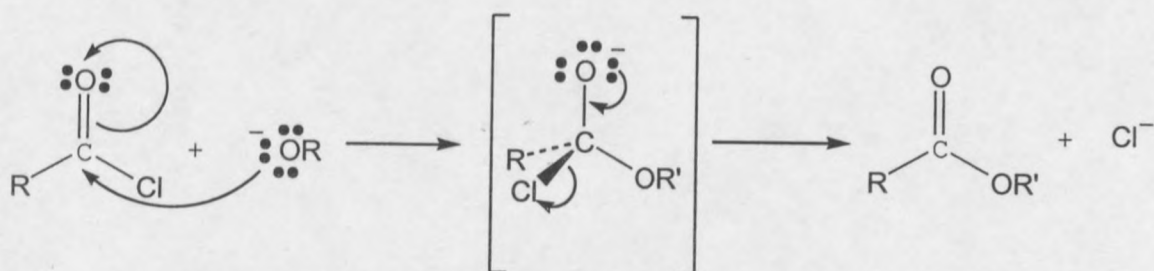


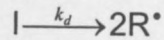
Figure 2.7: General mechanism for the esterification of alcohols with acid chlorides^[23].

2.6 Free radical polymerisation

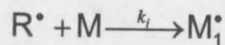
Free radical chain polymerisation is a chain reaction consisting of a sequence of steps: initiation, propagation and termination.

2.6.1 Initiation

An initiator I dissociates to form two initiator radicals R^\bullet :



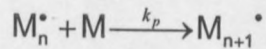
k_d is the rate constant for dissociation. The next step in the initiation is the formation of a chain initiating species M_1^\bullet by addition of radical R^\bullet to monomer M:



k_i is the rate constant for the initiation step.

2.6.2 Propagation

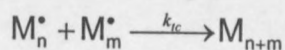
Propagation occurs when the initiating species M_1^\bullet (and longer chain growing radicals) adds to another monomer M. This forms another radical which is capable of adding successive monomer units, thus propagating to a long polymer chain:



k_p is the rate constant for the propagation step.

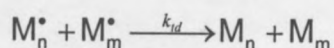
2.6.3 Termination

Termination of the propagating chains occurs in two ways. The first of these is when chain growth is stopped when two propagating chains M_n^\bullet and M_m^\bullet come together to form one dead chain. This process is called termination by combination and is illustrated as follows:



k_{tc} is the rate constant for termination by combination.

The other termination process occurs when a propagating chain M_n^* abstracts a hydrogen beta to the radical centre of another propagating radical M_m^* . Both chains stop growing with M_m containing a double bond. The process is called termination by disproportionation:



k_{td} is the rate constant for termination by disproportionation.

2.6.4 Homopolymerisation

Homopolymerisation is the polymerisation of a single monomer. This type of polymerisation limits the use / application of the monomer, in that only a few properties can be varied in the polymer. These properties are the molecular weight and its distribution, the molecular architecture, such as the degree of branching. Properties such as tacticity might be influenced by reaction conditions.

2.6.5 Copolymerisation

Copolymerisation is defined as polymerisation in which two or more structurally distinct monomers are incorporated into the same polymer chain, and copolymers are defined as polymers that contain two or more distinct structural units in the polymer chain. Copolymerisation is generally accepted as the most successful method for introducing systematic changes in polymer properties^[32]. It is widely used to produce commercial polymers, and in fundamental studies of structure-property relations. Copolymerisation modifies the symmetry of the polymer chain and modulates both intra- and inter-molecular forces. Properties such as melting point,

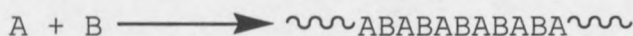
glass temperature, crystallinity, solubility, elasticity, permeability and chemical reactivity may be varied within wide limits^[32, 33].

There are four major classes of copolymers:

- statistical (random) copolymers – comonomers appear in irregular, unspecified sequences along the chain,



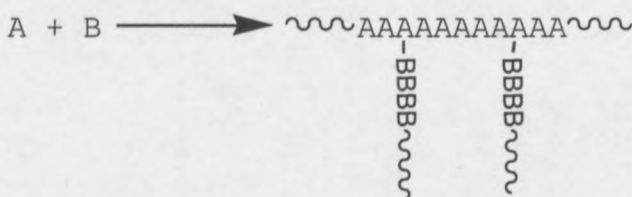
- alternating copolymers – comonomers alternate along the polymer chain,



- block copolymers – long linear sequences of comonomer A are joined to long linear sequences of comonomer B,



- graft copolymers – chains of one comonomer are pendant from a backbone of the other monomer,



2.6.6 Copolymerisation models

The main models proposed thus far to describe the propagation step of copolymerisation include^[34]:

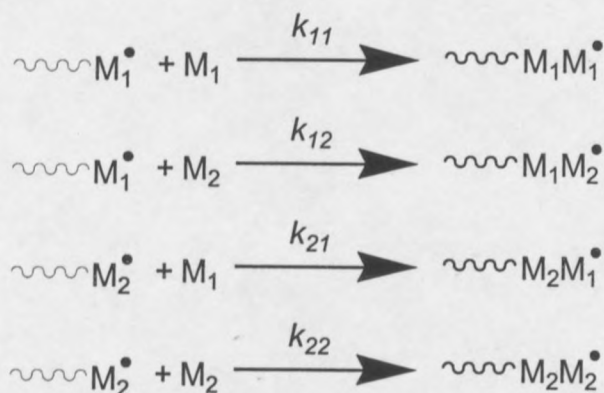
- the terminal model,
- the penultimate unit models; explicit and implicit,
- the radical-complex model,
- the monomer-complex-dissociation model, and
- the monomer-complex participation model.

The terminal model is the one that finds wide applicability. In cases where the terminal model fails to describe the polymerisation, use of the penultimate model is

usually made. The other models are rarely used. The derivation of the terminal model and the penultimate unit model is given below.

2.6.6.1 Terminal model

The terminal model is based on the assumption that the chemical reactivity of the propagating chain in a copolymerisation is dependent only on the identity of the monomer unit at the growing end, and independent of the chain composition preceding the last monomer unit. Mayo and Lewis^[35] are credited for this model. After failing to fit data for styrene and methyl methacrylate copolymerisation to the Wall equation^[36], Mayo and Lewis^[35] formulated the terminal model. Four propagation rate constants are considered:



where,

$\sim M_x^\bullet$ is the propagating polymer chain with the radical on monomer x,

$\sim M_x M_y^\bullet$ is the propagating polymer chain after the addition of monomer M_y ,

k_{xx} is the propagation rate constant for homopropagation,

k_{xy} is the propagation rate constant for cross-propagation.

The two monomers, M_1 and M_2 , are consumed at the following rates:

$$-d[M_1]/dt = k_{11}[M_1^\bullet][M_1] + k_{21}[M_2^\bullet][M_1] \quad (2.1)$$

$$-d[M_2]/dt = k_{12}[M_1^\bullet][M_2] + k_{22}[M_2^\bullet][M_2] \quad (2.2)$$

where $[M_1]$ and $[M_2]$ are monomer feed concentrations for monomers M_1 and M_2 and $[M_1^*]$ and $[M_2^*]$ are the concentrations of the propagating chain radicals with M_1 and M_2 radical ends, respectively.

Division of equation 2.1 by equation 2.2 gives,

$$d[M_1]/d[M_2] = (k_{11}[M_1^*][M_1] + k_{21}[M_2^*][M_1]) / (k_{12}[M_1^*][M_2] + k_{22}[M_2^*][M_2]) \quad (2.3)$$

$d[M_1]$ and $d[M_2]$ are changes in molar ratios of M_1 and M_2 in the copolymer.

Assumption of steady state concentrations of the radicals M_1^* and M_2^* in the system takes the form:

$$k_{21}[M_2^*][M_1] = k_{12}[M_1^*][M_2] \quad (2.4)$$

The propagating radicals concentration from equation 2.3 can be eliminated to give the copolymer equation as:

$$\frac{d[M_1]}{d[M_2]} = \frac{[M_1]}{[M_2]} \frac{(r_1[M_1] + [M_2])}{([M_1] + r_2[M_2])} \quad (2.5)$$

where r_1 and r_2 are reactivity ratios defined as the ratio of the rate constants of homo-propagation to cross-propagation:

$$r_1 = \frac{k_{11}}{k_{12}} \quad \text{and} \quad r_2 = \frac{k_{22}}{k_{21}}$$

When the concentrations of the monomers M_1 and M_2 are expressed as the mole fractions in the feed, f_1 and f_2 respectively, with:

$$f_1 = 1 - f_2 = \frac{[M_1]}{[M_1] + [M_2]} = \frac{[M_1]}{[M]_0} \quad (2.6)$$

where $[M]_0$ is the total initial monomer concentration.

In the copolymer, the concentration of the monomers M_1 and M_2 when expressed as mole fractions give F_1 and F_2 respectively:

$$F_1 = 1 - F_2 = \frac{d[M_1]}{d[M_1] + d[M_2]} = \frac{d[M_1]}{d[M]_0} \quad (2.7)$$

Substitution of equations 2.6 and 2.7 into equation 2.5 and eliminating F_2 , yields:

$$F_1 = \frac{r_1 f_1^2 + f_1 f_2}{r_1 f_1^2 + 2 f_1 f_2 + r_2 f_2^2} \quad (2.8)$$

Equation 2.8 is the copolymerisation equation for a binary monomer system relating the instantaneous copolymer composition to monomer composition and reactivity ratios.

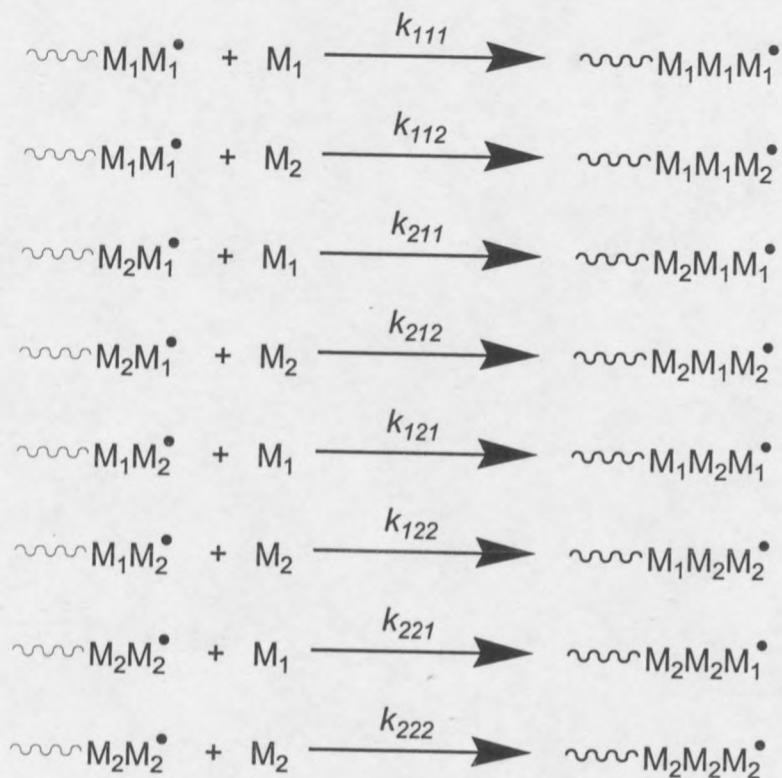
2.6.6.2 Penultimate unit model

The penultimate^[32, 37] unit model applies to systems where the relative rate of monomer addition at the end of the propagating copolymer chain is dependent not only on the identity of the last monomer unit (terminal) to be added but also on the identity of the monomer unit preceding it (penultimate). Two types of the penultimate unit model exist: the implicit and the explicit.

The implicit penultimate^[38, 39] unit effect assumes that the penultimate unit effect is absent from the monomer reactivity ratios, which are equivalent to the terminal model forms, but only exist in the radical reactivity ratios.

The explicit penultimate^[39, 40] unit effect assumes that both the terminal and the penultimate units of a polymer radical may affect the rate of the propagation reaction as shown below.

Because the penultimate unit is considered, there are eight distinct propagation steps:



where,

$\sim M_x M_x^\bullet$ is the propagating chain with the penultimate unit the same as the terminal unit,

$\sim M_x M_y^\bullet$ is the propagating chain with the penultimate unit different to the terminal unit,

$\sim M_x M_x M_x^\bullet$ is the propagating chain after adding another monomer unit similar to both the terminal and penultimate unit,

$\sim M_x M_x M_y^\bullet$ is the propagating chain after adding a monomer unit different to both the terminal and penultimate unit,

$\sim M_x M_y M_x^\bullet$ is the propagating chain after adding a monomer unit similar to the penultimate unit but different to the terminal unit,

k_{xxx} is the propagating rate constant for homo-propagation,

k_{xxy} is the propagating rate constant for cross-propagation,

k_{xyx} is the propagating rate constant for cross-propagation

There are also four reactivity ratios:

$$r_1 = \frac{k_{111}}{k_{112}} \quad r'_1 = \frac{k_{211}}{k_{212}}$$

$$r_2 = \frac{k_{222}}{k_{221}} \quad r'_2 = \frac{k_{122}}{k_{121}}$$

Each monomer has two reactivity ratios, one representing the propagating species in which the penultimate and terminal units are the same, and the other representing the propagating species in which the terminal and penultimate units are different. The molar ratio of the monomers in the formed copolymer is given by the rates of monomer consumption:

$$\frac{d[M_1]}{d[M_2]} = \frac{(k_{111}[M_1M^*_1][M_1] + k_{211}[M_2M^*_1][M_1] + k_{121}[M_1M^*_2][M_1] + k_{221}[M_2M^*_2][M_1])}{(k_{112}[M_1M^*_1][M_2] + k_{212}[M_2M^*_1][M_2] + k_{122}[M_1M^*_2][M_2] + k_{222}[M_2M^*_2][M_2])} \quad (2.9)$$

Assumption of steady-state concentrations of each of the four types of propagating radicals leads to:

$$[M_1M^*_1] = \frac{(k_{211}[M_2M^*_1][M_1])}{(k_{112}[M_2])} \quad (2.10)$$

$$[M_1M^*_2] = \frac{(k_{122}[M_1M^*_2][M_2])}{(k_{221}[M_1])} \quad (2.11)$$

$$[M_1M^*_2] = \frac{([M_2M^*_1](k_{211}[M_1] + k_{212}[M_2]))}{(k_{121}[M_1] + k_{122}[M_2])} \quad (2.12)$$

$$[M_2M^*_1] = \frac{([M_1M^*_2](k_{122}[M_2] + k_{121}[M_1]))}{(k_{211}[M_1] + k_{212}[M_2])} \quad (2.13)$$

where,

$[M_xM^*_x]$ is the concentration of the propagating chains with the same terminal and penultimate units,

$[M_xM^*_y]$ is the concentration of the propagating chains with the penultimate unit different to the terminal unit.

Substitution of the reactivity ratios and the steady state concentrations (equations 2.10 – 2.13) into equation 2.9 leads to:

$$\frac{d[M_1]}{d[M_2]} = \frac{1 + \frac{r'_1 X (r_1 X + 1)}{(r'_1 X + 1)}}{1 + \frac{r'_2 (r_2 + X)}{X (r'_2 + X)}} \quad (2.14)$$

with $X = \frac{[M_1]}{[M_2]}$.

Equation 2.14 is an expression relating copolymer composition to feed composition and reactivity ratios when there are penultimate unit effects in the system.

2.6.7 Compositional drift

The copolymerisation equation and its various forms is applicable to instantaneous feed and copolymer composition. In order to get conditions close to this, polymerisations are terminated at conversions below 10%. As the reaction progresses the copolymer becomes richer (though decreasingly so) in the more reactive comonomer and the monomer feed becomes continually richer in the less reactive comonomer, therefore there is a drift in composition of the system.

In order to accommodate compositional drift, the instantaneous copolymer composition must be expressed as a function of conversion. Wall's^[36] equation relating the copolymer composition to degree of conversion, reactivity ratios and initial feed composition was restricted to monomers with reactivity ratios that are inversely proportional to one another. Skeist's^[47] equation needed graphical or numerical methods of evaluation. Meyer and Lowry^[48] took an analytical solution of Skeist's equation and derived the integrated copolymer equation as shown below:

Equation 2.8 can be expressed as,

$$F_1 = \frac{(r_1 - 1)f_1^2 + f_1}{(r_1 + r_2 - 2)f_1^2 + 2(1 - r_2)f_1 + r_2} \quad (2.15)$$

Skeist derived the equation:

$$\ln \frac{[M]}{[M]_0} = \int_{f_{1,0}}^{f_1} \left[\frac{1}{F_1 - f_1} \right] df_1 \quad (2.16)$$

where $f_{1,0}$ is the mole fraction of monomer 1 in feed at time $t = 0$ and f_1 is the mole fraction of monomer 1 at any time during the reaction.

Fractional conversion is:

$$X = 1 - \frac{[M]}{[M]_0} \quad (2.17)$$

Graphical or numerical methods are needed to calculate the change in monomer mixture and copolymer composition.

Substitution of equation 2.15 into equation 2.16 and further rearranging, yields:

$$\ln \frac{[M]}{[M]_0} = \frac{1}{(2-r_1-r_2)} \int_{f_{1,0}}^{f_1} \frac{(r_1+r_2-2)f_1^2 + 2(1-r_2)f_1 + r_2}{f_1(f_1-1) \left(f_1 - \left(\frac{1-r_2}{2-r_1-r_2} \right) \right)} df_1 \quad (2.18)$$

Equation 2.18 can be re-written as:

$$- \int_{f_{1,0}}^{f_1} \frac{f_1}{(f_1-1)(f_1-\delta)} df_1 = \left[\left(\frac{f_1-1}{f_{1,0}-1} \right)^{\frac{(2-r_1-r_2)}{(r_1-1)}} \left(\frac{f_1-\delta}{f_{1,0}-\delta} \right)^{\frac{(r_2-1)}{(r_1-1)}} \right] \quad (2.19)$$

Integration of equation 2.19 yields the Meyer-Lowry equation:

$$\frac{[M]}{[M]_0} = \left(\frac{f_1}{f_{1,0}} \right)^\alpha \left(\frac{f_2}{f_{2,0}} \right)^\beta \left(\frac{f_{1,0}-\delta}{f_1-\delta} \right)^\gamma \quad (2.20)$$

with:

$$\alpha = \frac{r_2}{1-r_2}$$

$$\beta = \frac{r_1}{1-r_1}$$

$$\delta = \frac{1-r_1r_2}{(1-r_1)(1-r_2)} \text{ and}$$

$$\gamma = \frac{1-r_2}{2-r_1-r_2}$$

2.6.8 Estimation of reactivity ratios

The elucidation of copolymer structure (composition and monomer sequence distribution) and kinetics are the major concern for the prediction of copolymer properties, and the correlation between structure and properties. Among the various copolymerisation reactions, free radical copolymerisation is the most important since it does not demand rigorous experimental conditions, and can be applied to a large variety of monomers, leading to the formation of new materials^[49].

In systems about which little is known, the most sensible approach in the estimation of reactivity ratios is to use a pair of initial feed compositions that are far apart^[50]. Traditionally the reactivity ratio of a monomer pair was determined by preparation and isolation of a series of copolymers at low conversion, with molar composition ranging from 0 to 1. After the collection of the feed and copolymer molar fraction data, linear and non-linear methods are used to determine the most reliable reactivity ratios^[35, 51-53]. With new monomers that are either available in small quantities or are unstable, it is necessary to convert the monomers to high conversion. The number of possible experiments under these conditions is limited, hence the need to allow the reaction to go to high conversion, such that the copolymers can be isolated, purified and analysed^[54].

However, there are some problems and errors involved in these methods. The obtained copolymer is not the instantaneously formed copolymer corresponding to the initial feed composition, but an average copolymer formed during the entire

polymerisation history until the reaction was terminated. The isolation of the polymer may also lead to the presence of residual monomers or solvents^[55].

Spectroscopic methods such as ¹H NMR and Raman spectroscopy have been used successfully to study the kinetics of copolymerisation *in situ*. These methods have the advantages of being non-invasive, and measuring the instantaneous feed and copolymer composition is possible. This can be achieved by monitoring the continuous change in the intensity of resonance signals assigned unambiguously to the double bonds of the participating monomers^[55-57].

The various methods for the experimental determination of reactivity ratios after the collection of the feed and copolymer data proceeds with the use of the methods explained below^[52, 53]:

2.6.8.1 Approximation method

This method depends on the fact that the copolymer composition is almost completely dependent on r_1 at very low concentrations of monomer M_2 ^[52]. Under these conditions, the following relation holds:

$$r_1 = \frac{f_2}{F_2}$$

r_2 can also be determined by using a very low concentration of M_1 where this relation also holds:

$$r_2 = \frac{f_1}{F_1}$$

In order to determine the amount of monomer in copolymer, F_x , extremely sensitive analytical procedures are required. When $r_x < 1$ or $r_x > 10$, the estimated r_x values suffer from bias. The method also assumes that the copolymerisation equation is applicable and does not confirm or disprove that assumption.

2.6.8.2 Linearisation method

The Mayo-Lewis^[35] equation was rearranged by Fineman and Ross^[59] to give:

$$\frac{f_1(F_2 - F_1)}{f_2 F_1} = \left(-\frac{F_2 f_1^2}{F_1 f_2^2} \right) r_1 + r_2$$

A plot of $\frac{f_1(F_2 - F_1)}{f_2 F_1}$ versus $\left(-\frac{F_2 f_1^2}{F_1 f_2^2} \right)$ gives a straight line with slope r_1 and intercept r_2 .

2.6.8.3 Intersection method

The copolymerisation equation was rearranged by Mayo and Lewis^[35] to:

$$r_1 = r_2 \left(\frac{F_1 f_2}{F_2 f_1^2} \right) + \left(\frac{f_2}{f_1} \right) \left(\frac{F_1}{F_2} - 1 \right)$$

Assigning arbitrary values to r_2 , the equation can be solved for r_1 . The obtained r_1 and r_2 values can be plotted to give lines with slope $\left(\frac{F_1 f_2}{F_2 f_1^2} \right)$ and intercept $\left(\frac{f_2}{f_1} \right) \left(\frac{F_1}{F_2} - 1 \right)$.

The point where these lines intersect gives the most probable r_1 and r_2 values.

2.6.8.4 Curve-fitting method

The method consists of drawing a graph of the experimental F_1 versus f_1 and drawing a curve that fits equation:

$$F_1 = \frac{r_1 f_1^2 + f_1 f_2}{r_1 f_1^2 + 2 f_1 f_2 + r_2 f_2^2}$$

for various values of r_1 and r_2 . Different combinations of r_1 and r_2 are tried until a fit close to the observed curve is obtained. This method is tedious but has the following advantages, it provides:

- the experimenter a visual check on the validity of the model as the data used is generally over a wide range of monomer compositions
- a qualitative measure of the experimental error even in the absence of repetitive runs and
- in some cases a qualitative measure on how well the reactivity ratios are estimated.

One draw-back for this method is that the closeness of the theoretical curve to the experimental curve is determined by the eye of the experimenter. The non-linear least squares method is an improvement on this method and uses the sum of the squares of the deviations between theoretical and experimental values to test reliability of result.

2.6.8.5 Non-linear least-squares method

Tidwell and Mortimer^[52] modified the curve fitting method so that the values of r_1 and r_2 satisfy the condition that, for a selected pair of r_1 and r_2 the sum of squares of the differences between the observed and theoretical values is minimised. The acceptance of the r_1 and r_2 values here does not depend on the discretion of the experimenter but different people can reach the same solution provided they use the same data and manipulation process.

2.6.9 Types of copolymerisation behaviour

The values of the reactivity ratios determine the type of copolymerisation observed. The various possible combinations of r_1 and r_2 are listed below and their effect on the copolymerisation behaviour is also discussed.

$$2.6.9.1 \quad r_1 = r_2 = 0; (k_{11} \ll k_{12} \text{ and } k_{22} \ll k_{12})$$

In this case the propagating species shows a strong preference for the monomer that is not at its propagating end. In other words cross-propagation is preferred by both propagating species leading to an alternating copolymer structure. The Mayo-Lewis equation, equation 2.8 gets reduced to:

$$\frac{d[M_1]}{d[M_2]} = 1 \text{ and equation 2.7 becomes } F_1 = F_2 = 0.5 .$$

$$2.6.9.2 \quad r_1 = r_2 = 1, (k_{11} = k_{12} \text{ and } k_{22} = k_{12})$$

In this case both monomers show similar reactivity towards the propagating species. The copolymer composition is similar to that of the monomers in the feed and the monomer sequence distribution in the chain would be random. Equation 2.5 and 2.8 reduce to:

$$\frac{d[M_1]}{d[M_2]} = \frac{[M_1]}{[M_2]} \text{ and } F_1 = f_1 \text{ respectively.}$$

$$2.6.9.3 \quad r_1 > 1, r_2 < 1$$

Both propagating species show a preference for addition of one monomer type, M_1 in this case. The converse is true when $r_2 > 1$ and $r_1 < 1$. The copolymer will contain a large percentage of the more reactive monomer in random placement along the chain at low conversions.

$$2.6.9.4 \quad r_1 < 1, r_2 < 1$$

Each propagating species prefers cross-propagation to homo-propagation. The preference towards alternation becomes stronger as both r_1 and r_2 tend towards zero.

At the point where the F_1 vs f_1 curve crosses the line where $F_1 = f_1$, the copolymer formed has the same composition as the feed. Copolymerisation at this point occurs without a change in the feed composition. This copolymerisation is known as azeotropic copolymerisation.

2.6.9.5 $r_1 > 1, r_2 > 1$

Both types of propagating species prefer to homo-propagate resulting in either a tendency toward independent or concurrent homopolymerisation. This gives a structure with blocky sequences of either monomer along the polymer chain.

These types of polymerisation behaviour are illustrated in Figure 2.8.

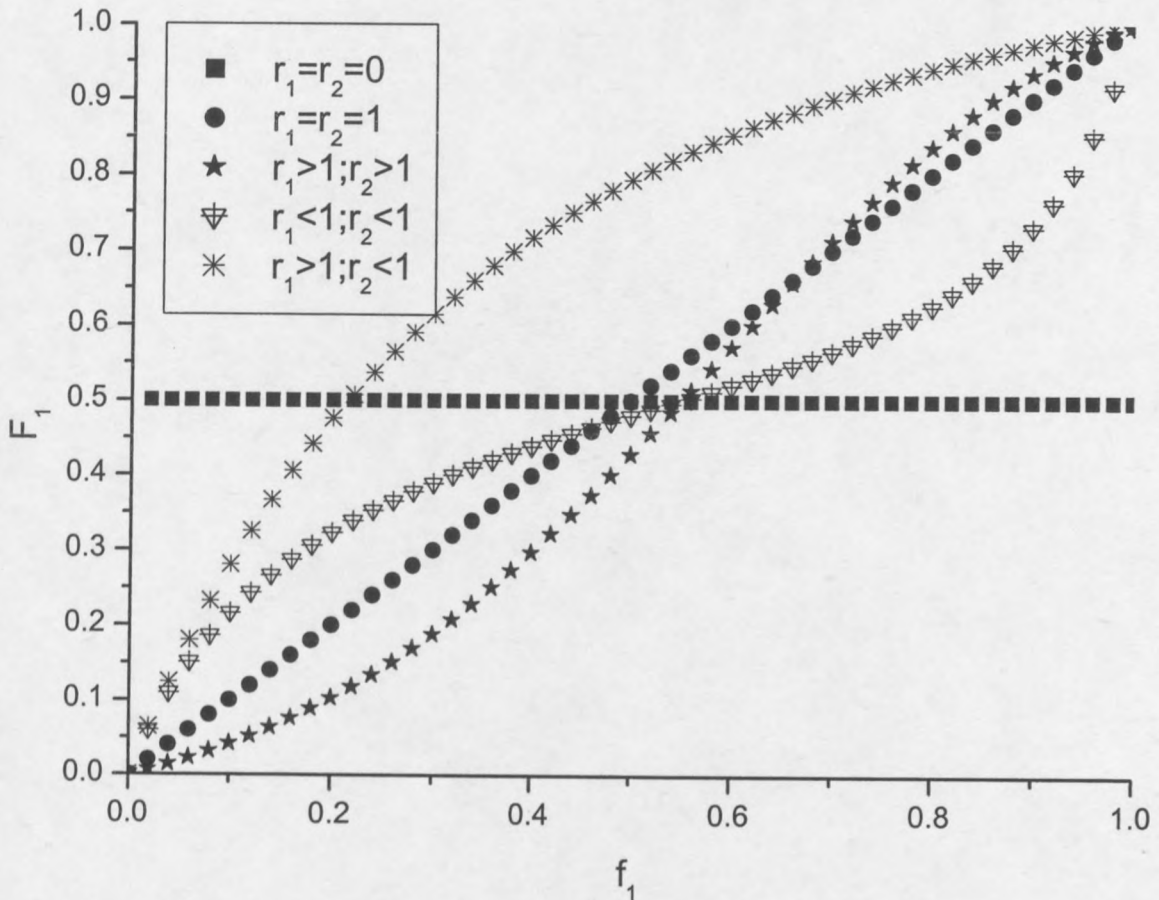


Figure 2.8: A graphical presentation of the dependence of the types of copolymerisations on reactivity ratios.

2.7 Acrylate copolymers

The combination of durability and versatility, and the ability to tailor molecules relatively easily to specific applications have made acrylic polymers prime candidates for numerous applications^[60]. Acrylate homopolymers and their copolymers are used in various fields, such as thin films, fibres, filaments, coatings, lithography, lacquers, adhesives, printing inks and binders^[61-64].

Polyacrylates are considerably different to polymethacrylates; the former are much softer as they lack the methyl groups on alternate carbon atoms on the polymer backbone chain that make the polymethacrylates more rigid. Polymethacrylates tend to be used as shaped objects, while polyacrylates find applications in areas that require flexibility and extensibility. Polymer products for non-rigid applications are

produced by solution and emulsion polymerisations. These find applications in coatings (interior, exterior and automotive paints), textiles (finishes for improving abrasion resistance, binding pigments, reducing shrinkage of wool, drapery and carpet backing), additives for engine oils, fluids, and sealants^[33].

2.8 References

1. Dry, M. E., *Catalysis Today*, 2002. **71**: p. 227 - 241.
2. Behr, A., *Ullman's Encyclopedia of Industrial Chemistry*. 5th ed, ed. Elvers, B., Hawkins, S., Ravenscroft, M., Schulz, G. Vol. A13, 1989, Weinheim: VCH Verlagsgesellschaft mbH, p. 238.
3. Lutz, E. F., *J. Chem. Educ.*, 1986. **63**(3): p. 202 - 203.
4. Skupinska, J., *Chem. Rev.*, 1991. **91**(4): p. 613 - 648.
5. Schulz, H., *Appl. Catal. A*, 1999. **186**: p. 3 - 12.
6. Reuben, B. and Wittcoff, H., *J. Chem. Educ.*, 1988. **65**: p. 605 - 607.
7. Yanjarappa, M. J. and Sivaram, S., *Prog. Polym. Sci.*, 2002. **27**: p. 1347 - 1398.
8. Brintzinger, H. H., Fischer, D., Mulhaupt, R., Rieger, B., and Waymouth, R. M., *Angew. Chem. Internat. Edit. Engl.*, 1995. **34**: p. 1143 - 1170.
9. Kolthammer, B. W. S., Mangold, D. J., and Gifford, D. R., *J. Polym. Sci. Part A: Polym. Chem.*, 1992. **30**: p. 1017 - 1026.
10. Christoffers, J. and Bergman, R. G., *J. Am. Chem. Soc.*, 1996. **118**: p. 4715 - 4716.
11. Wahner, U. M., Brull, R., Pasch, H., Raubenheimer, H. G., and Sanderson, R. D., *Angew. Makromol. Chem.*, 1999. **270**: p. 49 - 55.
12. Resconi, L., Piemontesi, F., Franciscono, G., Abis, L., and Fiorani, T., *J. Am. Chem. Soc.*, 1992. **114**: p. 1025 - 1032.
13. Hungenberg, K.-D., Kerth, J., Langhauser, F., Muller, H.-J., and Muller, P., *Angew. Makromol. Chem.*, 1995. **227**: p. 159 - 177.
14. Christoffers, J. and Bergman, R. G., *Inorg. Chim. Acta*, 1998. **270**: p. 20 - 27.
15. Nelson, D. J., Cooper, P. J., and Coerver, J. M., *Tetrahedron Letters*, 1987. **28**(9): p. 943 - 944.

16. Brown, H. C. and Subba, R., *J. Am. Chem. Soc.*, 1956. **78**: p. 5694 - 5695.
17. Brown, H. C. and Subba, R., *J. Org. Chem.*, 1957. **22**: p. 1136 - 1137.
18. Brown, H. C. and Subba, R., *J. Am. Chem. Soc.*, 1959. **81**: p. 6423 - 6437.
19. Brown, H. C. and Zweifel, G., *J. Am. Chem. Soc.*, 1961. **83**: p. 3834 - 3840.
20. Beyer, H. and Walter, W., *Handbook of Organic Chemistry*. 1996, London: Prentice Hall. p. 181.
21. Fukuzumi, S. and Kochi, J. K., *J. Am. Chem. Soc.*, 1981. **103**: p. 2783 - 2791.
22. Brown, H. C. and Geoghegan, P. J., *J. Am. Chem. Soc.*, 1967. **89**: p. 1522 - 1524.
23. McMurry, J., *Organic Chemistry*. 3rd ed. 1992, California: Brooks/Cole Publishing Company. p. 223.
24. Brown, H. C. and Geoghegan, P. J., *J. Org. Chem.*, 1970. **35**(6): p. 1844 - 1850.
25. Smith, M. B. and March, J., *March's Advanced Organic Chemistry - Reactions, Mechanisms and Structure*. 5th ed. 2001, New York: John Wiley and Sons, Inc. p. 484.
26. Balasubramanian, S. and Reddy, B. S. R., *Eur. Polym. J.*, 1996. **32**(9): p. 1073 - 1077.
27. Finkelmann, H. and Schafheutle, M. A., *Colloid and Polymer Science*, 1986. **264**: p. 786 - 790.
28. Subramanian, K., Nanjundan, S., and Reddy, A. V. R., *Eur. Polym. J.*, 2001. **37**(4): p. 691 - 698.
29. Thamizharasi, S., Srinivas, G., Sulochana, N., and Reddy, B. S. R., *J. Appl. Polym. Sci.*, 1999. **73**: p. 1153 - 1160.
30. Vijayaraghavan, P. G. and Reddy, B. S. R., *J. Appl. Polym. Sci.*, 1996. **61**: p. 935 - 943.
31. Acar, H. Y., Jensen, J. J., Thigpen, K., McGowen, J. A., and Mathias, L. J., *Macromolecules*, 2000. **33**: p. 3855 - 5859.
32. Tirell, D. A., *Encyclopaedia of Polymer Science and Engineering*. 2nd ed, ed. N.M.B. H. Mark, C. G. Overberger, G. Menges. Vol. 4. 1985, New York: John Wiley and Sons. p. 192.
33. Odian, G., *Principles of Polymerization*. 3rd ed. 1991, New York: Wiley-Interscience.
34. Fukuda, T., Kubo, K., and Ma, Y.-D., *Prog. Polym. Sci.*, 1992. **17**: p. 875 - 916.

35. Mayo, F. R. and Lewis, F. M., *J. Am. Chem. Soc.*, 1944. **66**: p. 1594 - 1601.
36. Wall, F. T., *J. Am. Chem. Soc.*, 1941. **63**: p. 1862 - 1866.
37. Merz, E., Alfrey, T., and Goldfinger, G., *J. Polym. Sci.*, 1946. **1**: p. 75.
38. Fukuda, T., Ma, Y.-D., and Inagaki, H., *Macromolecules*, 1985. **18**: p. 17 - 26.
39. Coote, M. L. and Davis, T. P., *Prog. Polym. Sci.*, 1999. **24**: p. 1217 - 1251.
40. Fukuda, T., Ma, Y.-D., and Inagaki, H., *Makromol. Chem., Rapid Commun.*, 1987. **8**: p. 495.
41. Seiner, J. A. and Litt, M., *Macromolecules*, 1971. **4**(3): p. 308 - 311.
42. Litt, M., *Macromolecules*, 1971. **4**(3): p. 312 - 313.
43. Litt, M. and Seiner, J. A., *Macromolecules*, 1971. **4**(3): p. 314 - 316.
44. Litt, M. and Seiner, J. A., *Macromolecules*, 1971. **4**(3): p. 316 - 318.
45. Cais, R. E., Farmer, R. G., Hill, D. T. J., and O'Donnell, J. H., *Macromolecules*, 1979. **12**(5): p. 835 - 839.
46. Hill, D. T. J., O'Donnell, J. H., and O'Sullivan, P. W., *Macromolecules*, 1983. **16**: p. 1295 - 1300.
47. Skeist, I., *J. Am. Chem. Soc.*, 1946. **68**: p. 1781 - 1784.
48. Meyer, V. E. and Lowry, G. G., *J. Polym. Sci. Part A: Polym. Chem.*, 1965. **3**: p. 2843 - 2851.
49. Stergiou, G., Dousikos, P., and Pitsikalis, M., *Eur. Polym. J.*, 2002. **38**: p. 1963 - 1970.
50. Plaumann, H. P. and Branston, R. E., *J. Polym. Sci. Part A: Polym. Chem.*, 1989. **27**: p. 2819 - 2822.
51. Wall, F. T., *J. Am. Chem. Soc.*, 1944. **66**: p. 2050 - 2057.
52. Tidwell, P. W. and Mortimer, G. A., *J. Polym. Sci. Part A: Polym. Chem.*, 1965. **3**: p. 369 - 387.
53. Dube, M. A., Sanayei, R. A., Penlidis, A., O'Driscoll, K. F., and Reill, P. M., *J. Polym. Sci. Part A: Polym. Chem.*, 1991. **29**: p. 703 - 708.
54. Czerwinski, W. K., *Polymer*, 1998. **39**(1): p. 183 - 187.
55. Aguilar, M. R., Gallardo, A., del Mar Fernandez, M., and Roman, J. S., *Macromolecules*, 2002. **35**(6): p. 2036 - 2041.
56. Ito, H., Dalby, C., Pomerantz, A., Sherwood, M., Sata, R., Sooriyakumaran, R., Guy, K., and Breyta, G., *Macromolecules*, 2000. **33**: p. 5080 - 5089.
57. Ito, H., Miller, D., Sveum, N., and Sherwood, M., *J. Polym. Sci. Part A: Polym. Chem.*, 2000. **38**: p. 3521 - 3542.

58. Fineman, M. and Ross, S., *J. Polym. Sci. Part A: Polym. Chem.*, 1950. **5**: p. 259.
59. Reghunandan, N. C. P., Chaumont, P., and Charmot, D., *Polymer*, 1999. **40**: p. 2111.
60. Balasubramanian, S. and Reddy, B. S. R., *J. Polym. Mater.*, 1995. **12**: p. 55.
61. Lungu, A. and Neckers, D. C., *J. Coating Technology*, 1995. **67**: p. 29.
62. Brar, A. S. and Malhotra, M., *Macromolecules*, 1996. **29**: p. 7470 - 7476.
63. Omidian, H., Hasheni, S. A., Saymes, P. G., and Meldrum, I., *Polymer*, 1999. **40**: p. 1753 - 1761.

CHAPTER 3

SYNTHESIS AND HOMOPOLYMERISATION OF THE OLEFIN-MODIFIED ACRYLIC MONOMER, 1-METHYL-1-PROPYL-HEXYL ACRYLATE

3.1 Introduction

In this investigation, the inexpensive monomer, 1-pentene, a by-product of the Fischer-Tropsch process, was converted into a polymerisable acrylate. The properties of the monomer, polymer, and the kinetics of the homopolymerisation process were investigated.

3.2 Experimental

This section describes the reagents used in the preparation of the monomer, 1-methyl-1-propyl-hexyl acrylate, and the analytical techniques used to characterise the intermediate products and the subsequently formed polymers.

3.2.1 Reagents used

1-Pentene (Aldrich, 95%) was dried over lithium aluminium hydride (LiAlH_4), distilled and stored under nitrogen over 4 Å molecular sieves. The co-catalyst, methylaluminoxane (MAO, Aldrich, 10% in toluene) and the catalyst, bis-cyclopentadiene zirconocene dichloride (Cp_2ZrCl_2 , Labchem, 98%), were used as received and handled under nitrogen in a glove box. Mercuric acetate ($\text{Hg}(\text{OAc})_2$, Merck, 96%), sodium borohydride (NaBH_4 , Merck) and tetrahydrofuran (THF, Saarchem, AR grade) were used as received. Toluene (Saarchem, AR grade) was dried by boiling under reflux over sodium metal flakes. Benzophenone was used to

indicate complete drying. The dry toluene was collected and stored under nitrogen over 4 Å molecular sieves. Diethyl ether (Labchem, CP grade), acryloyl chloride (Labchem, 98%) and triethylamine (Labchem, 99%) were all used as received. Deuterated toluene (Sigma-Aldrich) was used for the *in situ* NMR experiments. Methyl methacrylate (MMA, ICI Chemicals and Polymers, 99.9%) was purified by distillation under reduced pressure. Azobis(isobutyronitrile) (AIBN, Delta Scientific, 98%), the initiator, was dissolved in chloroform and recrystallised from methanol.

3.2.2 Analyses

A Varian VXR 300 dual channel broadband pulse Fourier transform NMR spectrometer was used to obtain ^1H (300 MHz) and ^{13}C (75 MHz) NMR spectra of the products. The NMR samples were dissolved in deuterated chloroform (CDCl_3), and spectra run at room temperature (25 °C).

A Perkin-Elmer Fourier transform infrared spectrophotometer (FTIR) was used to confirm the functional groups of the synthesised compounds. A drop of sample dissolved in THF was placed on a NaCl disc. The sample on the disc was dried to evaporate the THF. The dry sample was then inserted in the beam path of the spectrophotometer and 40 scans were obtained for each sample. A background scan of THF dried on a NaCl disc was subtracted from the result.

Gel permeation chromatographic (GPC) analysis of the polymers was performed on a system comprising a Waters 610 Fluid Unit, Waters 410 Differential Refractometer at 30 °C, a Waters 717_{plus} Autosampler and Waters 600E System Controller. Two PLgel 5 µm Mixed-C columns and a pre-column (PLgel 5 µm Guard) were used and the column oven was set at 30 °C. Data acquisition and analysis was done using the Millennium³² software. THF was used as the solvent at a flow rate of 1.0 mL/min. The samples were prepared by dissolving 5 mg of the polymer samples in 1 mL of HPLC-grade THF filtered through a 0.45 µm nylon filter. The volume of the injected samples was 100 µL. The system was calibrated with six narrow polystyrene standards ranging from 800 to 2×10^6 g/mol.

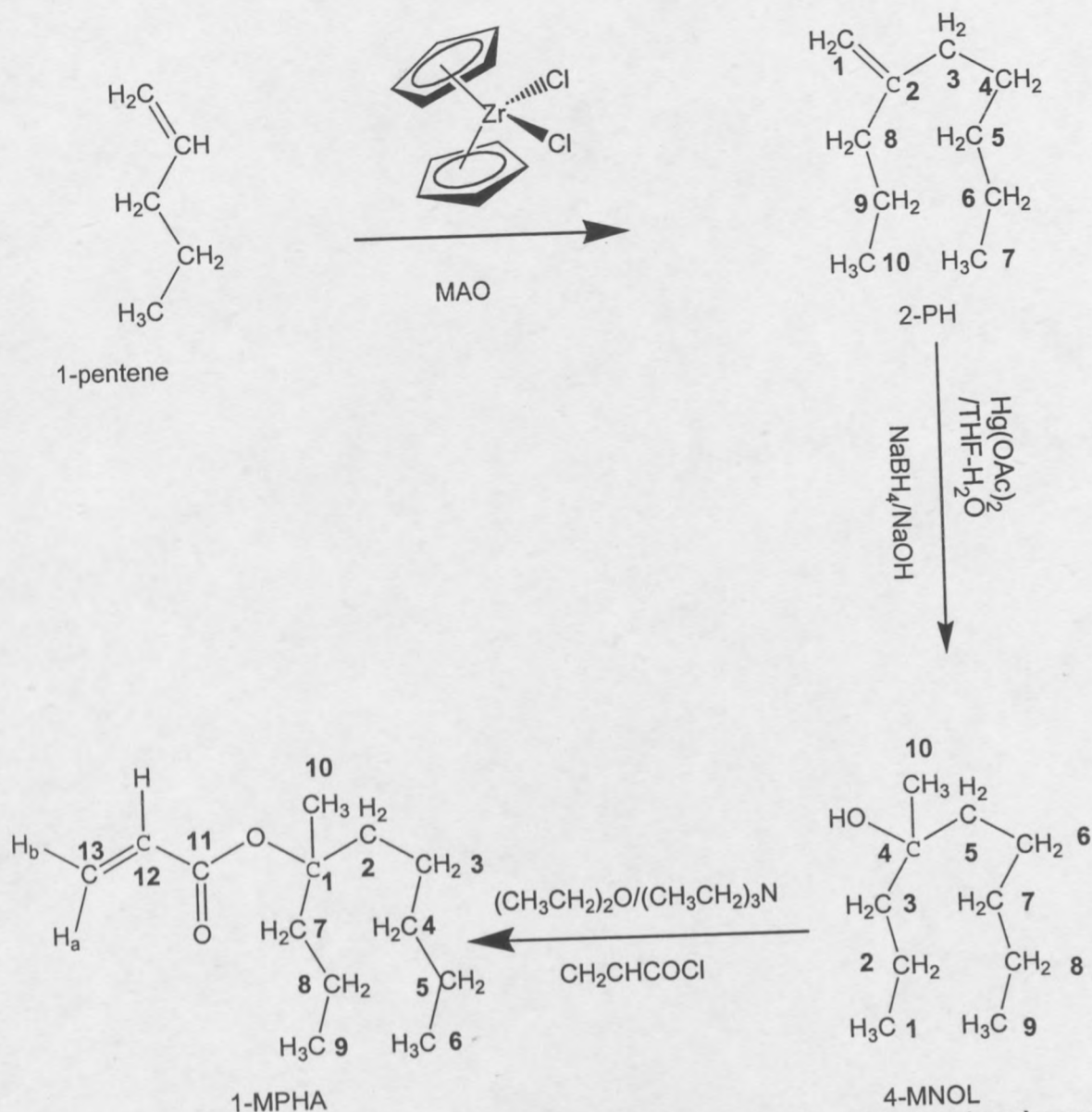
The *in situ* ^1H NMR kinetic studies were run on a Varian INOVA 600 dual fullband pulse NMR spectrometer at 70 °C and 600 MHz. The samples were prepared by weighing the monomer directly into an NMR tube. After adding AIBN dissolved in deuterated toluene to the NMR tube, nitrogen was bubbled through the sample for 2 minutes. The tube was closed with an NMR tube cap and inserted into the NMR apparatus. The sample temperature was raised to 70 °C. Scans were taken at 5-minute intervals. The data collected was processed using ACD Labs 7.0 ^1H NMR processor[®] integration software.

A Perkin-Elmer Thermogravimetric Analyser 7 was used to perform the thermogravimetric analyses. The samples were submitted in powder form. They were heated from room temperature to 900 °C at a rate of 10 °C/min.

A Perkin-Elmer Dynamic Mechanical Analyser was used to measure the mechanical responses of the samples when subjected to a heating programme at a frequency of 1 Hz. The samples were heated from -55 °C to 200 °C at a rate of 5 °C/min. The polymer samples used were pressed using a KBr disc mould and then annealed before running the temperature programme.

3.3 Synthesis of 1-methyl-1-propyl-hexyl acrylate

This section describes the 3-step synthetic pathway used, and the results obtained, in the process of converting 1-pentene to its dimer, 2-propyl-heptene (2-PH), to the corresponding alcohol 4-methyl-nonan-4-ol (4-MNOL), and finally to the ester, 1-methyl-1-propyl-hexyl acrylate (1-MPHA). See Scheme 3.1.



Scheme 3.1: Reaction scheme used for the preparation of 1-methyl-1-propyl-hexyl acrylate from 1-pentene.

3.3.1 Oligomerisation of 1-pentene

In the oligomerisation of 1-pentene, Bergman and co-workers^[1] used a 1:1 Al:Zr co-catalyst-to-catalyst ratio and obtained a product consisting of predominantly dimers. Wahner and co-workers^[2] used a 1000:1 Al:Zr ratio and obtained a range of products from dimers to tetramers. A ratio of 100:1 was used in this study, and the resulting product was predominantly dimeric. The ratio of 100:1 was chosen because it gave the intended results and it was more economical to use than the 1:1 ratio. A scheme

for the synthesis of low molar mass 1-pentene oligomers is shown in Scheme 3.1. The reaction was done in bulk, at room temperature, in a 2-L high-pressure steel reactor containing a glass reaction vessel. A typical feed consisted of 800 mL (7299.7 mmol) 1-pentene, 12.0 mL (24 mmol) MAO and 71.2 mg (0.24 mmol) Cp_2ZrCl_2 . After 8 hours the reaction was quenched with methanol and acidified with hydrochloric acid. The oligomers were purified by distilling the reaction mixture over a Vigreux column and collecting the dimeric product boiling at 119 °C at atmospheric pressure. The trimer and the tetramer were collected at a vacuum of about 2 mbar over a temperature range of 90 – 100 °C and 115 – 130 °C, respectively^[2].

Since toluene was not used as a solvent during the oligomerisation reactions, the pure dimer fraction was collected at 119 °C. When toluene was used as a solvent (boiling point at 110 °C) there was some contamination of the dimer fraction with the toluene. After all the dimer fraction had been collected, the temperature of the reaction mixture was lowered and the vacuum was maintained at 2 mbar. The collection of the trimer and tetramer fractions proceeded as stated above. The remaining fraction contained an insignificant amount of high waxy oligomers.

According to gas chromatography (GC) analysis a typical oligomer distribution of the product consisted of about 90% dimer, 7% trimer and 3% tetramer, see Figure A.1.

The structure of the dimer 2-propyl-heptene was confirmed by ^1H and ^{13}C NMR; see Figures A.2 – A.3 in Appendix A:

^1H NMR (CDCl_3 25 °C) (ppm): δ 0.85 (t, 3H, C7); 0.87 (t, 3H, C10); 1.22 (m, 6H, C4, C5, C6); 1.43 (m, 2H, C9); 1.93 (m, 4H, C3, C8); 4.69 (d, 2H, C1).

^{13}C NMR (CDCl_3 25 °C) (ppm): δ 13.65 (CH_3 , C7); 13.83 (CH_3 , C10); 20.74 (CH_2 , C9); 22.4 (CH_2 , C6); 27.4 (CH_2 , C4); 31.56 (CH_2 , C5); 35.9 (CH_2 , C3); 38.1 (CH_2 , C8); 108.6 ($=\text{CH}_2$, C1); 150.3 ($-\text{C}=\text{C}$, C2).

The subsequent reactions were based on 2-propyl-heptene, the dimer.

The ^1H and ^{13}C NMR spectra for the trimer oligomer of 1-pentene are shown in Figures E1 and E2 in Appendix E, respectively. The peaks are assigned to corresponding atoms unambiguously.

The ^1H and ^{13}C NMR spectra for the tetramer oligomer of 1-pentene are also shown in Figures F1 and F2 in Appendix F, respectively. The assignment of the carbon atoms was made challenging by peak overlap in the ^{13}C NMR spectrum.

3.3.2 Hydration of 2-propyl-heptene

The synthetic procedure followed in the hydration of 2-propyl-heptene was as reported by Brown and Geoghegan^[3]. A clean 3-necked flask fitted with a magnetic stirrer and a thermometer was charged with mercuric acetate $\text{Hg}(\text{OAc})_2$ (3.187g, 10 mmol), water (10 mL), tetrahydrofuran (THF, 10 mL) and 2-propyl-heptene (1.403 g, 10 mmol). After stirring for 2 minutes at room temperature the initial yellow colour of the reaction mixture changed to colourless. The reaction was allowed to run for a further 10 minutes before the addition of 3.0 mol/L sodium hydroxide (NaOH, 10 mL) and 0.5 mol/L sodium borohydride (NaBH_4 , 10 mL) in 3.0 mol/L NaOH. Addition of the NaBH_4 solution was done slowly to keep the temperature below 25 °C, since the reaction is highly exothermic. The reduction step is very fast and the reaction was completed as soon as the addition of the NaBH_4 solution was completed.

The mercury metal that formed during the reduction step was allowed to settle. NaCl was added to saturate the aqueous layer. The upper THF layer was separated, and from this layer the product 4-methyl-nonan-4-ol was obtained by removing the solvent on a rotary evaporator.

The Markovnikov addition of water to the double bond of 2-propyl-heptene leads to the formation of the tertiary alcohol 4-methyl-nonan-4-ol (4-MNOL). The general mechanism for oxymercuration/demercuration reaction is depicted in Figure 2.6.

The structure of 4-MNOL was confirmed by ^1H , ^{13}C NMR and IR spectroscopy; see Figures A.4 – A.6 in Appendix A:

^1H NMR (CDCl_3 25 °C) (ppm): δ 0.88 (t, 3H, C9); 0.91 (t, 3H, C1); 1.13 (s, 3H, C10); 1.31 (m, 8H, C2, C6, C7, C8,); 1.40 (m, 2H, C5); 1.42 (m, 2H, C3).

^{13}C NMR (CDCl_3 25 °C) (ppm): δ 13.7 (CH_3 , C9); 14.4 (CH_3 , C1); 16.8 (CH_2 , C2); 22.4 (CH_2 , C6); 23.3 (CH_2 , C8); 26.6 (CH_2 , C10); 32.2 (CH_2 , C7); 41.7 (CH_2 , C5); 44.0 (CH_2 , C3); 72.6 (C, C4).

IR (cm^{-1}): 3369 (-OH); 2936, 2863 (-CH).

The ^1H and ^{13}C NMR spectra for the hydration product of the trimer oligomer of 1-pentene are shown in Figures E3 and E4 with corresponding peak assignment. The FTIR spectrum of the alcohol is shown in Figure E5 in Appendix E.

The ^1H and ^{13}C NMR spectra for the hydration product of the tetramer oligomer of 1-pentene are shown in Figures F3 and F4. The peak assignment was made difficult by peak overlap.

3.3.3 Esterification of 4-methyl-nonan-4-ol

1-Methyl-1-propyl-hexyl acrylate (1-MPHA) was synthesised from the alcohol 4-MNOL by esterification with acryloyl chloride, as detailed in the work by Reddy and co-workers^[4]. 4-Methyl-nonan-4-ol (31.66 g, 0.2 mol) was dissolved in dry diethyl ether (100 mL), and added to triethylamine (31 mL, 0.22 mol) in a 3-neck 500 mL round-bottom flask. The mixture was stirred at 0 °C.

Acryloyl chloride (23 mL, 0.28 mol) was added dropwise from a dropping funnel, over a period of 1 hour. A white precipitate formed immediately, and a pale green colour developed with time. After all the acryloyl chloride was added, the reaction was allowed to run for a further hour at room temperature.

The crude reaction mixture was washed with water, and then with 1% sodium hydroxide solution to remove the unreacted acryloyl chloride. The product was dried over anhydrous sodium sulfate. After the sodium sulfate was removed by filtration, the ether was removed by evaporation. 1-Methyl-1-propyl-hexyl acrylate (1-MPHA) was purified by column chromatography (silica gel), using CH_2Cl_2 as the eluent.

The structure of 1-MPHA was confirmed by ^1H , ^{13}C NMR and IR spectroscopy; see Figures A.7 – A.9 in Appendix A:

$^1\text{H NMR}$ (CDCl_3 , 25 °C) (ppm): δ 6.28 (d, 1H, H13a); 6.0 (qua, 1H, H12); 5.7 (d, 1H, H13b); 1.85 (m, 2H, H2); 1.73 (m, 2H, H7); 1.43 (s, 3H, H10); 1.27 (m, 8H, H3, H4, H5, H8); 0.9 (t, 3H, H9); 0.87 (t, 3H, H6).

$^{13}\text{C NMR}$ (CDCl_3 , 25 °C) (ppm): δ 165.7, C11; 130.5, C13; 129.3, C12; 85.3, C1; 40.5, C7; 38.2, C2; 31.99, C4; 23.6, C10; 23.1, C5; 22.4, C3; 16.7, C8; 14.2, C9; 13.7, C6.

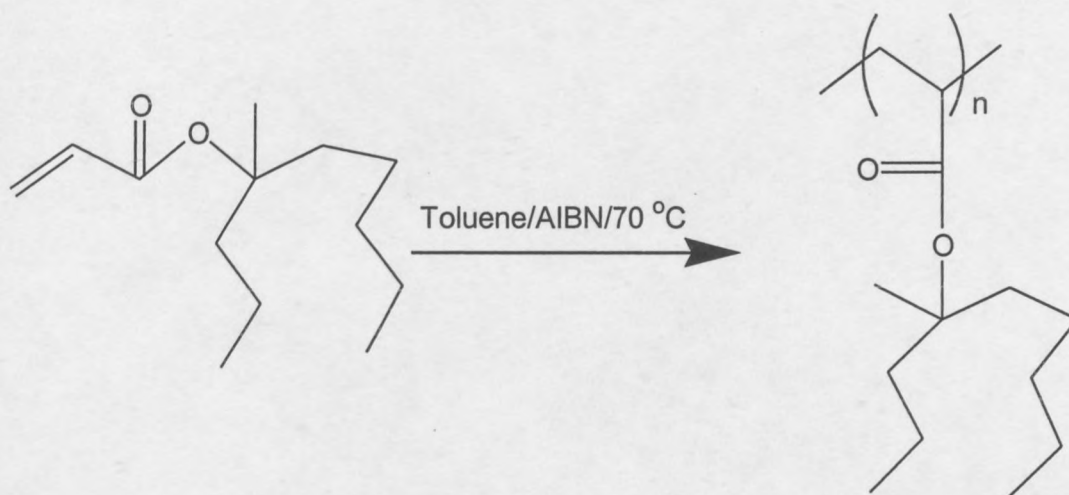
IR (cm^{-1}): 2956, 2863 (-CH); 1720 (-C=O stretching); 1619 (-C=C- stretching); 1401 (=CH₂ deformation); 1297 (=CH rock); 1203 (C-O asymmetric stretching); 1137; 1045 (=CH₂ rock); 988 (trans CH wag); 960 (=CH₂ wag); 810 (=CH₂ twist).

During the preliminary stages of the project dichloromethane was used as the reaction solvent for the esterification process. It was found that the use of dichloromethane made the purification process difficult as it is heavier than water, the water soluble impurities were not easily washed away. Also during the washing process, a strong colloidal phase is formed between the organic and aqueous phases which took a long time to break up. This led to premature polymerisation within the separating funnel when left at room temperature. The author found it necessary to leave the reaction mixture in a refrigerator overnight and separate the phases the following morning. Because of these challenges when dichloromethane is used as the solvent, the yields are very low and unpredictable.

Purification of the monomer by column chromatography is made difficult the lack of colour differentiation between the product and the impurities. This then requires the use of a lot of glassware to capture the eluent in small quantities which are later analysed to determine which ones contain the product. This process proved very tedious.

3.4 Homopolymerisation of 1-methyl-1-propyl-hexyl acrylate

The polymerisations of 1-MPHA were carried out in high-pressure Schlenk tubes. The solvent effect on the homopolymerisation was investigated by carrying out two reactions, one in toluene and the other in benzene as solvents over three days at 50 wt% monomer solution. 2 wt% AIBN was used as initiator and the reaction was conducted at 70°C. The reaction is depicted in Scheme 3.2.



Scheme 3.2: Scheme for the homopolymerisation of 1-MPHA with 2 wt% AIBN at 70 °C.

At the end of the three days, a sample was taken from each reaction for ^1H NMR analysis. The spectra of the reaction mixtures in the two solvents are shown in Figure 3.1. The spectrum of the benzene based reaction, Figure 3.1 (a), showed that much monomer still remained as indicated by the 1-MPHA double bond peaks between 5.6 to 6.4 ppm. The toluene based spectrum, Figure 3.1 (b), shows almost complete disappearance of the double bond peaks. Toluene was then chosen as the solvent in which all further reactions were carried out. The narrow peak at about 2.34 ppm in Figure 3.1 (b) is due to the toluene since the samples were submitted for the NMR analysis without precipitating and purifying them.

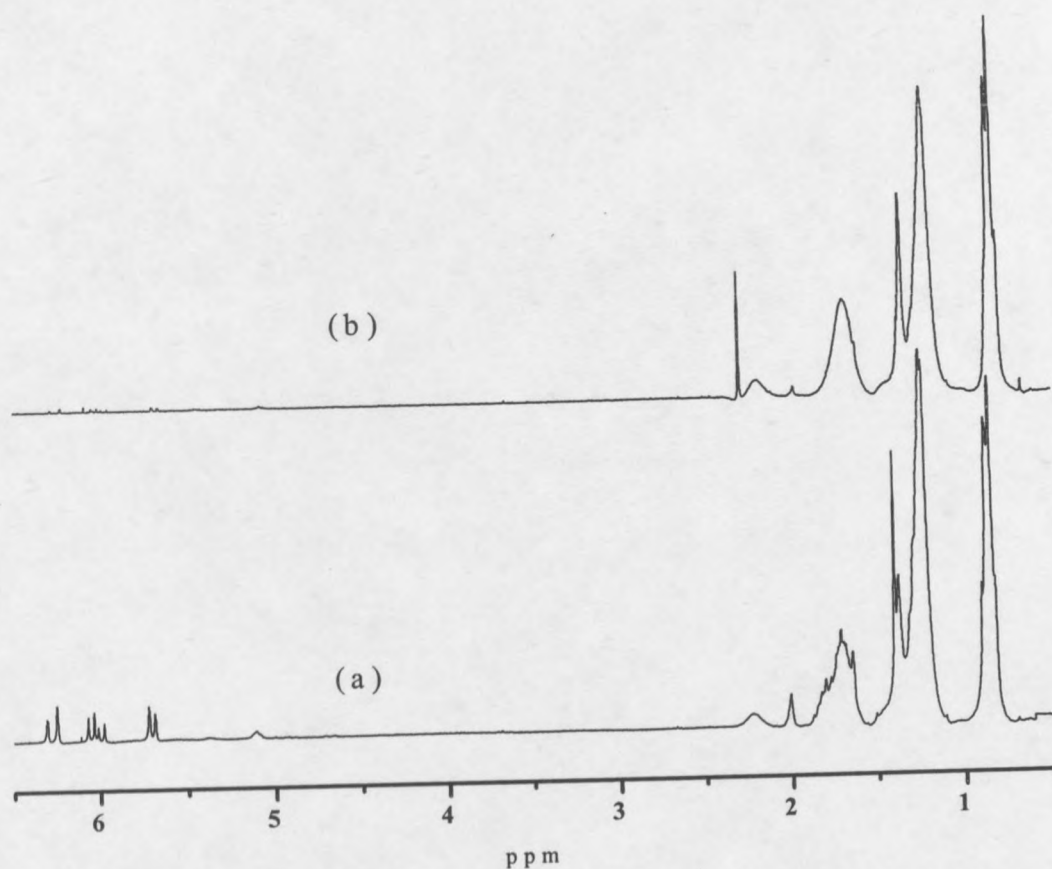


Figure 3.1: ^1H NMR spectra for the homopolymerisation of 1-MPHA in (a) benzene and (b) toluene, at 50 wt% solution, 2 wt% AIBN and 70 °C over three days.

Three monomer concentrations were investigated: in bulk, at 70 and at 50 wt% monomer in toluene. The initiator AIBN (2 wt% AIBN with respect to monomer) was used to initiate the reactions. The Schlenk tubes, containing the reaction mixtures, were subjected to three freeze-pump-thaw cycles to remove dissolved oxygen before immersion in an oil bath at 70 °C. The three respective reactions were allowed to run for 18 hours, and the products were recovered by pouring the contents of each reaction mixture into a 5-fold excess of methanol to precipitate the polymers. The polymers were removed by filtration and purified by dissolving in THF and reprecipitating in methanol. The polymer products were dried in a vacuum oven at 50 °C for 24 hours. Samples of the polymers were analysed by GPC, NMR, IR, TGA and DMA with results given in Sections 3.4 and 3.6.

Homopolymerisation in bulk was not carried out since the initiator was insoluble in the monomer. The yields for the homopolymerisation reactions were determined

gravimetrically. The yields and molecular weight data (with respect to polystyrene standards) for the polymerisations are summarised in Table 3.1. The polymer obtained with 70 wt% monomer solution in toluene was a high molecular weight polymer, with a wide polydispersity index (PDI). It is worth to note that the molar mass values obtained are relative to a polystyrene standards calibration and are not corrected. The polystyrene standards were used because they are readily available commercially and there are no standards for poly-(1-MPHA) as it is a novel polymer. The polymer obtained at 50 wt% monomer solution in toluene had a low weight average molar mass and a narrower polydispersity index than the former.

It should be noted that the light scattering GPC available in the Department which provides absolute molecular weights, was not used because it entailed a lot of work and for the purposes of this thesis there would have been no particular gain with this quantification.

Table 3.1: Molecular weight data for the products of homopolymerisation of 1-MPHA at various monomer concentrations

Sample	Yield (%)	\overline{M}_n	\overline{M}_w	PDI
Bulk	0	-	-	-
70 wt%	70	6100	342 300	-
50 wt%	78	6800	58 400	8.6

The ^1H NMR spectrum of the homopolymer of 1-MPHA in Figure 3.2 (b) shows a complete disappearance of the double bond peaks between 5.6 to 6.4 ppm (seen in Figure 3.2 (a)), and the emergence of a new polymer backbone peak at around 2.27 ppm, suggesting almost complete conversion of monomer to polymer. There is also a general broadening of the peaks and loss of multiplicity, indicating production of a high molecular weight polymer.

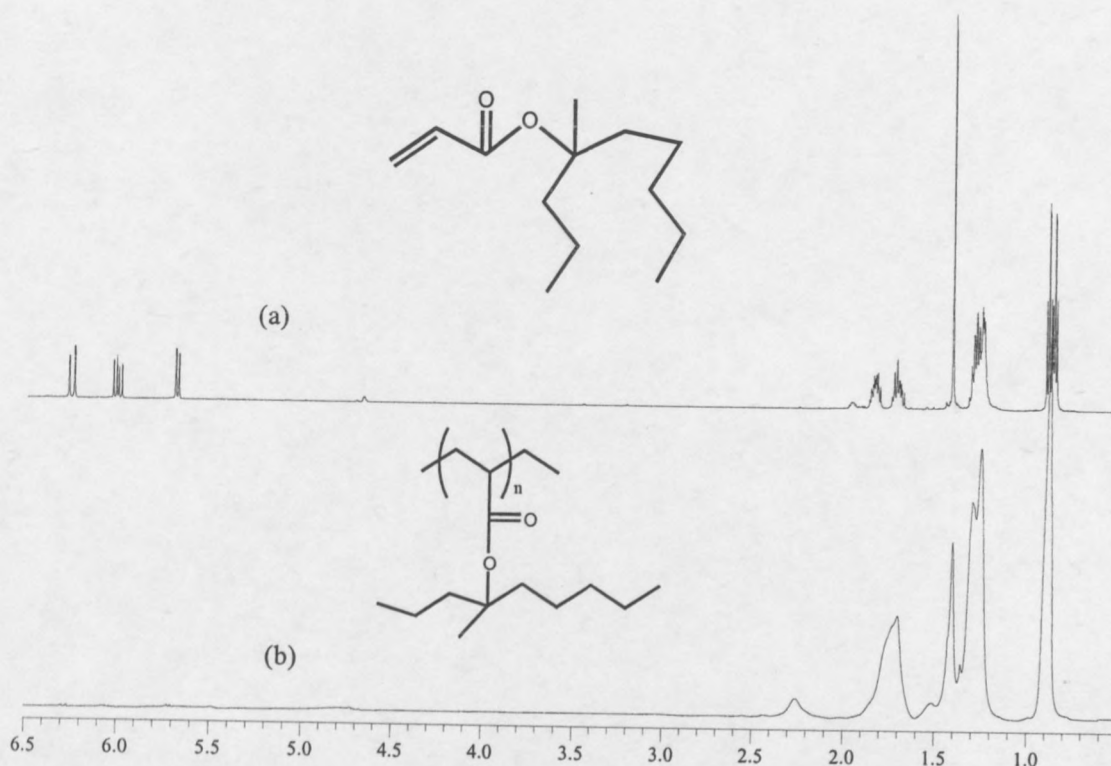


Figure 3.2: ^1H NMR spectra for (a) the monomer and (b) the homopolymer of 1-MPHA showing the disappearance of the double peaks between 5.6 to 6.4 ppm and the appearance of a new backbone peak at about 2.25 ppm in the homopolymer.

Figure 3.3 shows the FTIR spectrum of the 1-MPHA homopolymer. Complete disappearance of the carbon-carbon double bond peak of the 1-MPHA monomer at about 1619 cm^{-1} is observed.

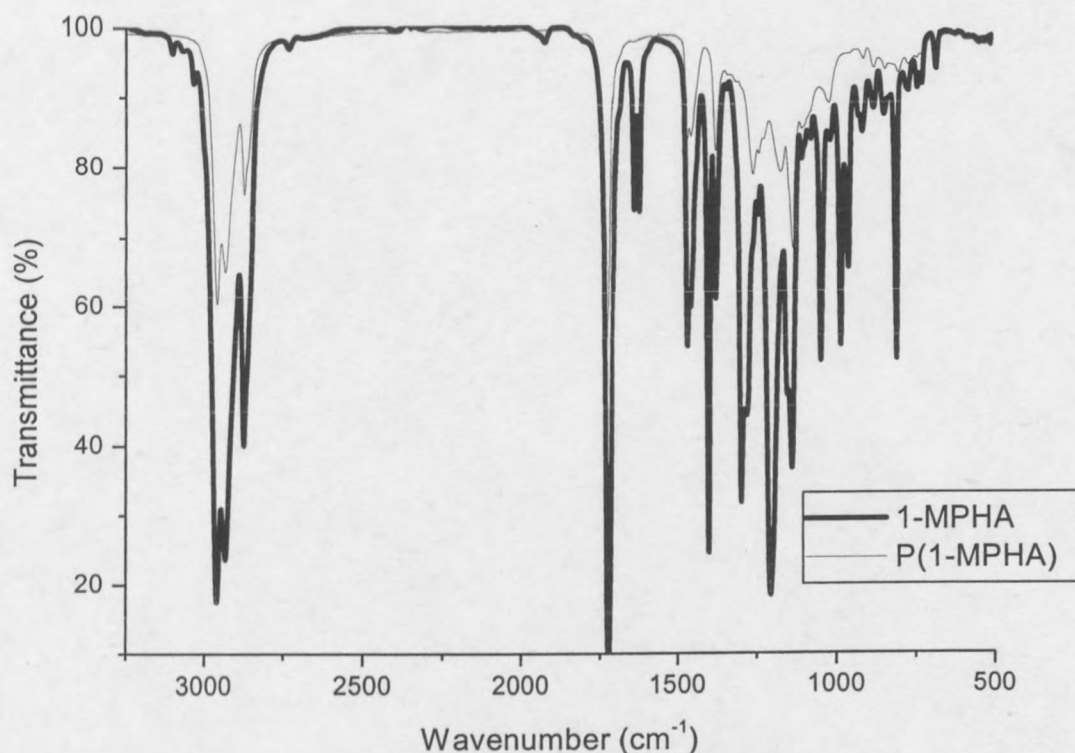


Figure 3.3: FTIR spectra of the 1-MPHA monomer (bold line) showing the disappearance of the homopolymer of 1-MPHA (normal line).

The data presented confirms that the 1-MPHA compound thus synthesised, is a monomer that is polymerisable by free radical means.

3.5 Kinetics of the homopolymerisation of 1-methyl-1-propyl-hexyl acrylate

The kinetics of the homopolymerisation reaction of 1-MPHA were studied as follows: a 50 wt% solution of the monomer 1-MPHA in toluene and 2 wt% AIBN (initiator) were mixed in a polymerisation vessel fitted with a rubber septum. The solution was heated to 70 °C, and samples were withdrawn throughout the reaction. ¹H NMR spectra of the samples were obtained by dissolving 60 mg of the reaction mixture in deuterated chloroform.

Figure 3.4 shows successive ¹H NMR spectra of the homopolymerisation reaction at different reaction times. The peaks that are of interest are the double bond peaks

between 5.6 and 6.4 ppm that are expected to disappear as the reaction progresses. Also, the peak at about 2.3 ppm, the polymer backbone peak due to proton H' in the generalised polymer chain $-\text{CH}_2-\text{CH}'\text{R}-$ should increase as the monomer is converted to the polymer. It was seen that a significant amount of polymerisation did not occur until after 16 hours, as shown by the appearance of the polymer backbone peak at about 2.3 ppm at 16 h. Such a long induction period is unusual, especially as the AIBN initiator concentration of 2 wt% was quite high. After the induction period, the rate of reaction increased significantly. The data from this experiment was used qualitatively as no internal standard was used, quantification would be unreliable.

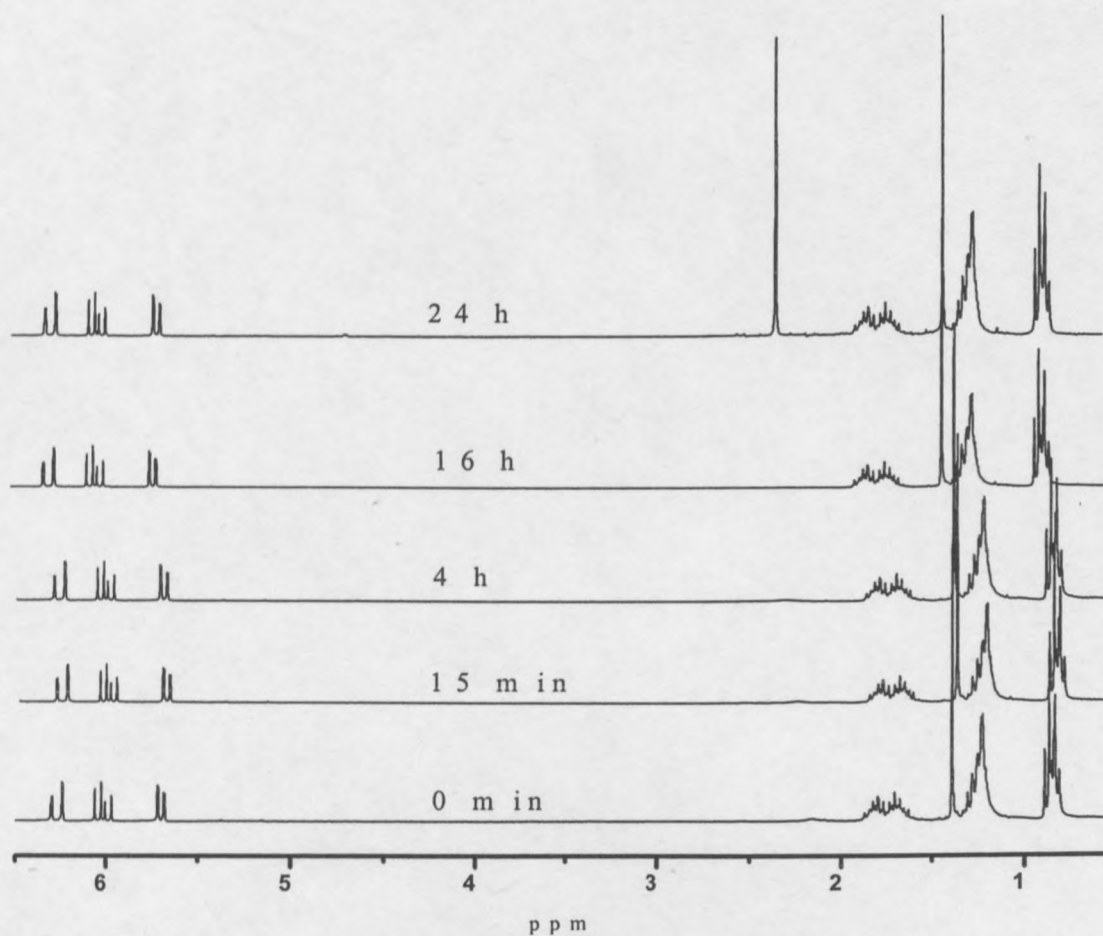


Figure 3.4: The homopolymerisation process of 1-MPHA showing ^1H NMR spectra drawn from the reaction mixture at the time intervals indicated. The reaction conditions were: 50 wt% monomer solution in toluene, 2 wt% AIBN and conducted at 70 °C.

Preliminary copolymerisation reactions with other monomers, including MMA, at the same reaction conditions as for the experiment whose results are presented in Figure

3.4, had previously given faster reactions with no noticeable inhibition (see Section 4.4.3). Thus, a small amount of MMA (1.5 and 5 wt%) was then added to 1-MPHA to investigate its effect on the length of the induction period and examine the reasons for this period. A possible reason for the long inhibition period during homopolymerisation of 1-MPHA is the formation of stable, non-propagating radicals. There could also be some radical impurities in the form of radical scavengers in the reaction mixture which preferentially attack the cyanoisopropyl radicals from AIBN. Reactive impurities rapidly consume reactive free radicals in a polymerisation system, thereby preventing radical growth (propagation)^[5].

Samples from the homopolymerisation of 1-MPHA with small amounts of MMA (1.5 and 5 wt% MMA), were analysed by ¹H NMR at various time intervals. Figure 3.5 shows the ¹H NMR spectra of the vinyl region of the homopolymerisation of 1-MPHA (5.7, 6.04 and 6.28 ppm) with 5 wt% MMA at various time intervals.

MMA was consumed rapidly, as indicated by the complete disappearance of the MMA double bond peaks after 8 hours. The 1-MPHA monomer in the "activated" reaction was consumed in significant amounts very early in the reaction whereas the pure 1-MPHA monomer reaction showed a prolonged induction period of up to 8 hours over the time intervals investigated. Almost 70 % conversion of 1-MPHA had occurred after 4 hours in the "activated" reaction. The use of 5 wt% MMA resulted in unobservable induction period. The MMA competes favourable for the cyanoisopropyl radicals and provides the 1-MPHA monomer with a base for further addition and propagation.

After 24 hours, almost complete conversion of 1-MPHA to polymer had taken place. Because only the double bonds of the 1-MPHA were monitored during the polymerisation, the conversion reported is only that of the 1-MPHA and not overall monomer conversion.

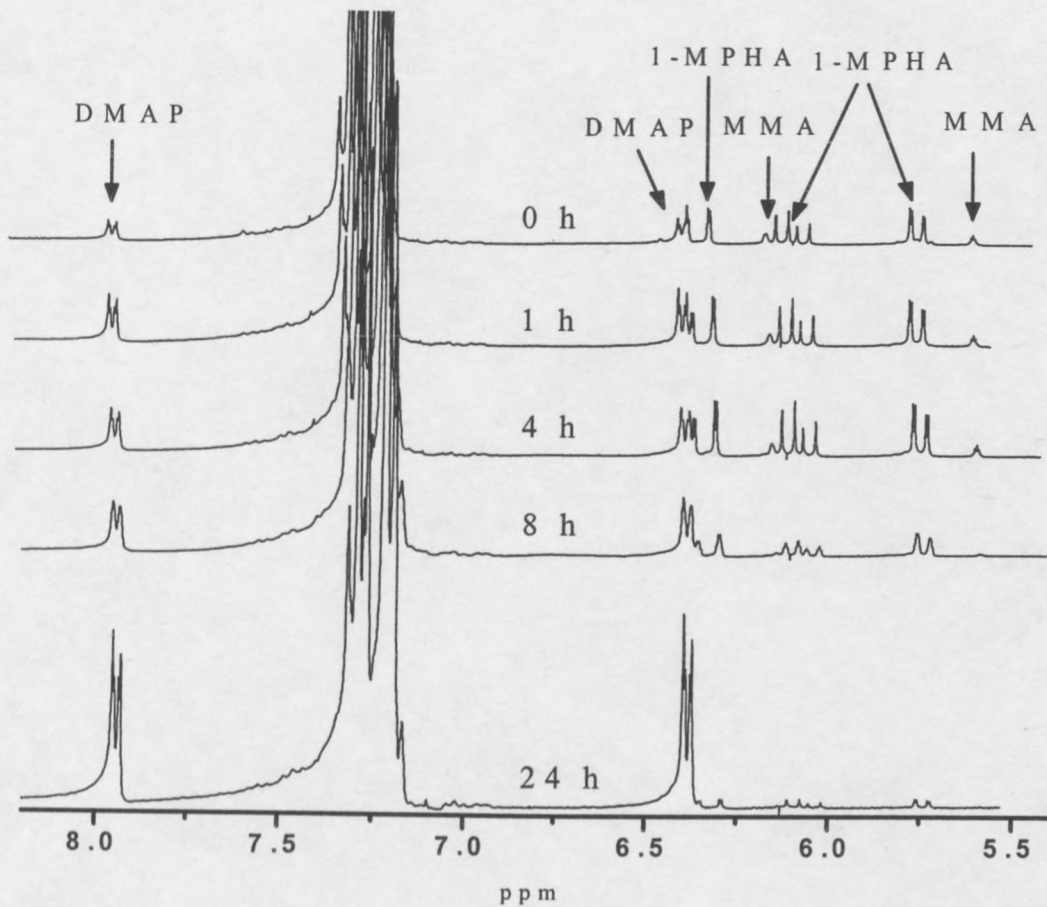


Figure 3.5: ¹H NMR spectra of the polymerisation of 1-MPHA with 5 wt% MMA at different reaction times, showing the vinyl peaks of the monomer and DMAP (the internal standard).

A graphical representation of the conversion against time is depicted in Figure 3.6. A comparison is made between homopolymerisation with and without MMA.

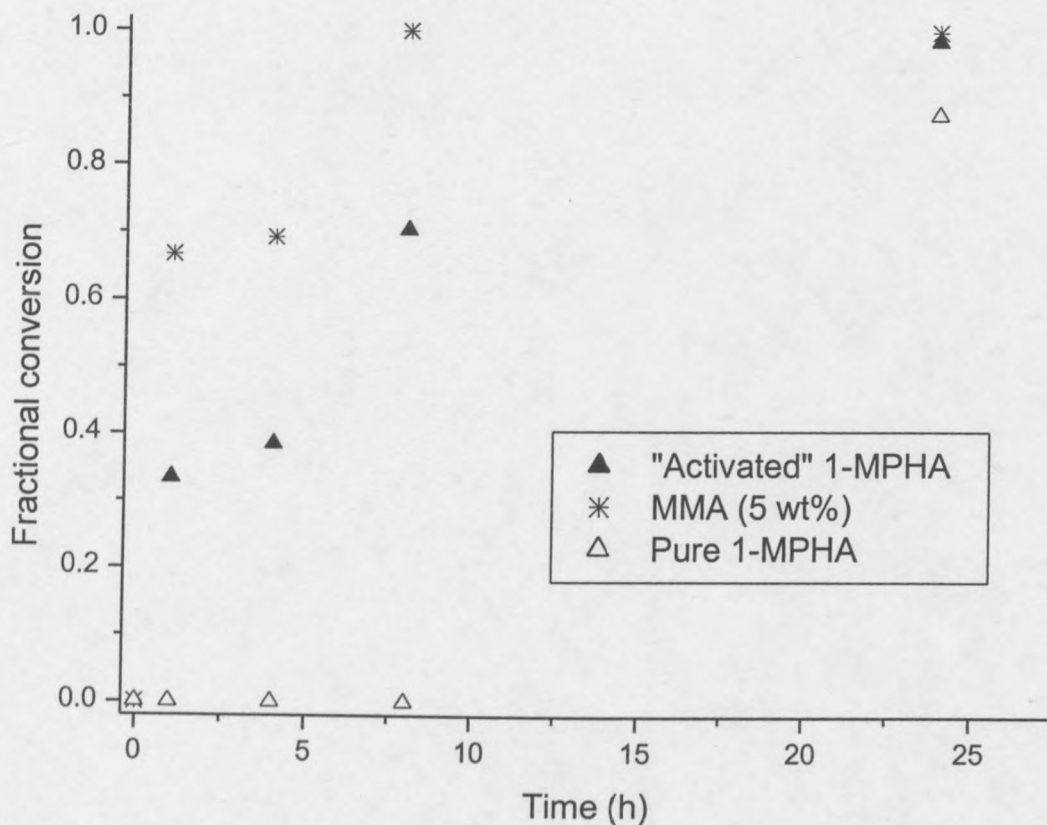


Figure 3.6: A graphical representation of the homopolymerisation results, conversion vs reaction time, as monitored by ^1H NMR, for the 1-MPHA reaction "activated" with MMA and the reaction of pure 1-MPHA.

In order to find the origin of the induction effect, a study of the entire polymerisation process was undertaken. The reactions were conducted in NMR tubes and ^1H NMR scans were recorded at 5-minute intervals. These *in situ* ^1H NMR experiments were conducted to eliminate outside interference during the polymerisation process and were carried out on the pure 1-MPHA samples only as they were the only ones that displayed an induction period. Deuterated toluene was used as the solvent to make up 50 wt% monomer solutions. Due to the very slow reaction and the very long induction period, an unusually high concentration of AIBN (10 wt%) was used. An internal standard of pyrazine with a few drops of deuterated benzene was used to normalise the double bond peak area integrations. The reaction temperature was 70 °C. Figure 3.7 shows the peaks monitored during the reaction. The concentration of the monomer was calculated by means of equation 3.1:

$$C_{1\text{-MPHA}} = \frac{H_1 + H_2 + H_3}{R} \times C_0 \quad (3.1)$$

Where C_{1-MPHA} is the concentration of 1-MPHA, H_1 to H_3 are the areas under the peaks from H_1 to H_3 of the 1-MPHA double bond protons, C_0 is the initial concentration of 1-MPHA added in the NMR tube and R is the intensity of the signal for the internal standard, pyrazine.

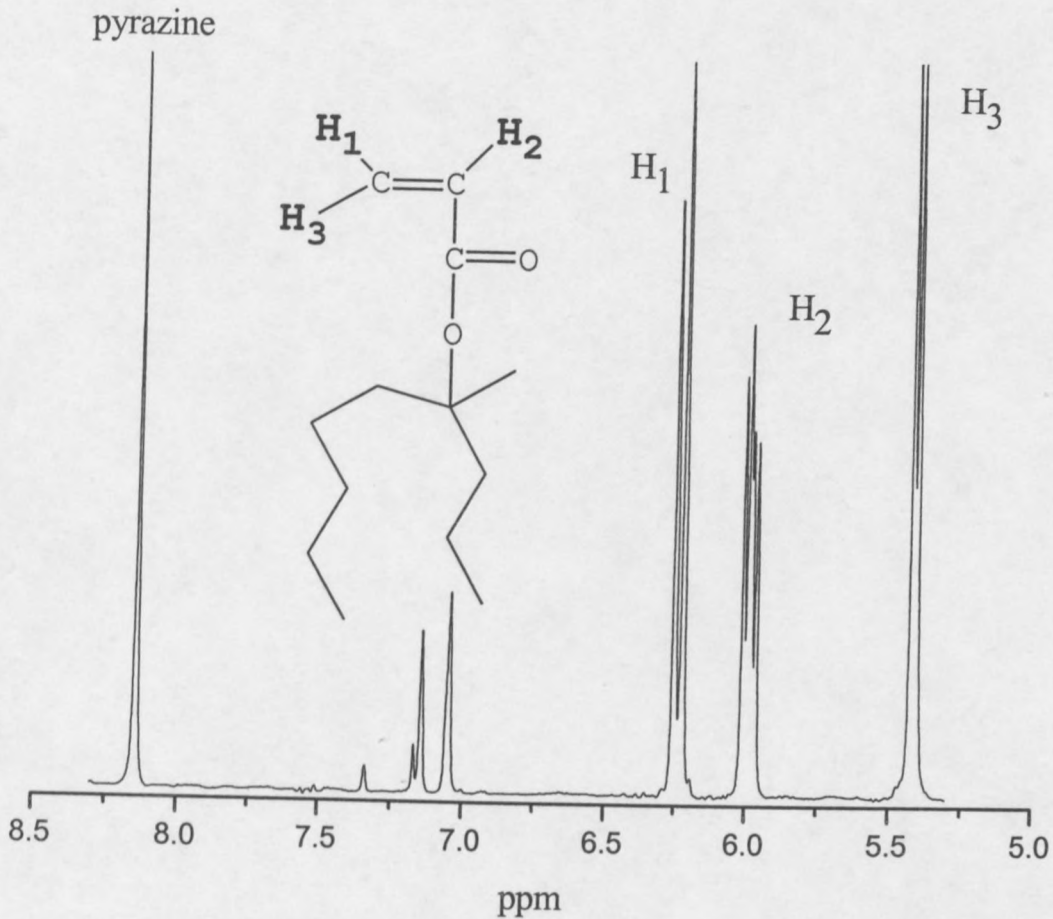


Figure 3.7: The ^1H NMR spectrum of the peaks used to monitor reaction progress for the polymerisation of 1-MPHA at 50 wt% solution in deuterated toluene and 10 wt% AIBN at 70 °C *in situ* an NMR apparatus.

The data obtained from the *in situ* ^1H NMR homopolymerisation reactions of 1-MPHA are shown in Figure 3.8.

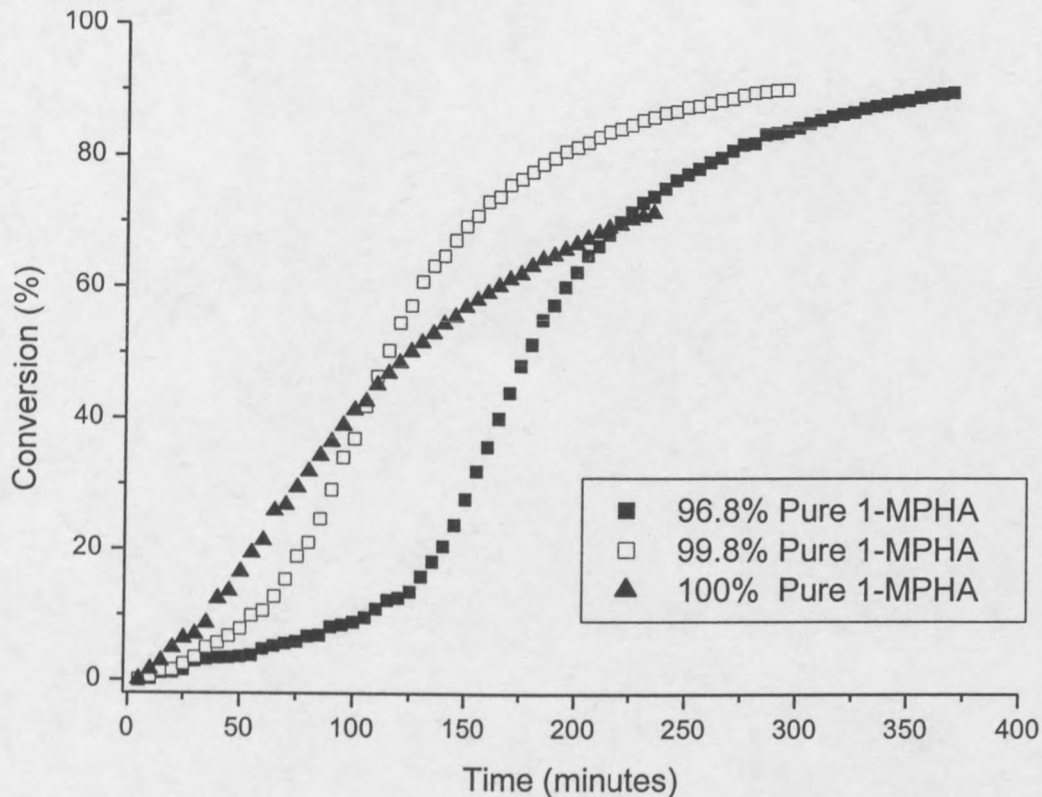


Figure 3.8: Conversion data for the homopolymerisation of 1-MPHA of various purity levels: 100% purified by 3 columns, 99.8% purified by 2 columns and 96.8% purified by 1 column. The reaction conditions were 50 wt% monomer solutions in deuterated toluene, 10 wt% AIBN as initiator and run at a temperature of 70 °C.

Observations from three *in situ* ^1H NMR homopolymerisation experiments of 1-MPHA (50 wt% 1-MPHA in deuterated toluene, 10 wt% AIBN and run at 70 °C) in Figure 3.8 are explained below. In the first experiment with the monomer that was purified by column chromatography through a silica gel stationary phase with dichloromethane as eluent, there is a long induction period of up to about two hours, after which the reaction rate increases rapidly until it slows down at around 75 % conversion. The reaction was run with 1-MPHA monomer purified by one pass through a silica gel column using dichloromethane as the eluent.

Close examination of the data showed an extra species to those expected in the reaction mixture that was consumed rapidly during the polymerisation reaction. Its disappearance coincided with the increase in the reaction rate of the 1-MPHA homopolymerisation. See Figure 3.9(a). This species was present as an impurity appearing in the double bond region of the ^1H NMR spectrum. It should be noted that the concentration of the impurity is so low that it is not possible to observe it in

normal ^1H NMR traces, see Figure 3.7. In Figures 3.9 (a) and (b) a different scale is used for the impurity and the double bond proton peaks.

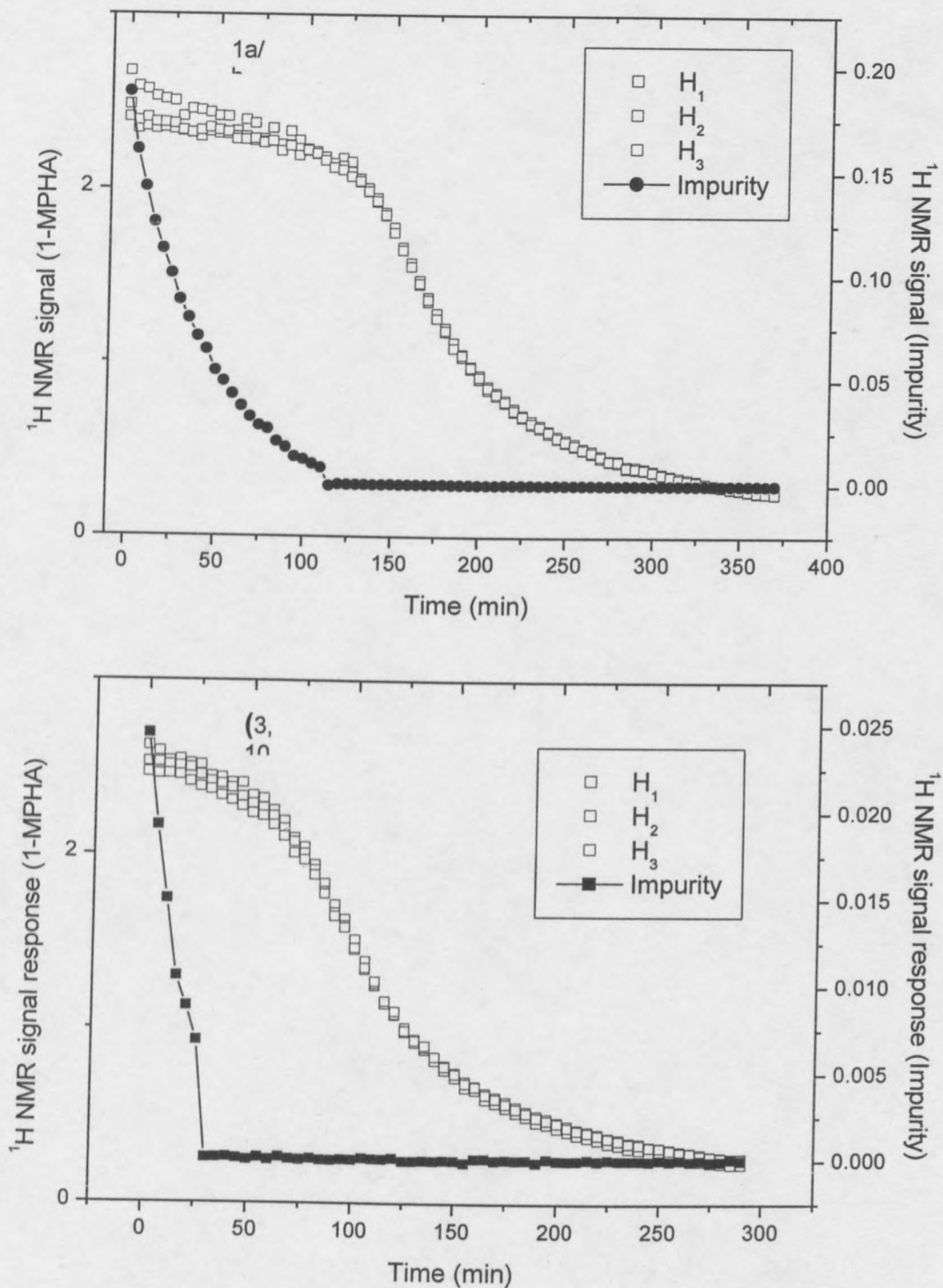


Figure 3.9: Plots of the ^1H NMR signal for the three double bond proton peaks (H_1 , H_2 and H_3) of 1-MPHA as a function of time illustrating the effect of an extra radical scavenging species, the impurity, on reaction progress. In (a) the induction period is 110 minutes and in (b) after further purification the induction period decreased to 25 minutes. The reaction conditions for both experiments were 50 wt% 1-MPHA solution in deuterated toluene, 10 wt% AIBN and were conducted at 70 $^\circ\text{C}$.

Since the presence of this impurity appeared to inhibit the polymerisation, further purification of the monomer 1-MPHA and kinetic investigation of its homopolymerisation were necessary. The purification of the monomer 1-MPHA was repeated a second time by column chromatography under the same conditions as the first. The conversion data for the homopolymerisation of the 1-MPHA monomer after further purification is shown in Figure 3.8. Here a shorter induction period of about 25 minutes was observed. The conversion curve followed the same trend as that obtained for the purification with 1 column. The raw data showing the ^1H NMR signal response for the 1-MPHA double bond peaks with that of the impurity after purification with the second column is shown in Figure 3.9(b).

When the impurity was removed to levels that could not be detected on the NMR by subjecting the monomer to a third column chromatography pass, no induction period was observed (see Figure 3.8 - 100 % pure 1-MPHA). This shows that the induction period is due to a competition between the monomer and the impurity for the initiator radicals. It should be noted that the reaction is still slow as a very high initiator concentration was used in order to get appreciable reaction within the limited NMR instrument time. The identity of the impurity could not be ascertained from the NMR data. The shape of the conversion curve for the pure 1-MPHA is different to the other two and seems to level off earlier at about 60% conversion.

The impurity seems to very effectively compete for the cyanoisopropyl radicals from AIBN, and then not propagate, so that little monomer gets consumed. This suggests that the cyanoisopropyl radicals add to the impurity much faster than to the monomer 1-MPHA. Thus the rate coefficient for addition to impurity is much greater, since its concentration is lower than that of the monomer ($k_{\text{add,impurity}} \gg k_{\text{add,monomer}}$). The formed radical species does not seem to copolymerise with the 1-MPHA monomer, and probably undergoes fairly rapid termination.

In an industrial process the presence of the impurity would be undesirable as it seriously hinders the start of the reaction and this would mean a loss in time, reagents and energy since the reaction is run at 70 °C.

3.6 Thermal properties of poly-(1-methyl-1-propyl-hexyl acrylate)

The TGA trace of the 1-MPHA homopolymer shown in Figure 3.10 indicates that the homopolymer is stable to a temperature slightly above 200 °C and has two stages of thermal degradation. The initial decomposition of 1-MPHA starts at about 170 °C which is similar to the initial decomposition of PMMA. This stage is due to the decomposition of the least thermally stable hindered linkages formed during the termination by combination of propagating radicals during polymerisation^[6], see Scheme 3.3. There is a rapid degradation from about 200 °C with some arrest at about 300 °C. This stage, which is about 100 °C lower than that of PMMA, accounts for major weight loss in the poly-(1-MPHA) homopolymer and therefore must be from the decomposition of the main part of the polymer chains. The charred residue left above 550 °C is due to the burning of the hydrocarbon chains.

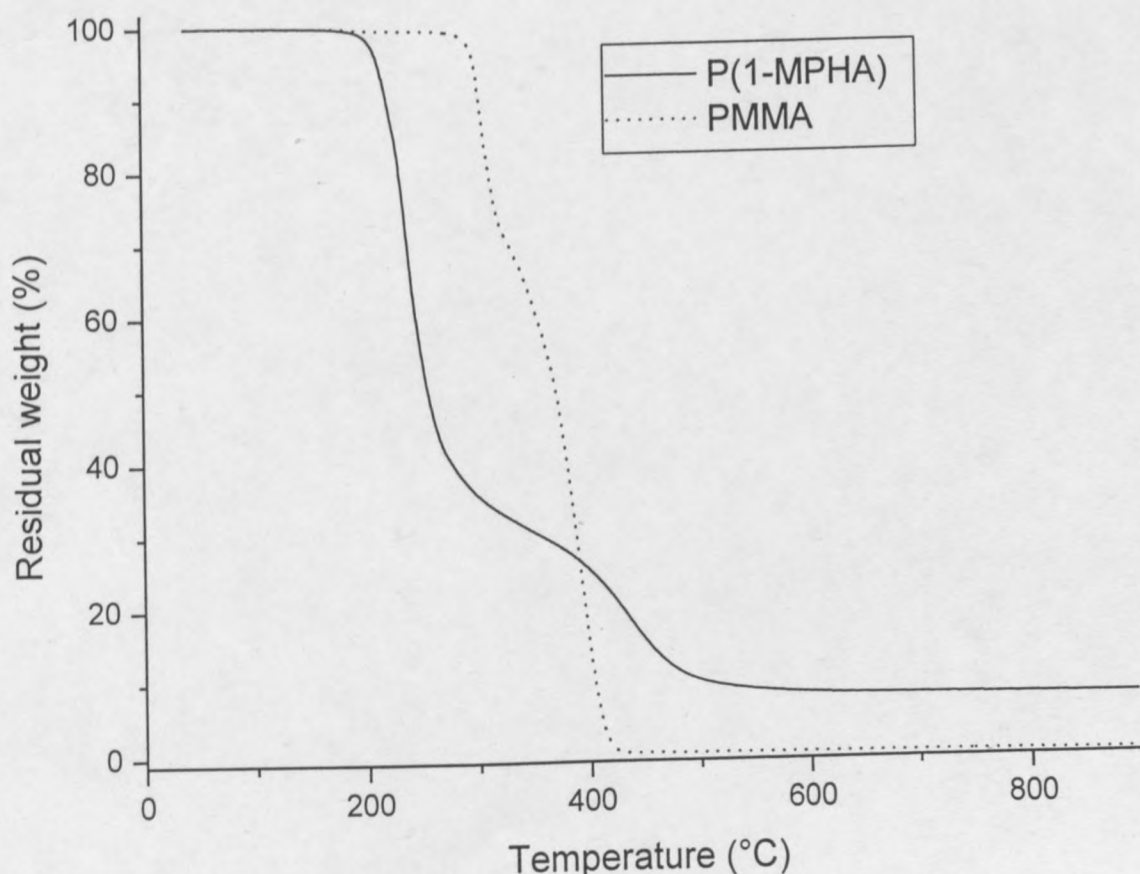
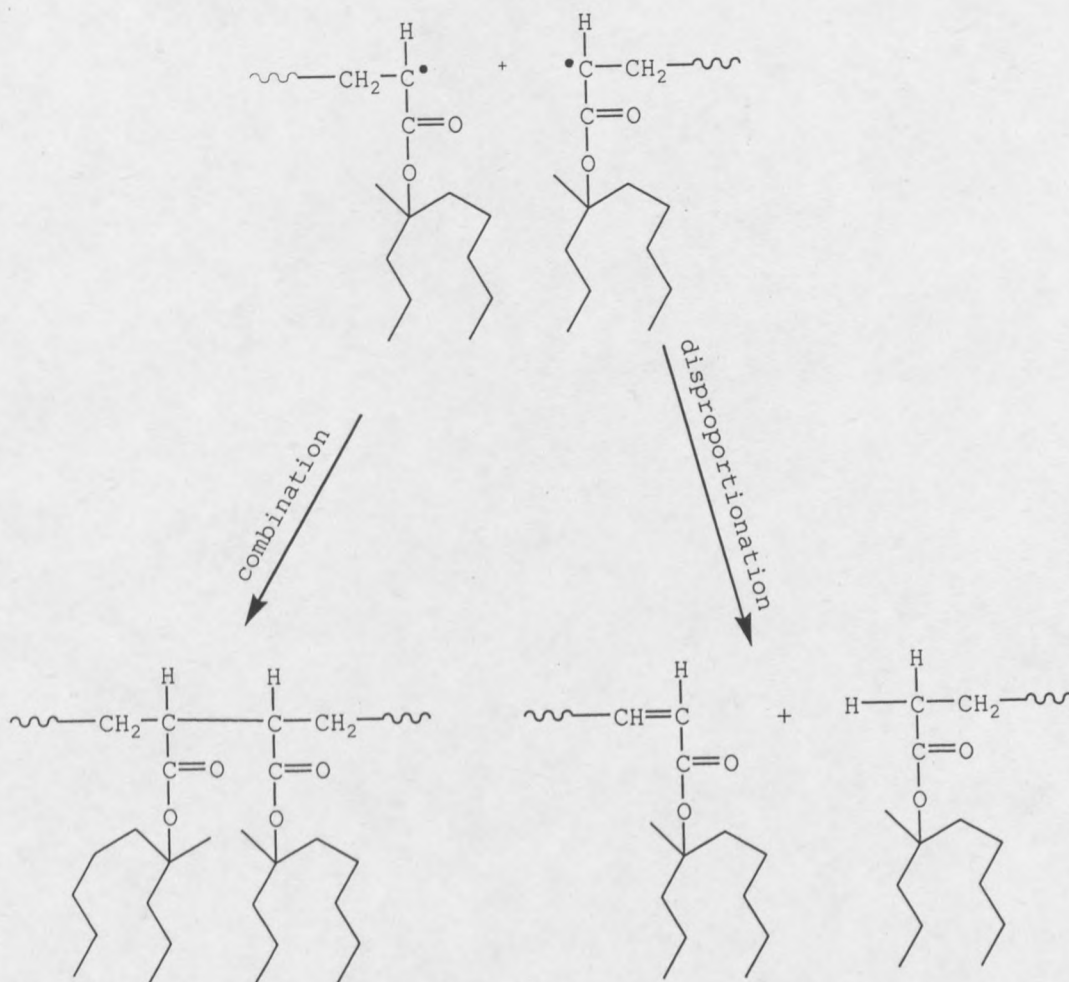


Figure 3.10: TGA traces for the homopolymers of PMMA and poly-(1-MPHA).



Scheme 3.3: Free radical termination by combination and disproportionation of poly-(1-MPHA) radicals.

Figure 3.11 shows DMA traces of the thermo-mechanical properties of the homopolymer. Cooling limitations with the mechanical cooling system used meant the temperature could not be reduced below $-56\text{ }^{\circ}\text{C}$. The estimation of the T_g value from both the tan delta trace and the storage modulus trace is complicated by the closeness of the values to the lower temperature limit of the cooling system. The value for T_g is estimated to be about $-46\text{ }^{\circ}\text{C}$, close to the limit of the cooling system. The leathery region between -56 and $-46\text{ }^{\circ}\text{C}$ is not pronounced and the sample quickly reaches the rubbery plateau around $0\text{ }^{\circ}\text{C}$. The tan delta trace is broad, with two local maxima. It is surmised that these two peaks are due to the formation of nano-domains due to phase separation of the backbone versus the hydrophobic side groups. This suggests that there are some thermal events such as liquid-liquid

transition that are occurring beyond the glass transition temperature. These might be a result of movements either in the backbone or side chains. At room temperature the polymer is soft because of the very low T_g .

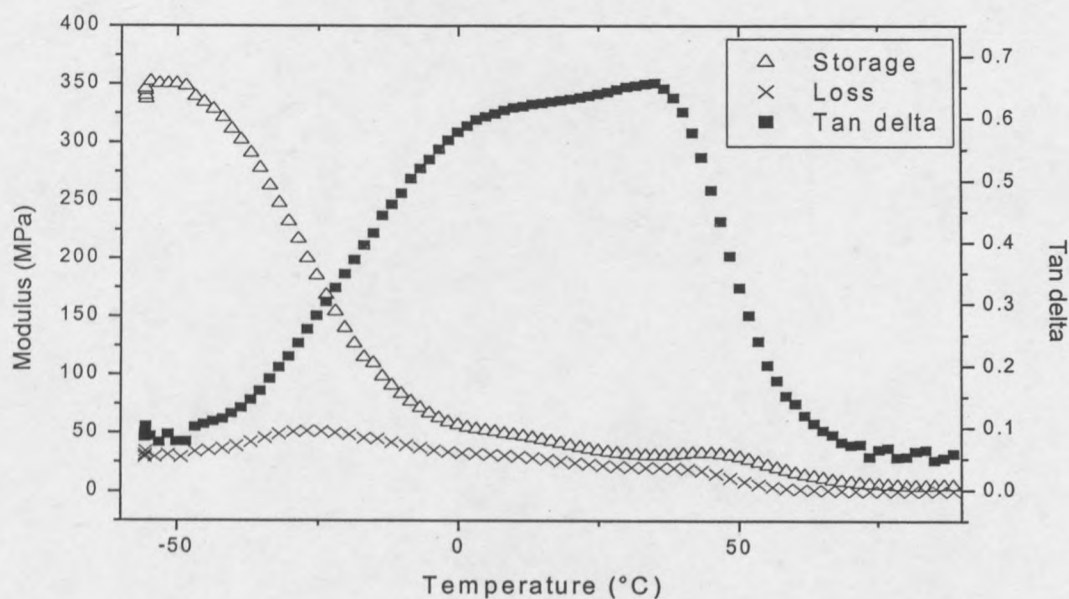


Figure 3.11: DMA results for the homopolymer of 1-MPHA.

3.7 Conclusions

The dimer of 1-pentene, 1-propyl-heptene, was successfully converted into the acrylic monomer, 1-methyl-1-propyl-hexyl acrylate (1-MPHA) via esterification of 4-methyl-nonan-4-ol (4-MNOL). The structure of 1-MPHA was confirmed by NMR and FTIR data. 1-MPHA was successfully homopolymerised, as confirmed by GPC, NMR and FTIR data. ^1H NMR kinetic data revealed an extremely long induction period that was subsequently traced to the presence of a very low concentration of an as yet unknown impurity. When MMA was added to 1-MPHA to encourage the homopolymerisation of 1-MPHA, the reaction was much faster. This is presumably because the MMA competes favourably with the impurity for addition of the initiator-derived cyanoisopropyl radicals, and provides radicals that are able to add to 1-MPHA. Further purification of the monomer managed to prevent the induction period. TGA results for the homopolymer show stability up to about 200 °C and then a rapid degradation to about 40 % of original mass.

Poly-(1-MPHA) has a low T_g , making it attractive to use 1-MPHA as a comonomer for polymers with high T_g s. Many other uses could be found for the homo- or copolymers of 1-MPHA, such as the utilisation of its hydrophobic nature in coatings applications.

3.8 References

1. Christoffers, J. and Bergman, R. G., *Inorg. Chim. Acta*, 1998. **270**: p. 20 - 27.
2. Wahner, U. M., Brull, R., Pasch, H., Raubenheimer, H. G., and Sanderson, R. D., *Angew. Makromol. Chem.*, 1999. **270**: p. 49 - 55.
3. Brown, H. C. and Geoghegan, P. J., *J. Org. Chem.*, 1970. **35**(6): p. 1844 - 1850.
4. Subramarian, K., Nanjundan, S., and Reddy, A. V. R., *Eur. Polym. J.*, 2001. **37**(4): p. 691 - 698.
5. Landry, R., Penlidis, A., and Duever, T. A., *J. Polym. Sci. Part A: Polym. Chem.*, 2000. **38**: p. 2319 - 2332.
6. Smith, S. D., Long, T. E., and McGrath, J. E., *J. Polym. Sci. Part A: Polym. Chem.*, 1994. **32**: p. 1747 - 1753.

CHAPTER 4

COPOLYMERISATION OF 1-METHYL-1-PROPYL-HEXYL ACRYLATE WITH METHYL METHACRYLATE

4.1 Introduction

The elucidation of copolymer structure (composition and monomer sequence distribution) and kinetics are of major importance for the prediction of copolymer properties and the correlation between structure and properties. Among the various types of copolymerisation reactions, radical copolymerisation is probably the most important since it does not demand rigorous experimental conditions and can be applied to a large variety of monomers, leading to the formation of new materials^[1,2].

The most sensible approach to the estimation of reactivity ratios in systems about which little is known is to use a pair of initial feed compositions that differ significantly^[3]. Conventionally, the reactivity ratio of any monomer pair is determined by preparing, at low conversion and by isolation of, a series of copolymers with fractional molar compositions of monomer feed ranging from 0 to 1. After the collection of the feed and copolymer molar fraction data, linear and non-linear methods are used to determine the most reliable reactivity ratios^[4-7], (see section 2.6.3). There are, however, some problems and errors involved in this method. The obtained copolymer is not the instantaneously formed copolymer corresponding to the initial feed composition, but a summation of all copolymer formed until the reaction is terminated at low conversion. Moreover, the isolation of the polymer may lead to the presence of residual monomers or solvents^[8].

Spectroscopic methods such as ¹H NMR and Raman spectroscopy have been used successfully to study the kinetics of copolymerisation *in situ*^[8-10]. These methods have the advantages of being non-invasive, and instantaneous determination of feed

and copolymer composition is possible by monitoring the continuous change in the intensity of resonance signals assigned unambiguously to the double bonds of the participating monomers.

The novel monomer 1-methyl-1-propyl-hexyl acrylate (1-MPHA), prepared as described in chapter 3, was copolymerised with methyl methacrylate (MMA). The copolymers obtained were analyzed by chemical and thermal techniques, and the kinetics of the copolymerisation studied.

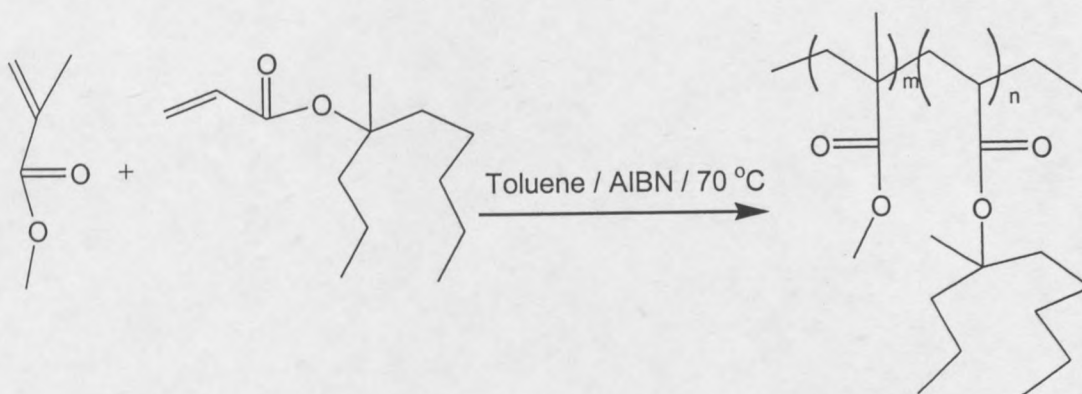
4.2 Experimental

4.2.1 Reagents used

The 1-methyl-1-propyl-hexyl acrylate (1-MPHA) monomer was synthesised and purified as detailed in Chapter 3. The methyl methacrylate, MMA (Merck, 96%) was purified by distillation under reduced pressure. The initiator azobis-isobutyronitrile, (AIBN, Delta Scientific, 98%) was recrystallised from methanol. The solvent toluene (Saarchem, AR grade) was dried and distilled over sodium metal flakes. Benzophenone was used as indicator to determine complete drying.

4.2.2 Copolymerisation of 1-MPHA with MMA

Five copolymers with different initial feed weight fractions of 1-MPHA and MMA were prepared in order to study the effect of 1-MPHA on the properties of MMA when copolymerised. Scheme 4.1 shows the scheme for the copolymerisation process. The structure of the copolymer is not intended to represent a block copolymer as depicted in the schematic, but rather varying monomer placement in the chain.



Scheme 4.1: Schematic representation for the copolymerisation of 1-MPHA with MMA. (NB – structure not intended to represent a block copolymer).

All the copolymerisations were reacted at 50 wt% total monomer solution with respect to toluene, and 2 wt% AIBN with respect to total monomer weight was used as initiator. The polymerisations were carried out in Schlenk tubes. After addition of the measured amounts of monomers, initiator and solvent, the Schlenk tubes were subjected to three freeze-pump-thaw cycles and then immersed in an oil bath thermostated at 70 °C. The reactions were allowed to run for 18 hours.

The reaction products were obtained by adding the reaction mixture into five-fold excess methanol and precipitating the copolymer. The copolymers were purified by dissolving the filtered precipitate in chloroform and reprecipitating in methanol three times.

4.2.3 Analyses

The copolymers were characterised by ^1H and ^{13}C NMR, infrared spectroscopy, gel permeation chromatography, thermogravimetry and dynamic mechanical analysis. The backgrounds for these analytical procedures are detailed in Section 3.2.2 of Chapter 3.

4.2.4 Determination of the kinetics of the copolymerisation of 1-MPHA with MMA

Knowledge of reactivity ratios enables prediction of reaction progress and the microstructure of the copolymer. In order to determine the reactivity ratios for the 1-MPHA and MMA copolymer system, *in situ* ^1H NMR copolymerisation experiments were conducted.

In order to obtain feed compositions at which the errors in the estimated reactivity ratios would be minimum, preliminary copolymerisation results were used to determine the initial feed composition for the copolymerisations according to Tidwell and Mortimer^[5]. By using these feed compositions, a set of reactivity ratios with the smallest possible confidence region is obtained. From the preliminary results r_{MMA} (the reactivity ratio of MMA) and r_{1-MPHA} (the reactivity ratio of 1-MPHA) were found to be 1.52 and 0.36 respectively.

The reactivity ratios r_{MMA} and r_{1-MPHA} are defined as the ratios of the rate coefficients for homo- and cross- propagation for monomers MMA and 1-MPHA respectively. They are expressed as follows:

$$r_1 = \frac{k_{11}}{k_{12}} \quad (4.1)$$

$$r_2 = \frac{k_{22}}{k_{21}} \quad (4.2)$$

Subscripts 1 and 2 represent MMA and 1-MPHA respectively and k is the rate coefficient of propagation.

To determine the upper and lower limits of MMA in the feed, for optimal reactivity ratios, preliminary values of $r_{MMA} = 1.52$ and $r_{1-MPHA} = 0.36$ were used in the following equations^[5]:

$$f'_{MMA} = \frac{2}{2 + r_{MMA}} = 0.57 \quad (4.3)$$

$$f''_{MMA} = \frac{r_{1-MPHA}}{2 + r_{1-MPHA}} = 0.15 \quad (4.4)$$

Where,

f_{MMA} is the upper limit of the ratio of MMA in the feed and f''_{MMA} is the lower limit of the ratio of MMA in the feed.

To determine the reactivity ratios, the following experiments were carried out: pre-determined concentrations of 1-MPHA, MMA and AIBN (see Table 4.1) in deuterated toluene were added to an NMR tube through which nitrogen was bubbled to expel air. A thin capillary tube (isolated from the reaction mixture) containing pyrazine and a few drops of deuterated benzene was inserted into the reaction tube to act as an internal standard.

Table 4.1: Concentration of the reagents used in the copolymerisation of 1-MPHA with MMA

Reaction	1-MPHA (mmol)	MMA (mmol)	f_{MMA}	AIBN (mg)	Toluene (mL)
1	0.49	0.79	0.23	3.6	0.39
2	0.67	0.42	0.39	3.6	0.38
3	0.75	0.23	0.62	3.6	0.40

The polymerisation reactions proceeded in a 600 MHz NMR instrument at 70 °C. ^1H NMR scans were collected at 5-minute intervals. The reactions were allowed to run for at least 3 hours. Integration of the double bond peaks over the time intervals enabled the monitoring of the consumption of monomers with time. This allowed the instantaneous determination of the monomer concentration at 5-minute intervals throughout the reaction. The data collected was manipulated using ACD Labs 7.0 ^1H NMR Processor® integration software. The peaks used for the integration are as shown in Figure 4.1. The peak areas were normalised by dividing the area under the double bond proton peaks by the area of the pyrazine peak, the internal standard. An average of the peak areas was used for the relative monomer concentration calculations, i.e.

$$C_{1-MPHA} = \frac{H_1 + H_2 + H_3}{3R} \times C_{1-MPHA,0} \quad (4.5)$$

$$C_{MMA} = \frac{H_4 + H_5}{2R} \times C_{MMA,0} \quad (4.6)$$

where,

C_{1-MPHA} is the relative 1-MPHA monomer concentration, C_{MMA} is the relative MMA monomer concentration, H_1 to H_3 are the intensities of the signal integrals for H_1 to H_3 in 1-MPHA and H_4 to H_5 are the intensities of the signal integrals for H_4 to H_5 in MMA and R is the intensity of the integral of the pyrazine peak, the internal standard, $C_{1-MPHA,0}$ and $C_{MMA,0}$ are the initial concentrations of 1-MPHA monomer and MMA monomer added to the NMR tube at the start of the reaction, respectively (see Figure 4.1).

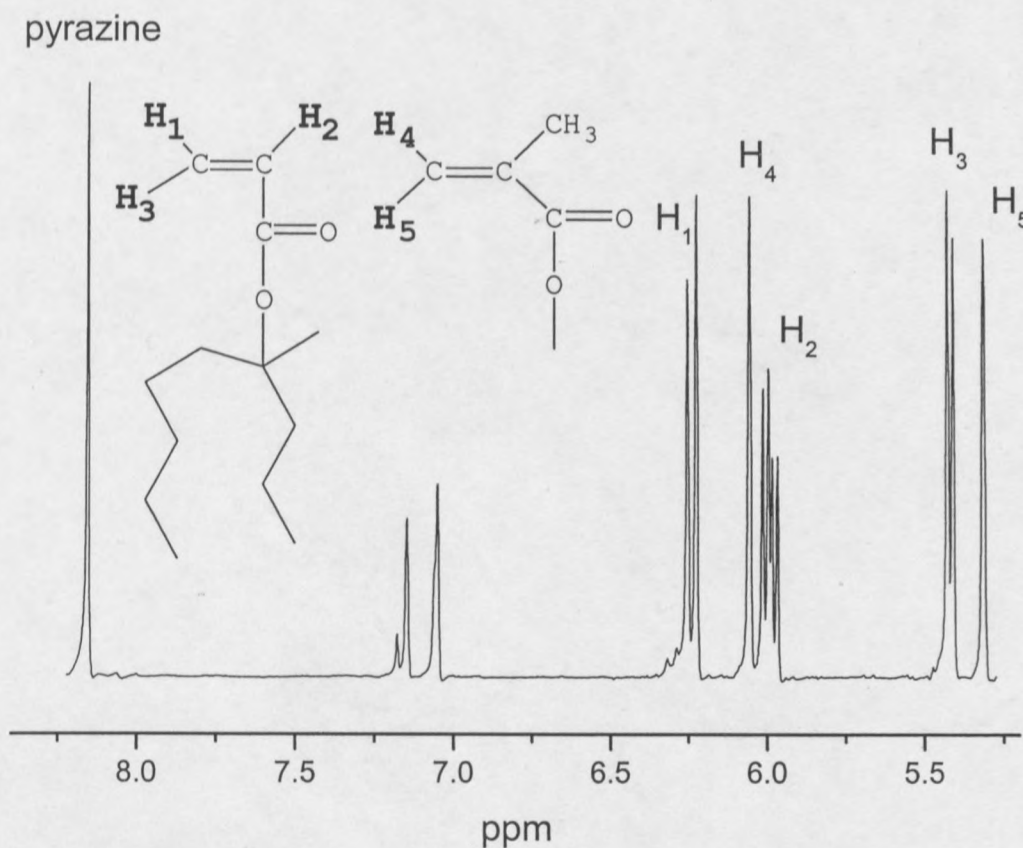


Figure 4.1: ^1H NMR peaks monitored for the monomer consumption determination in the *in situ* copolymerisation of 1-MPHA with MMA.

The data obtained was used to estimate the reactivity ratios of the two monomers, MMA and 1-MPHA, by non-linear least squares fitting to the integrated solution of the copolymer equation (Eq. 4.7),

$$F_1 = \frac{r_1 f_1^2 + f_1 f_2}{r_1 f_1^2 + 2f_1 f_2 + r_2 f_2^2} \quad (4.7)$$

where F_1 is the molar fraction of monomer 1 incorporated into the copolymer chain, r_1 is the reactivity ratio of monomer 1, r_2 is the reactivity ratio of monomer 2, f_1 is the molar fraction of monomer 1 in feed, and f_2 is the molar fraction of monomer 2 in feed.

The integrated solution of Eq. 4.7 gives the theoretical conversion equation (Eq. 4.8) as^[11],

$$X = 1 - \left(\frac{f_1}{f_{10}} \right)^\alpha \left(\frac{1-f_1}{1-f_{10}} \right)^\beta \left(\frac{f_{10} - \delta}{f_1 - \delta} \right)^\gamma \quad (4.8)$$

where X is the total monomer conversion, f_{10} is the initial molar fraction of monomer 1 in feed at time $t = 0$.

The other variables are defined below,

$$\alpha = \frac{r_1}{1-r_2}$$

$$\beta = \frac{r_1}{1-r_1}$$

$$\delta = \frac{1-r_1 r_2}{(1-r_1)(1-r_2)}$$

$$\gamma = \frac{1-r_2}{2-r_1-r_2}$$

The experimental conversion is given by Eq 4.9,

$$X = 1 - \frac{[M]}{[M]_0} \quad (4.9)$$

Where $[M]$ is the total monomer concentration at any time during the reaction and $[M]_0$ is the total initial monomer concentration at time $t = 0$.

The Microsoft Excel® program (Microsoft XP Professional) *Solver* was used to optimise the r_1 and r_2 values by minimising the sum of the squares of the residuals between theoretical (Eq. 4.8) and experimental (Eq. 4.9) conversion. A global solution for the reactivity ratios was obtained by combining the three sets of data and getting the optimum r_1 and r_2 by minimising the sum of the squares of the residuals.

The non-linear least squares method was used to estimate r_1 and r_2 because of the advantages that it has over the other methods discussed in section 2.6.8.5, such as the independence of the result on the experimenter as long as the same set of data is used.

The uncertainty in the reactivity ratios was determined by using the equation 4.10^[12]:

$$S = S_R \left[1 + \frac{p}{n-p} F_\alpha(p, n-p) \right] \quad (4.10)$$

with S being the contour that encloses the uncertainty region, S_R is the sum of squares of the residuals, n is the number of data points, $p = 2$ is the number of parameters and $F_\alpha(p, n-p)$ is the F distribution at 95% confidence level. The uncertainty region is the area where the computed reactivity ratios are most probable to be found after all the contributing statistical errors have been taken into account.

4.3 Results and discussion

4.3.1 Chemical analyses

4.3.1.1 NMR

^1H NMR was used to determine the amount of 1-MPHA monomer incorporated into the copolymer chains. ^1H NMR scans are shown in Figure 4.2 for the copolymers obtained after the reactions were allowed to run to completion at the extreme copolymer compositions: Figure 4.2(a) is that of a copolymer containing 25 mole% 1-MPHA and Figure 4.2(b) is that containing 7 mole% 1-MPHA in the copolymer chains.

The peak at about 3.7 ppm was assigned unambiguously to the MMA methoxy group protons of the copolymer. The integral of this peak was used relative to the rest of the spectrum to determine the molar percentage incorporation, see Table 4.2. The mole fraction of the monomers in copolymers was determined according to the following equation, derived by considering the intensities of the NMR peaks that could be assigned unambiguously. The equation is based on the eight protons in MMA and the twenty four protons in 1-MPHA, with the three methoxy peaks at 3.7 ppm unambiguously assigned^[13]:

$$\frac{\text{Intensity of MMA methoxy protons } (I_{\text{CH}_3})}{\text{Intensity of total protons } (I_{\text{T}})} = \frac{3m_2}{8m_2 + 24m_1}$$

$$\frac{I_{\text{CH}_3}}{I_{\text{T}}} = \frac{3m_2}{8m_2 + 24(1 - m_2)}$$

$$m_2 = \frac{24I_{\text{CH}_3}}{16I_{\text{CH}_3} + 3I_{\text{T}}}$$

where m_2 is the mole fraction of MMA in copolymer, $m_1 = 1 - m_2$, is the mole fraction of 1-MPHA in copolymer, I_{CH_3} is the integrated peak intensity for MMA methoxy protons and I_{T} is integrated peak intensity of total protons.

There seems to be only a limited amount of 1-MPHA incorporation into the copolymers, as at 81 mole% 1-MPHA starting concentration there is almost 75

mole% MMA incorporated. It is surmised that it is difficult for the 1-MPHA monomer to be incorporated into the copolymer because of its bulky nature, which results in steric hindrance to homo- or co-propagation.

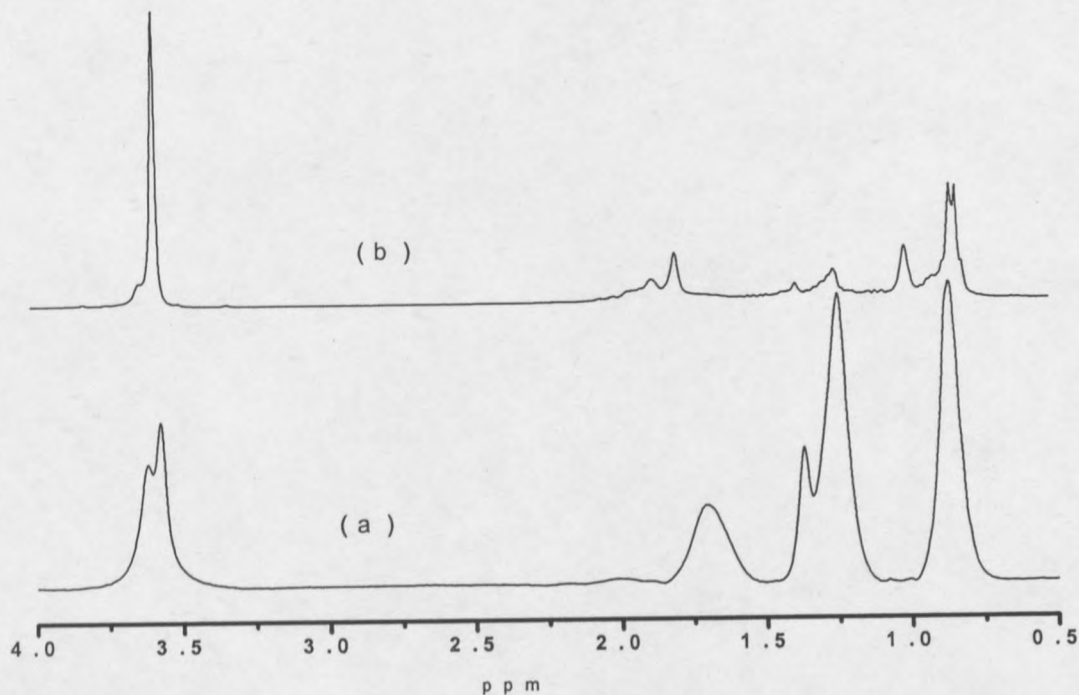


Figure 4.2: ^1H NMR spectra of poly-(1-MPHA-co-MMA) with (a) 25 mole% 1-MPHA and (b) 7 mole% 1-MPHA in copolymer precipitated in methanol after 18 hours at 70 °C.

4.3.1.2 GPC

The molar mass data for the copolymers as determined by GPC and based on polystyrene standards are also reported in Table 4.2. The polymers cover the 90 000 to 300 000 weight average molar mass range. There is a relatively narrow distribution in molar mass. The weight average molar mass, \overline{M}_w , as well as the polydispersity index decrease with decreasing 1-MPHA content. Sample DM19 containing 7 mole% 1-MPHA seems to be an exception as it has a lower molar mass and a broad polydispersity index. This result could be an outlier.

The number average molar mass, \overline{M}_n , seems to be constant with decrease in 1-MPHA content in the feed as the values range from 51 000 to 62 000 in no particular

order, except for sample DM19 which displays a very low \overline{M}_n at 1500. It should be noted that the values are not absolute as they are calculated with reference to a polystyrene calibration curve and are not corrected.

Table 4.2: Chemical analysis results of the poly-(1-MPHA-co-MMA) polymers

Sample	f_{1-MPHA} (%)	F_{1-MPHA} (%)	\overline{M}_n	\overline{M}_w	PDI
DM91	81	25	51000	295000	5.79
DM73	52	24	62000	128000	2.06
DM55	32	19	57000	100000	1.75
DM37	17	11	52000	91700	1.78
DM19	5	7	1500	6800	4.39

4.3.2 Thermal analyses

4.3.2.1 TGA

Figure 4.3 shows a plot of the residual weight for the poly-(1-MPHA-co-MMA) copolymers as a function of temperature. All the copolymers show a lower temperature for the early decomposition stage compared to both the homopolymers. This suggests that there is some copolymer fraction that is less thermally stable in the copolymers. As the amount of the comonomer MMA increased, the copolymers became more thermally stable than the 1-MPHA homopolymer in the 250 °C to 400 °C temperature range. The decomposition of DM91, the sample that contains 25 mole% 1-MPHA, shows a decomposition behaviour that is different to the other copolymers but similar to that of the 1-MPHA homopolymers. Even though the 1-MPHA content in sample DM91 is about 1 mole% higher than in sample DM73, there could be a higher percentage of 1-MPHA homopolymers domains in sample DM91 as the phase separation displayed in the DMA results suggests, hence the relation in decomposition behaviour to that of the 1-MPHA homopolymers.

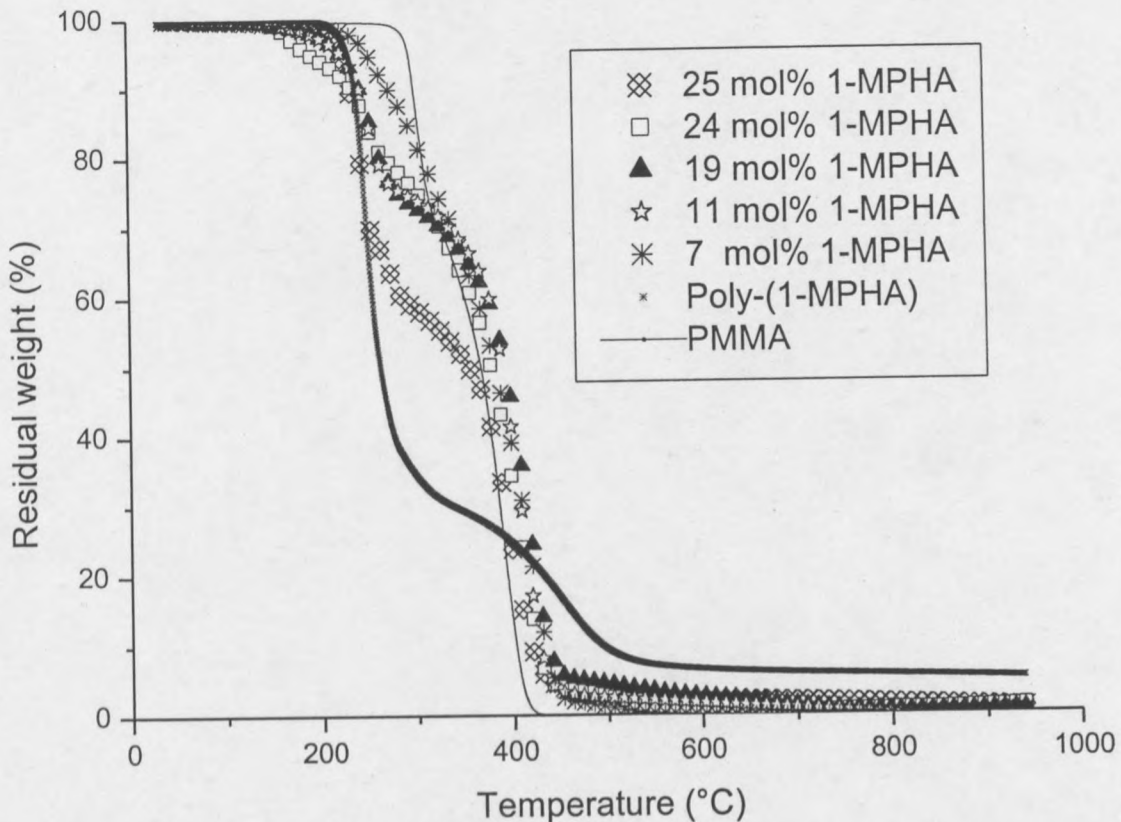


Figure 4.3: A plot of the TGA data for the homopolymers and copolymers of 1-MPHA and MMA.

Table 4.3 contains data extracted from Figure 4.3, showing the decomposition stages for the polymers. The decomposition stages for the copolymer samples were determined as the point of inflection of the weight loss regions. The amount of polymer lost is reported in parentheses as percentage weight loss. All the copolymer samples display weight loss around 240 °C, with an increase in amount lost with increase in amount of 1-MPHA in copolymer. This stage corresponds with the first decomposition stage in the poly-(1-MPHA) homopolymer. The copolymers with the highest 1-MPHA content show a decomposition stage that is earlier than that of the two homopolymers at around 200 °C.

In the copolymers that display three decomposition stages, the second decomposition stage is around 300 °C and corresponds to the first decomposition stage of the PMMA homopolymer. The copolymers containing an intermediate amount of 1-MPHA in copolymer composition show two stages of decomposition, with the first stage corresponding to the first decomposition stage of poly-(1-MPHA)

homopolymer and the second one corresponds to the second decomposition stage of the PMMA homopolymer.

All the copolymer samples have their final decomposition stages above 400 °C, which is higher than the final decomposition stage of PMMA. This phenomenon suggests that even a small amount of 1-MPHA in the copolymers is able to provide a residual at about 400 °C. The deviation of the decomposition behaviour of the copolymers from that of the homopolymers is evidence for the formation of true copolymers and not a mixture of homopolymers.

Table 4.3: TGA results of the poly-(1-MPHA-co-MMA) polymers

Sample (F_{1-MPHA} %)	180 – 270 (°C)	270 – 340 (°C)	340 – 540 (°C)
DM91 (25)	243.4 (21.7)	305.0 (53.1)	427.1 (82.3)
DM73 (24)	246.7 (19.8)	294.5 (37.6)	406.4 (67.7)
DM55 (19)	246.3 (16.8)		405.2 (67.1)
DM37 (11)	249.9 (13.1)		412.9 (75.2)
DM19 (7)	251.9 (3.4)	306.7 (20.4)	420.8 (79.6)
PMMA (0)		303.3 (9.5)	392.6 (75.3)
P(1-MPHA)	237.2 (28.2)		440.8 (82.5)

*The number in parentheses is cumulative percentage weight loss.

Another way of representing the data is shown in Figure 4.4, where a bar chart of the temperature at which 0, 50% and maximum weight loss occurs for the 1-MPHA/MMA copolymers is shown. Maximum weight loss occurs at about 450 °C for all the copolymers. The 1-MPHA homopolymer has its maximum weight loss at about 550 °C whereas that of PMMA is at about 425 °C. All the copolymer samples with the exception of sample DM91 have higher decomposition temperatures at 50% weight loss.

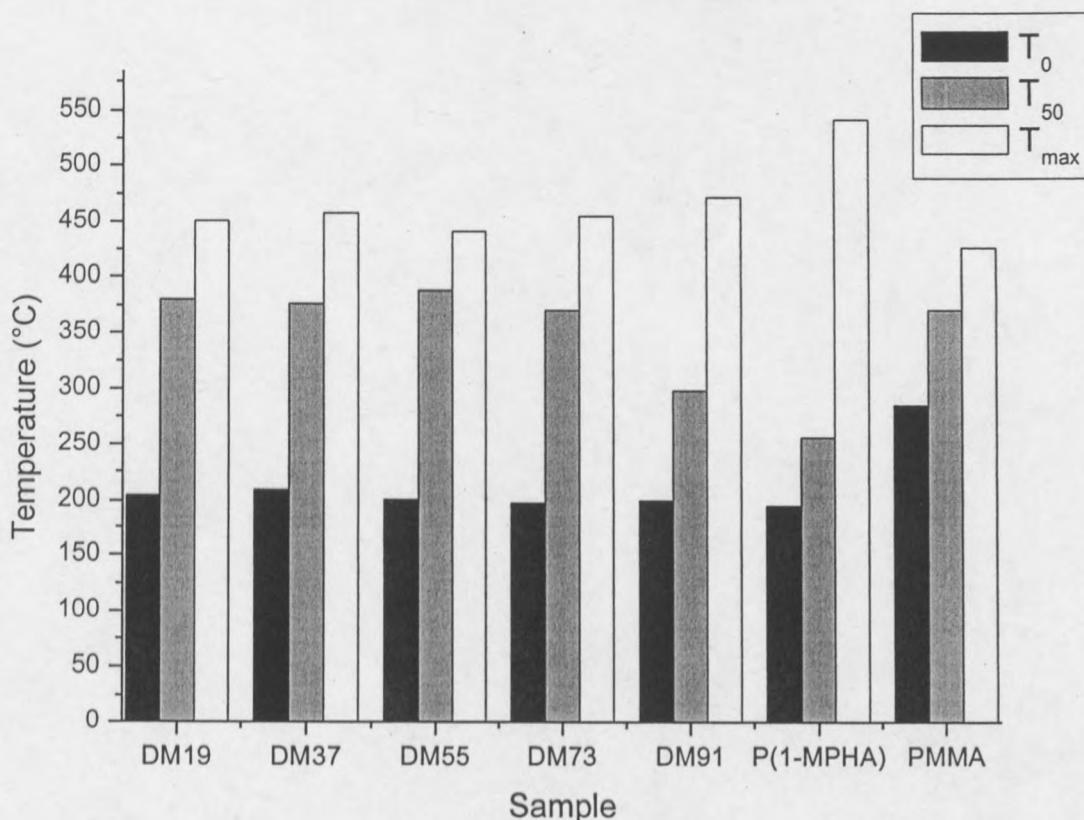


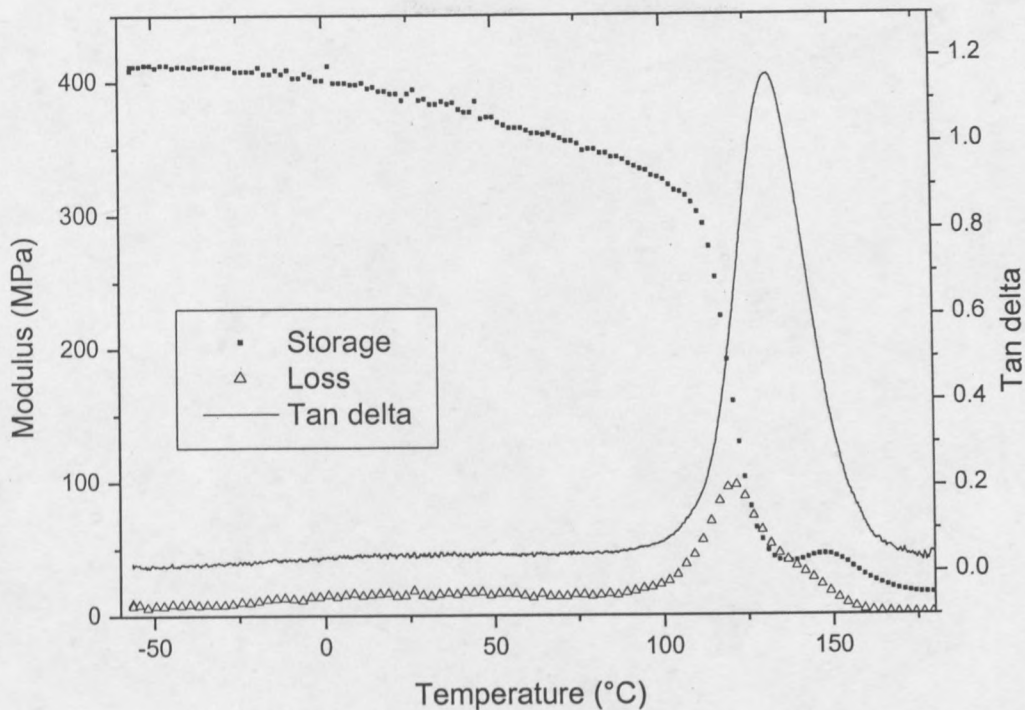
Figure 4.4: A plot of the temperatures at which 0, 50% and maximum weight loss occurs during the degradation of the poly-(1-MPHA-co-MMA) polymers.

4.3.2.2 DMA

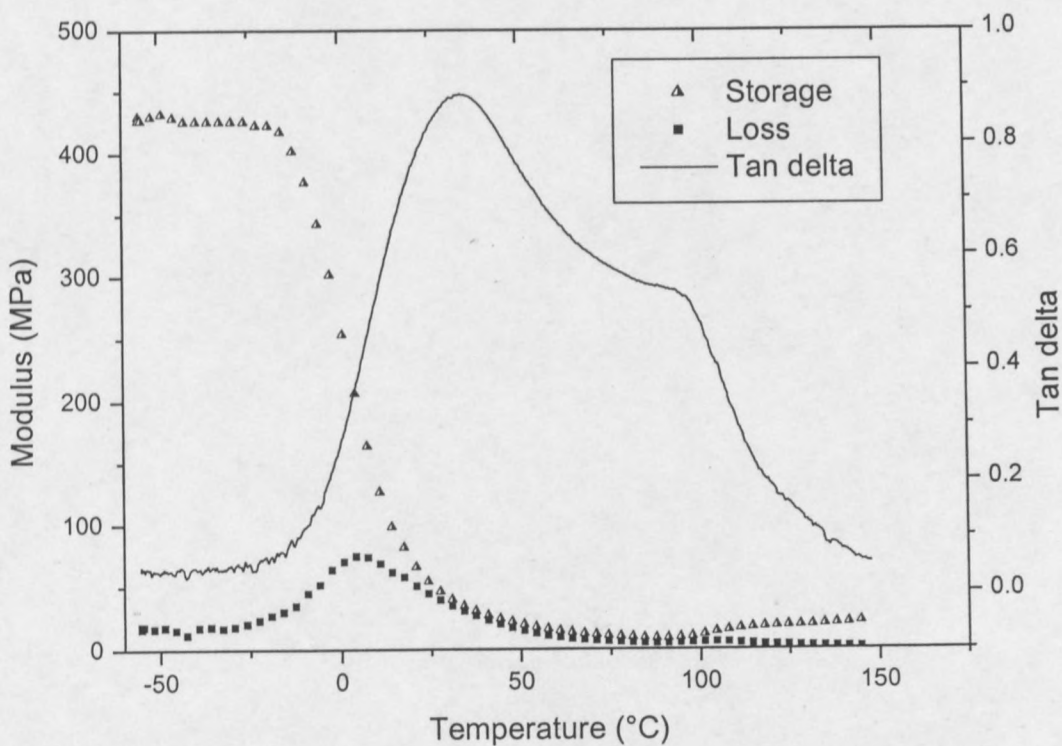
Figure 4.5(a) shows a plot of the DMA data for sample DM19 (7 mole% 1-MPHA) that contained 90 wt% MMA and 10 wt% 1-MPHA in the starting feed. The onset of the glass transition temperature (T_g) of the copolymer is at about 100 °C which is closer to the T_g for PMMA at 105 °C. Figure 4.5(b) shows a plot of the DMA data for sample DM91 (25 mole% 1-MPHA). A significant decrease in T_g onset to -25 °C is observed. This value is closer to the T_g for poly-(1-MPHA) of -46 °C. The tan delta plot for DM91 shows extensive broadening and two local maximum peaks which is normally indicative of partial phase separation in the copolymer. Sample DM73 containing 24 mol% 1-MPHA shown in Figure 4.6 shows behaviour similar to that of sample DM91. The peak broadening and the presence of two local peaks are observed in copolymers with high 1-MPHA content and in the 1-MPHA homopolymer. The peak broadening in the copolymers is different to that in the 1-MPHA homopolymer in that in the homopolymer the peak broadening is a result of nano-

domain formation due to local phase separation of the backbone versus the hydrophobic side groups, whereas the peak broadening in the copolymers is due to phase separation through association of the 1-MPHA components at a nanoscopic level. The copolymers display broader and more pronounced separation of the peaks which suggests that the peaks are not due to local effects.

The storage modulus of both copolymers, representing stiffness, is just above 400 MPa. This value is higher than the storage modulus for both the homopolymers of PMMA and poly-(1-MPHA). The poly-(1-MPHA) storage modulus starts dropping rapidly at about -50 °C whereas that of PMMA dropped gradually. The structure of the 1-MPHA monomer (long and branching chains) offered entanglements that help to reinforce the stiffness of the chains when copolymerised with MMA, as displayed by the improvements in storage modulus even at low 1-MPHA incorporation. Sample DM19 (7 mole% 1-MPHA) gradually loses its stiffness over a wide temperature range (-55 to 103 °C), whereas the stiffness of sample DM91 (25 mole% 1-MPHA) drops rapidly at around -25 °C. Addition of 1-MPHA onto PMMA lowered the T_g values of the copolymers with respect to PMMA, whereas there is little effect on the storage modulus. This could indicate favourable room temperature properties under various conditions of usage and could form a part of a new structure-property study with low additions of 1-MPHA as in DM19.



(a)



(b)

Figure 4.5: DMA data for (a) DM19 containing 7 mole% 1-MPHA and (b) DM91 containing 25 mole% 1-MPHA.

Figure 4.6 shows the tan delta traces for all of the 1-MPHA/MMA copolymers. A distinct change in T_g onset is observed with change in the copolymer composition. As the amount of MMA increases, the T_g onset also becomes higher, with the onset for sample DM91 at -25 °C and that of sample DM19 at 100 °C. T_g onset for PMMA is at 105 °C.

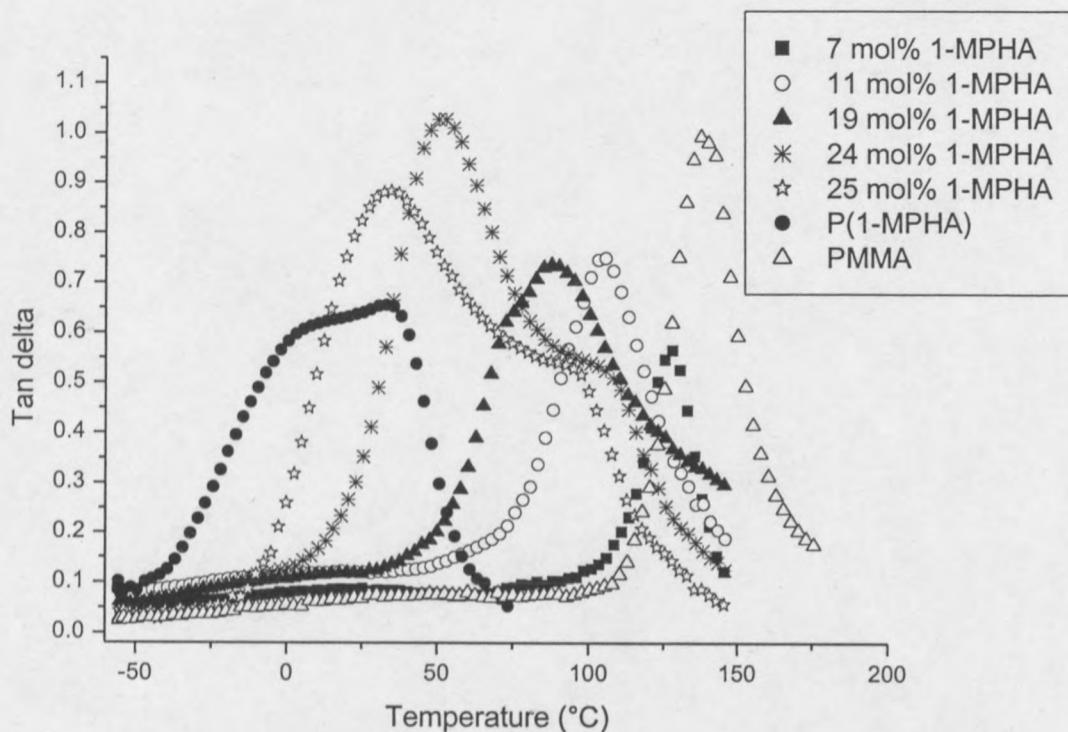


Figure 4.6: A plot of tan delta as a function of temperature for poly-(1-MPHA-co-MMA) polymers.

Figure 4.7 is a plot of the glass transition temperature as a function of 1-MPHA incorporated into the copolymers. The data obtained could not fit the Flory-Fox equation. This suggests that the microstructure of the copolymer is not random in nature. The glass transition temperature (T_g) is reported in three ways: T_1 – as the first maximum in the tan delta traces, T_2 – in broad tan delta traces a second maximum is also reported and T_g – as the onset of the rise in the tan delta trace taken as the intersection of the tangent between the horizontal and vertical part of the tan delta traces. The copolymers containing high 1-MPHA content ($F_{1\text{-MPHA}} = 25$ mole% and $F_{1\text{-MPHA}} = 24$ mole%) show low T_g values and broad traces with two local maxima.

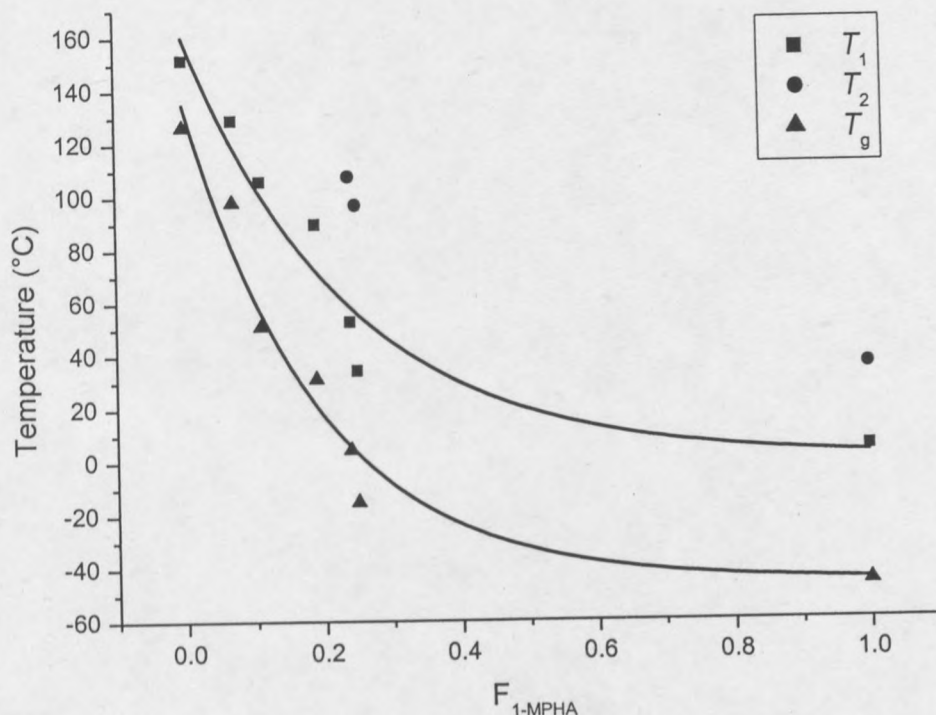


Figure 4.7: A plot of the glass transition temperature for the poly-(1-MPHA-co-MMA) polymers as a function of amount of 1-MPHA in the copolymers.

The copolymers with high 1-MPHA incorporation have two tan delta maxima. This phenomenon suggests phase separation. Since the polymers are not blends but true copolymers, this indicates that the copolymers show association of the 1-MPHA components at a nanoscopic level (i.e. tend to phase separate probably in a micellar structure). Further evidence for this is the fact that it only occurs at a narrow concentration range as it is less likely to happen at high or low 1-MPHA concentrations, where ordering is hampered by availability. The fact that the two maxima form a plateau means that the separation is not complete but rather partial in various stages of perfection, from mixed to separated. One expects therefore various stages of enrichment in the separation, depending on 1-MPHA placement in the chains and the amount of dilution by interstitial MMA insertions.

4.4.3 Kinetics of the copolymerisation of 1-MPHA with MMA

Figure 4.8 shows plots of monomer consumption as a function of time for MMA and 1-MPHA for the three molar feed ratios used in the *in situ* NMR polymerisations. The reaction conditions were: $f_{MMA} = 0.62$ (0.79 mmol MMA, 0.49 mmol 1-MPHA), $f_{MMA} = 0.39$ (0.42 mmol MMA, 0.67 mmol 1-MPHA) and $f_{MMA} = 0.23$ (0.23 mmol MMA, 0.75 mmol 1-MPHA). The reactions were initiated with 3.6 mg of AIBN in 0.39 mL deuterated toluene at 70 °C. There is a rapid consumption of both monomers for the system containing 0.62 MMA: 0.38 1-MPHA molar feed fractions.

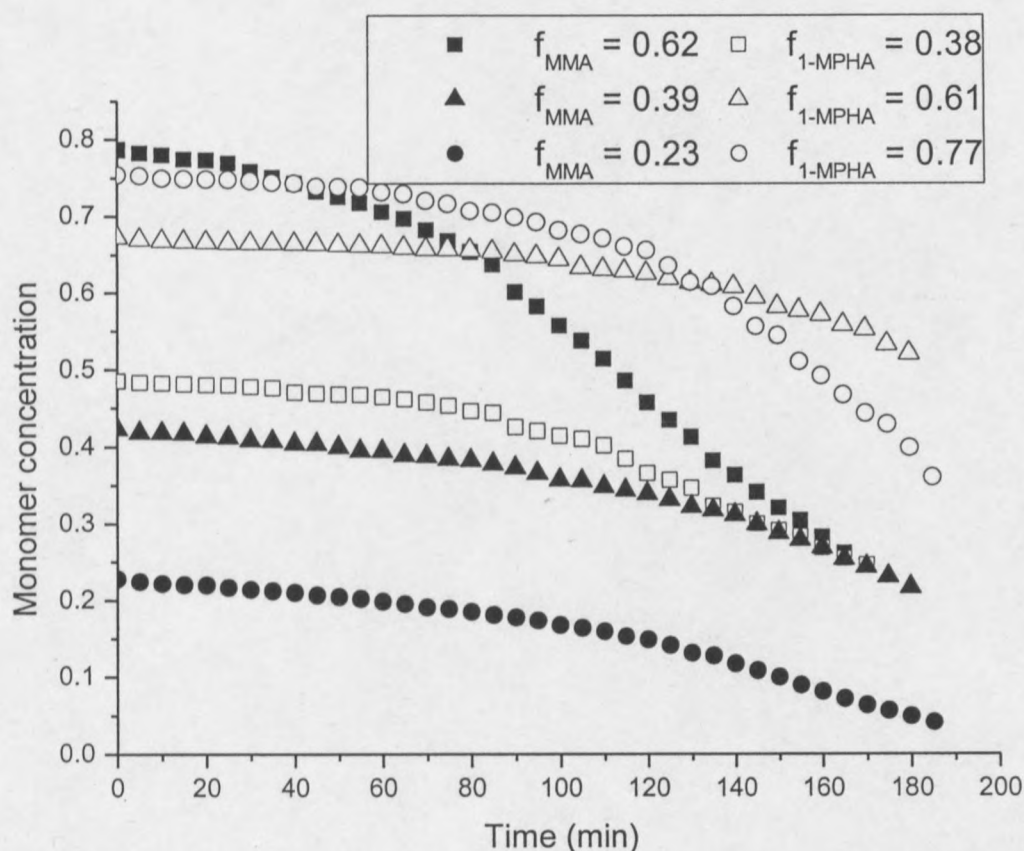


Figure 4.8: ^1H NMR signal versus time for the *in situ* ^1H NMR copolymerisation of 1-MPHA with MMA. The solid symbols represent MMA and the open symbols represent 1-MPHA.

A plot of the relative reaction rate for the three NMR *in situ* copolymerisation reactions for the 1-MPHA/MMA system is shown in Figure 4.9. The reaction containing 62 mole% MMA (highest content) in the starting feed showed the most rapid consumption of the 1-MPHA monomer whereas the reaction containing 23

mole% MMA (lowest content) in the starting feed showed an intermediate rate in the consumption of the 1-MPHA monomer. In Figure 4.9, it was observed that the faster the rate at which the MMA monomer was consumed, the faster also the rate at which the 1-MPHA monomer was consumed.

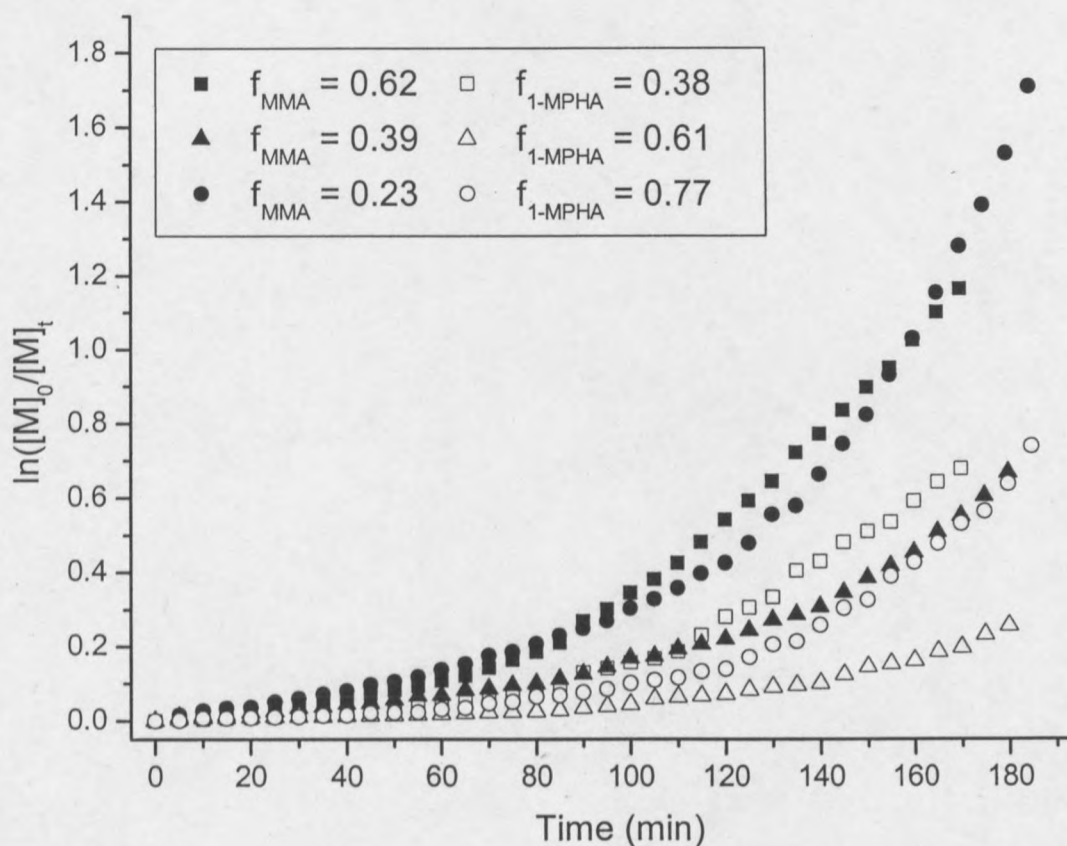


Figure 4.9: Rate of monomer consumption as a function of time for the *in situ* kinetic reactions in the copolymerisation of 1-MPHA with MMA. The solid symbols are MMA and the open symbols are for 1-MPHA.

The plot of monomer fraction as a function of theoretical (Eq. 4.8) and experimental (processed in Eq. 4.9) conversion data in Figure 4.10 was used to estimate the reactivity ratios for the copolymerisation of 1-MPHA and MMA. The results for the three monomer fraction compositions are tabulated in Table 4.4. The optimum reactivity ratios are obtained by minimising the sum of squares of the residuals between the experimental and theoretical conversion. The combined reactivity ratios are obtained by combining the three data sets and minimising the sum of squares of the residuals between the experimental and theoretical conversion for the whole set.

According to Van den Brink *et al*^[14] and Plaumann *et al*^[4] at least two experiments are needed to get a good estimate of the reactivity ratios. The experiments should be carried out at very different starting feed compositions and in this study the feed compositions chosen at 23 and 62 mole% MMA are very different and the choice was also informed by the estimates from the Tidwell-Mortimer^[5] equations (Eq. 4.3 and 4.4). There is a good fit between the theoretical and experimental conversion data.

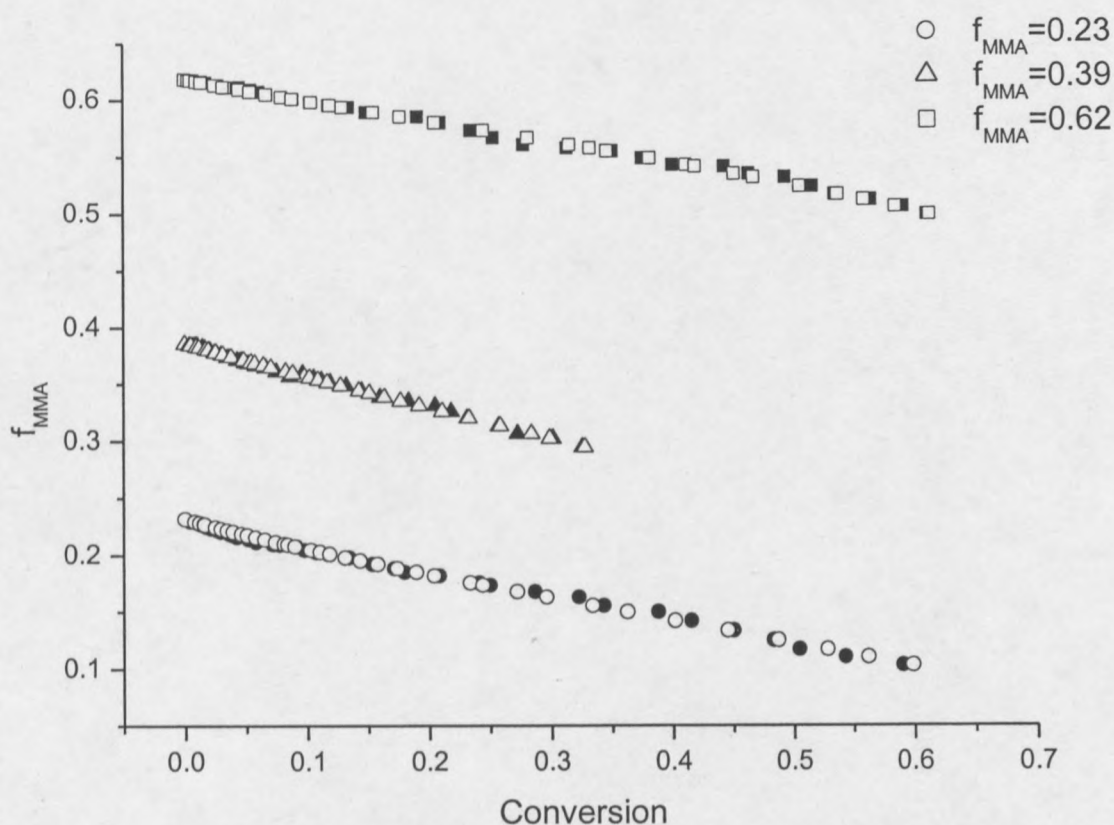


Figure 4.10: Mole fraction MMA in feed as a function of experimental and calculated conversion from *in situ* NMR studies by monitoring double bond signals with time (solid markers – experimental conversion: Equation 4.9 and open markers – calculated conversion: Equation 4.8).

Table 4.4: Results of the reactivity ratio determination

Reaction	n	f_{MMA}	r_{MMA}	r_{1-MPHA}	S
1	38	0.23	2.03 [1.94–2.11]	0.57 [0.56-0.59]	0.005
2	37	0.39	1.97 [1.81–2.24]	0.61 [0.58-0.64]	0.001
3	35	0.62	1.26 [1.25–1.26]	0.82 [0.82-0.83]	0.006
Combined	110		2.31 [2.26–2.40]	0.15 [-0.05-0.2]	0.171

- the numbers in the square brackets are the range of the reactivity ratios and S is the contour that encloses the 95% confidence level region. n is the number of data points used in the calculations.

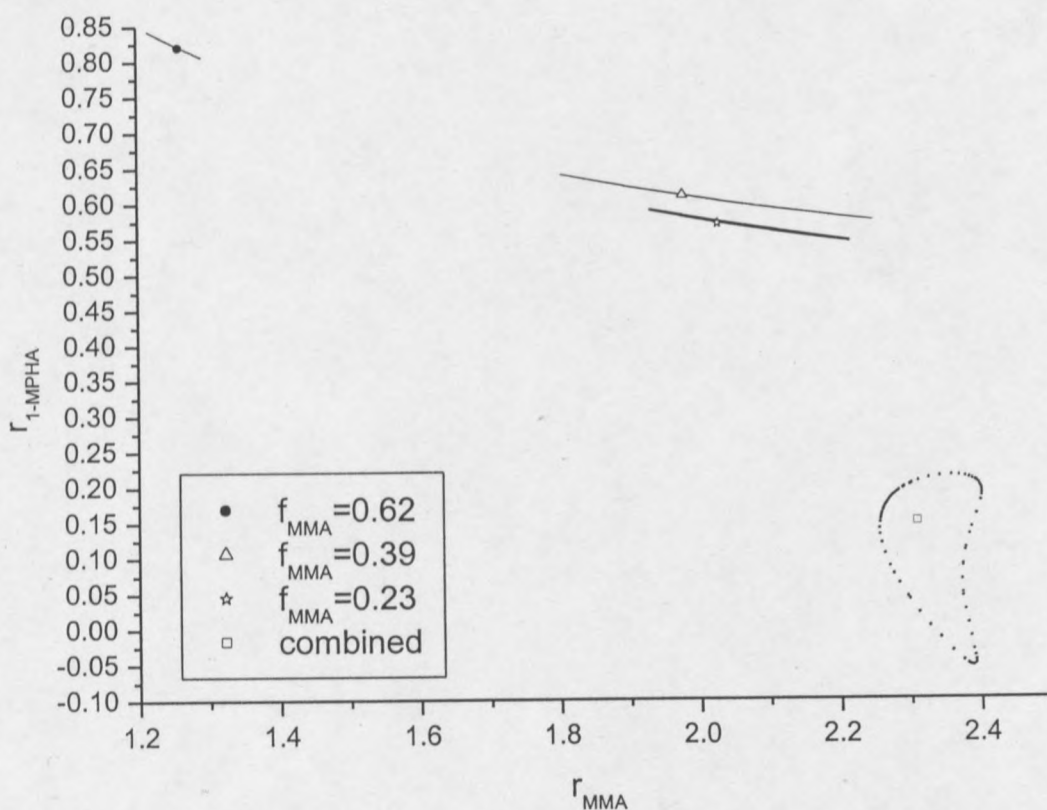


Figure 4.11: A plot of the confidence regions for the reactivity ratios of the MMA/1-MPHA copolymer system.

The calculation method used to determine the reactivity ratios does not discriminate between the various copolymerisation models. The values obtained for the r_{MMA} and r_{1-MPHA} were 2.31 [2.26-2.40] and 0.15 [-0.05-0.2] respectively. Figure 4.11 shows

the confidence regions for the reactivity ratios at the three starting feed ratios and also for the combined data. The individual confidence regions are very narrow and elongated along the horizontal axis. The confidence region for the combined data is broader than for the individual data sets. There is a variation in the reactivity ratios with feed ratio of MMA in the starting feed for the individual reaction sets. A high content of MMA in the starting feed generally led to a high r_{1-MPHA} and a low r_{MMA} value.

The variation in the reactivity ratios between the different runs at the different feed compositions might be indicative of a penultimate unit kinetic behaviour. The penultimate unit effect might be expected in the MMA/1-MPHA system as the 1-MPHA monomer is highly bulky and therefore can cause steric hindrance. This means that chains rich in 1-MPHA and having MMA as the terminal monomer would find it difficult to add another 1-MPHA monomer because of the steric repulsion between the 1-MPHA monomer in the propagating chain and the incoming 1-MPHA monomer.

4.4 Conclusions

1-Methyl-propyl-hexyl acrylate (1-MPHA) was successfully copolymerised with methyl methacrylate (MMA) over a wide composition range. There is limited incorporation of 1-MPHA into the copolymer chain; about 25 mole% of 1-MPHA is incorporated when the initial feed contained about 90 wt% 1-MPHA. This limitation in incorporation is surmised to be due to the steric hindrance of the 1-MPHA monomer, reducing its propagation rate coefficients.

The thermogravimetric data shows an increase in the stability of the copolymers with increasing MMA content. Presence of 1-MPHA results in residue above 400 °C in poly-(1-MPHA-co-MMA) polymers. The DMA data shows that an increase in 1-MPHA dramatically reduces the T_g onset, with very little change in storage modulus below T_g . The deviations in the thermal behaviour of the copolymers from that of the homopolymers proves that the copolymers made were true copolymers.

The kinetic data gives a good fit between the theoretical and experimental conversion data and the reactivity ratios at 70 °C were estimated to be $r_{MMA} = 2.31$ [2.26-2.40] and $r_{I-MPHA} = 0.15$ [-0.05-0.2].

4.5 References

1. Stergiou, G., Dousikos, P., and Pitsikalis, M., *Eur. Polym. J.*, 2002. **38**: p. 1963 - 1970.
2. Selvamalar, C. S. J., Krithiga, T., Penlidis, A., and Nanjundan, S., *Reactive and Functional Polymers*, 2003. **56**: p. 89 - 101.
3. Plaumann, H. P. and Branston, R. E., *J. Polym. Sci. Part A: Polym. Chem.*, 1989. **27**: p. 2819 - 2822.
4. Wall, F. T., *J. Am. Chem. Soc.*, 1944. **66**: p. 2050 - 2057.
5. Tidwell, P. W. and Mortimer, G. A., *J. Polym. Sci. Part A: Polym. Chem.*, 1965. **3**: p. 369 - 387.
6. Dube, M. A., Sanayei, R. A., Penlidis, A., O'Driscoll, K. F., and Reill, P. M., *J. Polym. Sci. Part A: Polym. Chem.*, 1991. **29**: p. 703 - 708.
7. Mayo, F. R. and Lewis, F. M., *J. Am. Chem. Soc.*, 1944. **66**: p. 1594 - 1601.
8. Aguilar, M. R., Gallardo, A., del Mar Fernandez, M., and Roman, J. S., *Macromolecules*, 2002. **35**(6): p. 2036 - 2041.
9. Ito, H., Dalby, C., Pomerantz, A., Sherwood, M., Sata, R., Sooriyakumaran, R., Guy, K., and Breyta, G., *Macromolecules*, 2000. **33**: p. 5080 - 5089.
10. Ito, H., Miller, D., Sveum, N., and Sherwood, M., *J. Polym. Sci. Part A: Polym. Chem.*, 2000. **38**: p. 3521 - 3542.
11. Meyer, V. E. and Lowry, G. G., *J. Polym. Sci. Part A: Polym. Chem.*, 1965. **3**: p. 2843 - 2851.
12. Box, G. E. P., Hunter, W. G., and Hunter, J. S., *Statistics for Experimenters - An Introduction to Design, Data Analysis and Model Building*. 1978, New York: John Wiley & Sons, Inc. 485.

13. Mathakiya, I., Rao, P. V. C., and Rakshit, A. K., *J. Appl. Polym. Sci.*, 2001. **79**: p. 1513 - 1524.
15. van den Brink, M., Smulders, W., van Herk, A. M., and German, A. L., *J. Polym. Sci. Part A: Polym. Chem.*, 1999. **37**: p. 3804 - 3816.

CHAPTER 5

COPOLYMERISATION OF 1-METHYL-1-PROPYL-HEXYL ACRYLATE WITH VINYL ACETATE

5.1 Introduction

The importance of copolymerisation has been discussed in Section 4.1 of Chapter 4. Emulsions of polyvinyl acetate find industrial applications in exterior and interior architectural coatings, adhesives and paints^[1, 2]. Copolymerisation of vinyl acetate with other monomers such as vinyl chloride^[3] and acrylates^[1] produce useful latexes having a wide range of properties. The vinyl acetate/butyl acrylate emulsion copolymer is one of the most important industrial latexes, that is widely used in the architectural coatings market. This system has been a subject of investigation by a number of workers, e.g. mechanism of degradation^[4] and kinetic studies^[5].

Emulsion copolymers of vinyl acetate and VEOVA 10 (vinyl ester of a highly branched decanoic acid, Shell Trade mark^[6] (note: this is a mixture of isomers)) are widely used for architectural paints, including those for indoor decoration based on highly pigmented emulsion paints (i.e. containing a high proportion of pigments plus low cost extenders and having a pigment volume concentration (PVC) of about 80%)^[7].

The use of VEOVA 11^[8] as a comonomer finds wide application in coatings. Hydrophobicity is one of the properties that are of interest. The effect of copolymerising small amounts of 1-MPHA on the properties of vinyl acetate copolymers is of interest because 1-MPHA is an acrylate analogue of VEOVA 11, which is a vinyl ester of versatic acid 11, a synthetic monocarboxylic acid of a highly branched alkane structure containing eleven carbon atoms. The hydrophobicity of the poly-(1-MPHA-co-VAc) polymers was therefore also investigated.

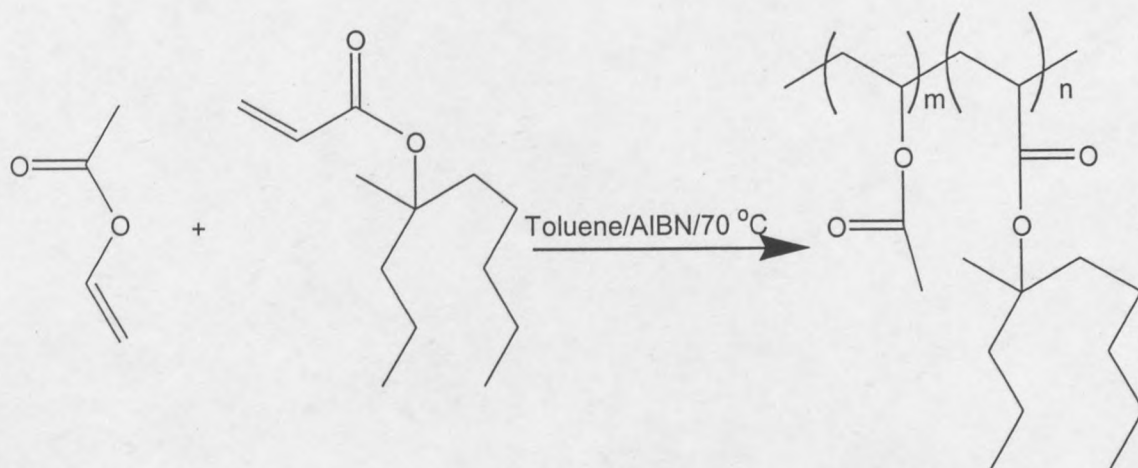
5.2 Experimental

5.2.1 Reagents used

The 1-methyl-propyl-hexyl acrylate (1-MPHA) monomer was synthesised and purified as detailed in Chapter 3, Section 3.2. The vinyl acetate, VAc (Merck, 96%) was purified by distillation under reduced pressure. The initiator azobis-isobutyronitrile, (AIBN, Delta Scientific, 98%) was recrystallised from methanol and dried under vacuum. The toluene solvent was dried and distilled over sodium metal flakes. Benzophenone was used as indicator to determine complete drying.

5.2.2 Copolymerisation of VAc with 1-MPHA

The polymerisation reactions were carried out in Schlenk tubes. The initial monomer feed compositions contained 2, 4, 8 and 16 wt% 1-MPHA, with the remainder being vinyl acetate. The total monomer concentration was 50 wt% in toluene. AIBN at 2 wt% with respect to total monomer was used as initiator. Scheme 5.1 shows a scheme for the copolymerisation process. The structure of the copolymer depicted does not represent a block copolymer.



Scheme 5.1: Schematic representation of the copolymerisation of 1-MPHA with VAc.

The sealed Schlenk tubes were subjected to three freeze-pump-thaw cycles before immersion in an oil bath thermostated at 70 °C. The reactions were allowed to run for 18 hours.

The reaction products were obtained by adding the reaction mixture into a five-fold excess hexane to precipitate the copolymers. The copolymers were purified by dissolving the filtered precipitate in chloroform and reprecipitating in hexane three times. Samples were then analysed by GPC, NMR, TGA and DMA.

5.2.3 Analyses

The copolymers were characterised by ^1H and ^{13}C NMR, gel permeation chromatography, thermogravimetry and dynamic mechanical analysis. These analytical procedures were detailed in Section 3.2.2.

Hydrophobicity tests were performed on the copolymers by measuring the contact angle when a drop of distilled water is put on the surface of the copolymer sample. In order to ensure a uniform surface, the copolymer films were obtained by spin coating the copolymer samples dissolved in chloroform onto a glass substrate. Under a magnifying glass, the film surfaces were smooth and uniform. No further surface analysis was undertaken. The samples were dried under vacuum at room

temperature for 24 hours before the tests were carried out. A digital camera was used to take pictures of the water droplets (put on the copolymer samples with a 1 μ L syringe) through a magnifying glass. An average of five measurements was reported. The captured images were transferred to a computer in order to measure the width and the height of the droplet using the Microsoft Photo Editor® 3.0.2.3 program.

The solubility parameter of the copolymers (δ) was estimated using the methods proposed by van Krevelen^[9] by considering the group contributions.

5.2.4 Determination of the kinetics of copolymerisation of VAc with 1-MPHA

In order to study the kinetics of the copolymerisation of 1-MPHA with VAc, *in situ* ^1H NMR copolymerisations were conducted. Three initial feed compositions were considered, $f_{1\text{-MPHA}} = 0.3, 0.59$ and 0.76 . The reactions were initiated with 2 wt% AIBN and the solutions were made to 50 wt% solution in deuterated toluene. Pyrazine was used as the internal standard. The reactions were run at 70 °C *in situ* in a 600 MHz NMR instrument. Figure 5.1 shows the double bond peaks of the comonomers, the intensities of which were monitored in order to quantify the monomer consumption.

The monomer concentrations for 1-MPHA and VAc monomers were calculated using equations 5.1 and 5.2 respectively:

$$C_{1\text{-MPHA}} = \frac{H_1 + H_2 + H_3}{3R} \times C_{1\text{-MPHA},0} \quad (5.1)$$

$$C_{\text{VAc}} = \frac{H_4 + H_5 + H_6}{3R} \times C_{\text{VAc},0} \quad (5.2)$$

H_1 to H_3 are areas due to the resonance peaks of the 1-MPHA comonomer and H_4 to H_6 are areas due to the peaks of vinyl acetate, R is the area due to pyrazine, the

internal standard, $C_{1-MPHA,0}$ and $C_{VAc,0}$ are the initial concentrations of 1-MPHA and VAc monomers respectively.

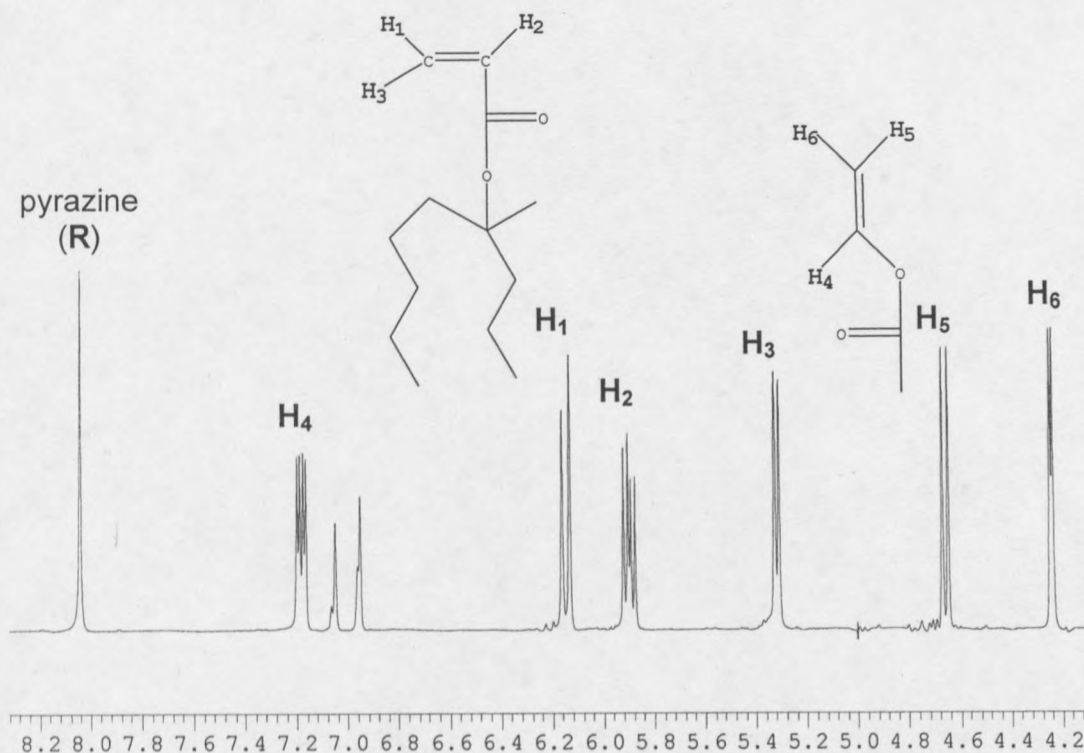


Figure 5.1: ¹H NMR spectrum showing the peaks used to monitor monomer consumption in the *in situ* NMR copolymerisation of 1-MPHA with VAc.

5.3 Results and Discussion

5.3.1 Chemical analyses

5.3.1.1 NMR

Figure 5.2 shows an overlay of the ¹H NMR spectra for copolymers of vinyl acetate containing 2 and 8 mole% of 1-MPHA. The composition of the copolymers as the amount of incorporation of 1-MPHA into vinyl acetate was determined by using the peak at 4.82 ppm, corresponding to one proton of the backbone of vinyl acetate, and the total integrated peak intensity of the entire spectrum. Equation 5.3 below is based on the six protons of VAc and the twenty four protons of 1-MPHA, with the one

backbone proton in polyvinyl acetate resonating at 4.82 ppm unambiguously assigned^[10]:

$$\frac{\text{Intensity of VAc backbone proton } (I_{\text{CH}})}{\text{Intensity of total protons } (I_{\text{T}})} = \frac{m_2}{6m_2 + 24m_1}$$

$$\frac{I_{\text{CH}}}{I_{\text{T}}} = \frac{m_2}{6m_2 + 24(1 - m_2)}$$

$$m_2 = \frac{24I_{\text{CH}}}{18I_{\text{CH}} + I_{\text{T}}} \quad (5.3)$$

where m_2 is the mole fraction of vinyl acetate in the copolymer, $m_1 = 1 - m_2$, is the mole fraction of 1-MPHA in the copolymer, I_{CH} is the integrated peak intensity for the backbone proton due to VAc in the copolymer and I_{T} is the total integrated peak intensity of the protons measured.

The incorporation data is given in Table 5.1. There is an increase in the amount of 1-MPHA incorporated in the copolymer as the amount of 1-MPHA in the starting feed increases.

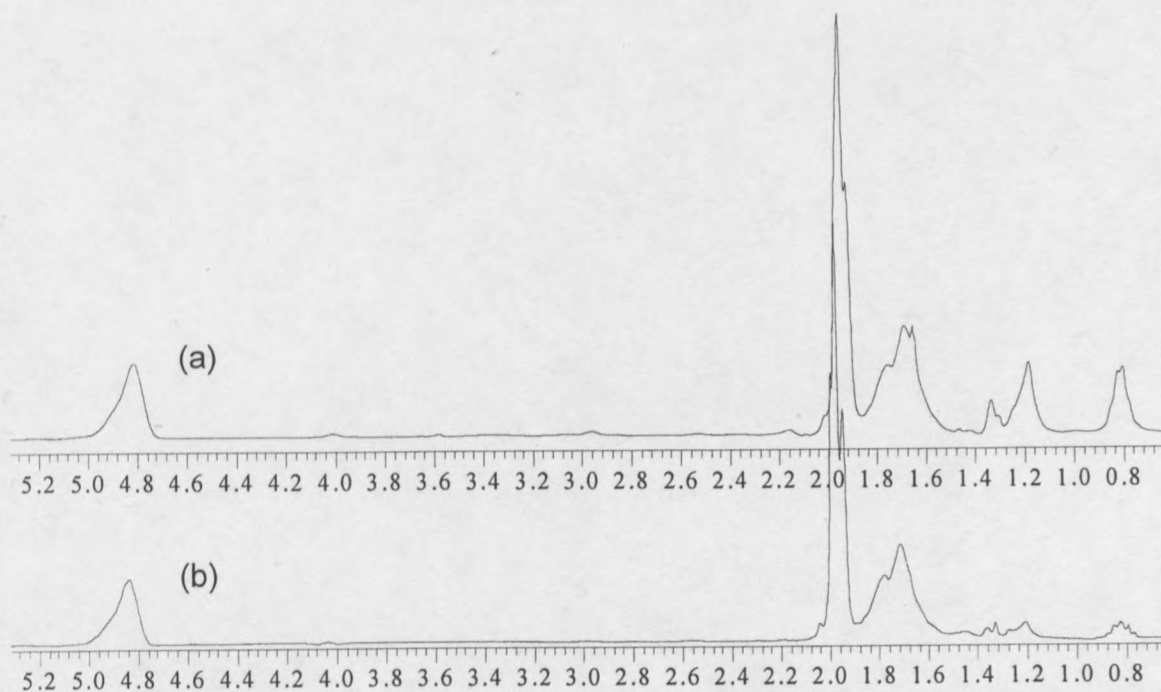


Figure 5.2: ¹H NMR spectra for the poly-(1-MPHA-co-VAc) polymers with copolymer compositions (a) 8 and (b) 2 mole% 1-MPHA.

5.3.1.2 GPC

The molecular weight data for the copolymers as determined by GPC with polystyrene standards is presented in Table 5.1. The copolymers have low molecular weight and a narrow polydispersity index. There is a slight decrease in the molecular weight and an increase in polydispersity index with an increase in the amount of 1-MPHA incorporated. It should be noted that the values reported in Table 5.1 can not be regarded as the absolute values of the molar mass data as they are calculated with reference to a polystyrene calibration curve and not corrected.

Table 5.1: Chemical analysis data for poly-(1-MPHA-co-VAc) polymers

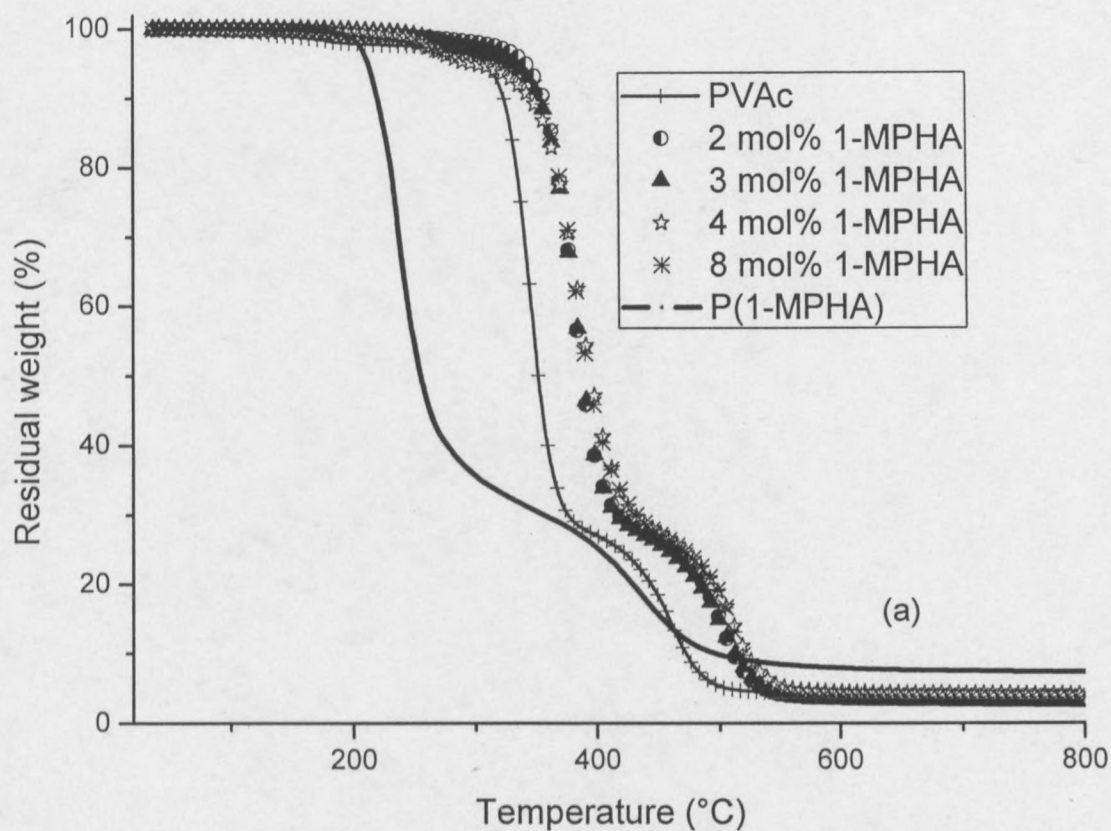
Sample	F_{1-MPHA} (mole%)	\bar{M}_n	\bar{M}_w	PDI
DVac-2	2	9500	15500	1.6
DVac-3	3	8100	14000	1.7
DVac-4	4	6600	13500	2.0
DVac-8	8	6800	12800	1.9

5.3.2 Thermal analyses

5.3.2.1 TGA

Figure 5.3 (a) shows the plot of the residual weights of the poly-(1-MPHA-co-VAc) polymers as a function of temperature. The copolymers seem to be more stable than the homopolymers as the decomposition temperatures are higher than for the individual homopolymers. Duquesne *et al*^[4] also observed a stabilisation in vinyl acetate and butyl acrylate copolymers which they said might result from either a crosslinking promoting reaction or a modification of the kinetics of degradation. In the composition range investigated, the copolymers show a two stage decomposition mechanism which is similar to that of polyvinyl acetate; the major component. The

copolymers with 4 and 8 mole% 1-MPHA show an early decomposition as shown in the expanded figure in Figure 5.3 (b) but above 400 °C they show better thermal stability. The deviation of the decomposition behaviour of the copolymers from that of the homopolymers proves that the polymers formed are true copolymers.



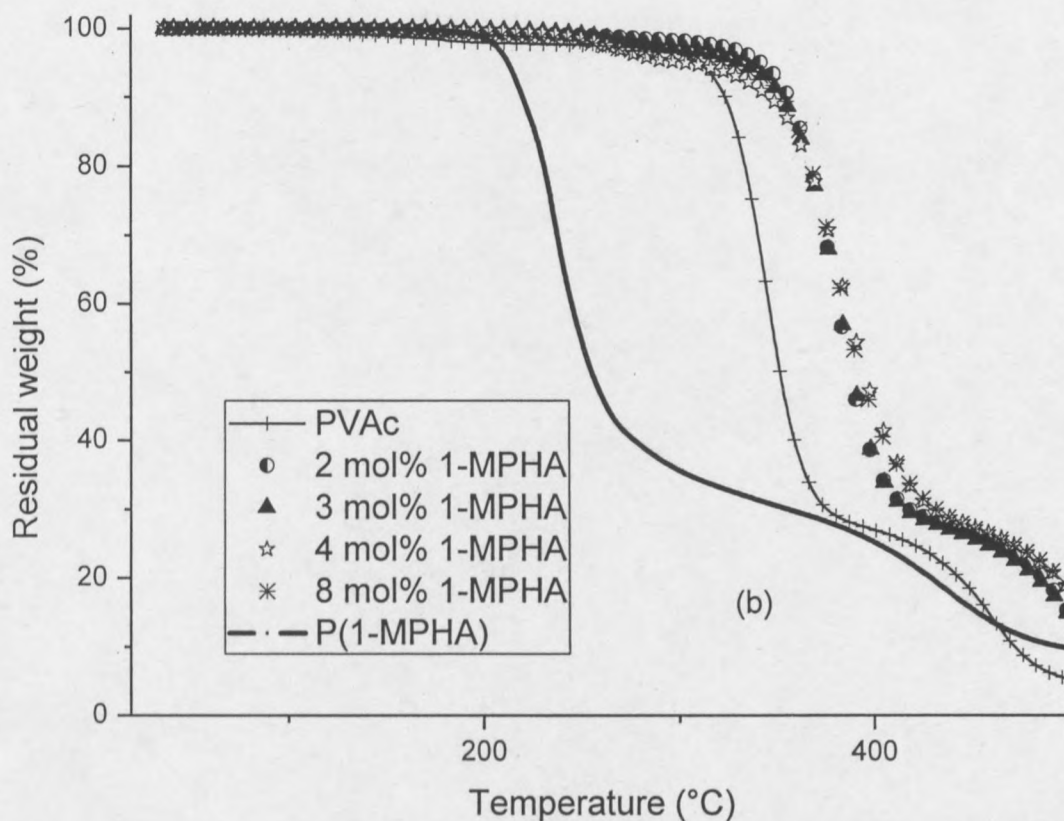


Figure 5.3: Plots of the TGA data for the poly-(1-MPHA-co-VAc) polymers (a) over the whole temperature range and (b) showing the early decomposition in samples containing high 1-MPHA content.

5.3.2.2 DMA

Figure 5.4 shows the plot of the storage modulus as a function of temperature for the poly-(1-MPHA-co-VAc) copolymers. There is an increase in storage modulus as the amount of 1-MPHA increases in the samples from 2 mole% in DVAc-2 to 8 mole% in DVAc-8. The storage modulus results are summarised in Table 5.2. The 1-MPHA comonomer contributes towards the stiffening of the copolymers. This could be due to the increased entanglement that results from the long and branched chain structure of the 1-MPHA comonomer. There is a strong synergistic effect from both monomers as the storage modulus of both homopolymers is lower than that of the copolymers. It is surmised that in the temperature range studied the 1-MPHA homopolymer is already approaching its glass transition temperature and hence the low storage modulus but when it is used as a property modifier to vinyl acetate, the vinyl acetate offers the necessary support as the polyvinyl acetate has a high glass transition temperature 45 °C.

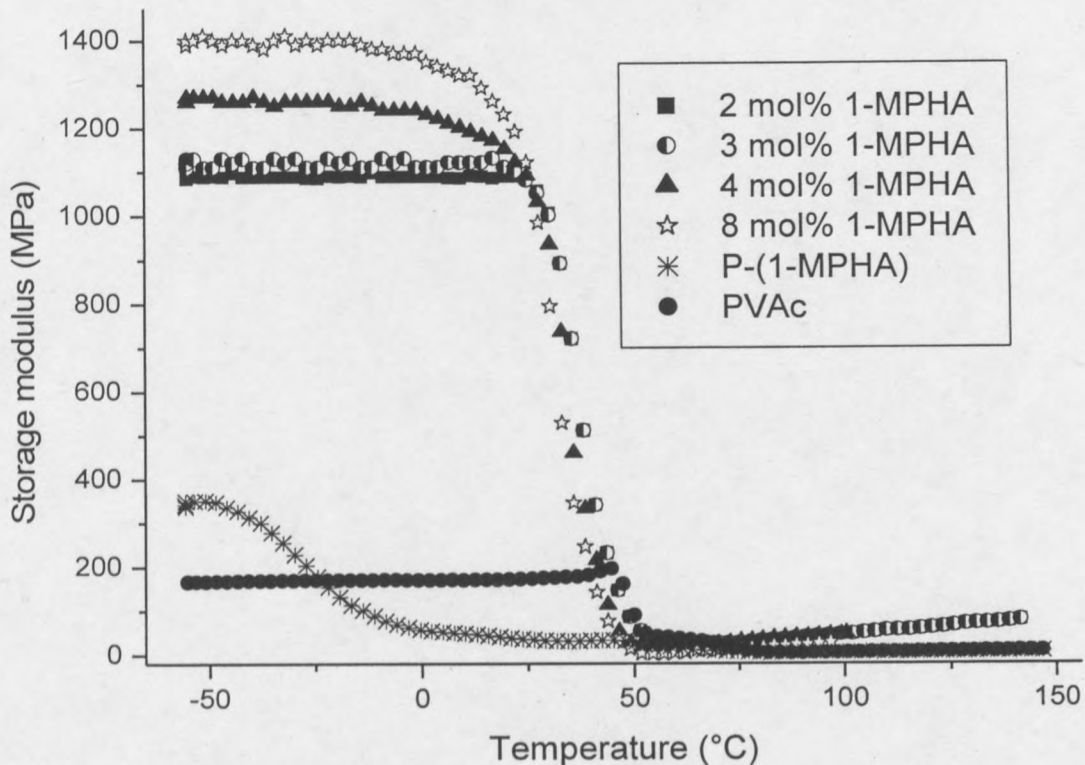


Figure 5.4: Storage modulus as a function of temperature for the poly-(1-MPHA-co-VAc) polymers.

Figure 5.5 is a plot of tan delta against temperature for the poly-(1-MPHA-co-VAc) copolymers. The glass transition temperature decreases slightly with increasing 1-MPHA fraction in the copolymer. The glass transition temperature taken as the maximum of the peak in the tan delta trace is presented in Table 5.2. At 2 mole% 1-MPHA (DVAc-2) there is a significant lowering in T_g of polyvinyl acetate from 54 to 40.5 °C. There is a drop of about 5 °C in the T_g taken as the maxima in the tan delta traces from the DVAc-2 to DVAc-8 which contain 2 and 8 mole% 1-MPHA in the copolymers. The deviations in the T_g 's of the copolymers from the T_g 's of the homopolymers is further evidence that the polymers made are true copolymers.

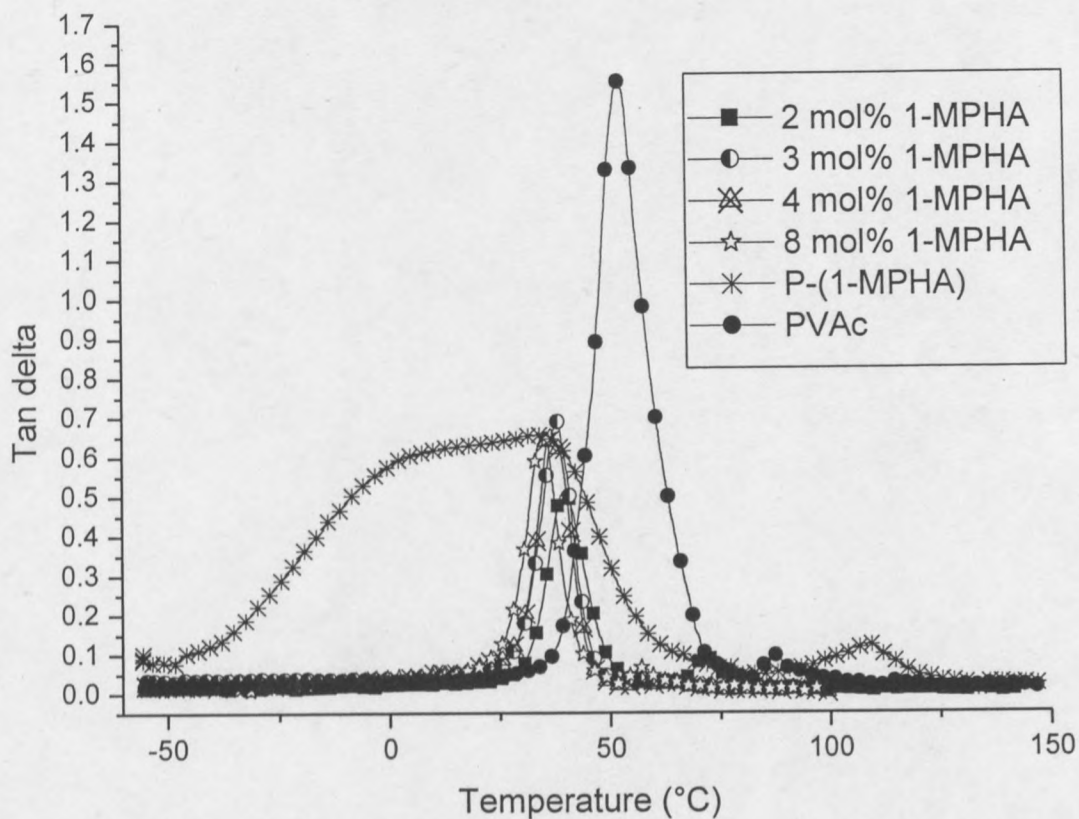


Figure 5.5: A plot of tan delta as a function of temperature for the poly-(1-MPHA-co-VAc) polymers.

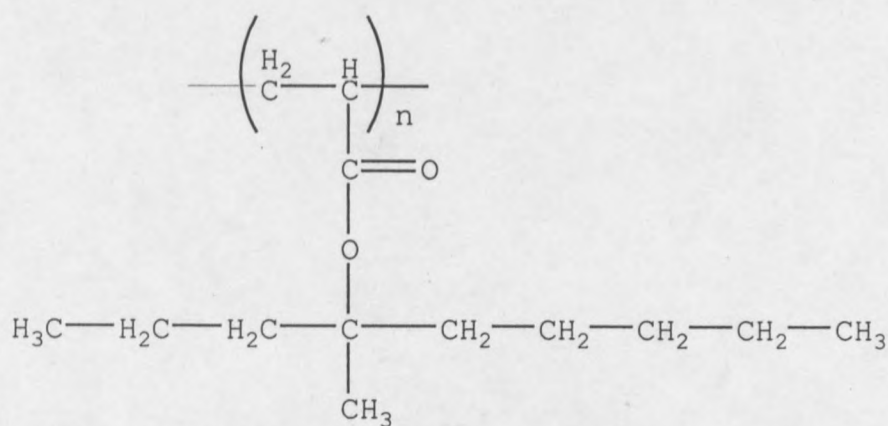
Table 5.2: Summary of the DMA results for the poly-(1-MPHA-co-VAc) polymers and poly-(1-MPHA).

Sample	Storage modulus (MPa) at -50 °C	Glass transition temperature (°C)
DVAc-2	1088	40.5
DVAc-3	1090	38.6
DVAc-4	1269	37
DVAc-8	1389	36
P(1-MPHA)	350	-46
PVAc	195	54

5.3.3 Physical analysis

5.3.3.1 Determination of solubility parameters

The solubility parameter δ (equation 5.5) quantifies the strength of the bonds between the components of a material. It is related to the square root of the cohesive energy, E_{COH} , (equation 5.4) which is the energy required to break all of the intermolecular physical links in a unit volume of the material^[11]. In low molecular weight liquids E_{COH} is easily calculated from the molar heat of evaporation or from the vapour pressure as a function of temperature. High molecular weight polymers present a problem as they do not evaporate. Tables for the estimation of group contribution to estimate E_{COH} for polymers are available^[9, 11]. In order to predict the solubility parameter of 1-MPHA, the methods of van Krevelen were used by considering the group contributions of poly-(1-MPHA) represented in Scheme 5.2 below^[9]. The solubility of a polymer in a given solvent is dependent on the similarity between the δ values of the polymer and the solvent. Factors such as crosslinking, crystallinity and increasing molecular weight generally tend to reduce the solubility of a polymer.



Scheme 5.2: A schematic of poly-(1-MPHA) showing the various groups that contribute to the solubility parameter.

Table 5.3: Group contributions to the solubility parameter of poly-(1-MPHA)

Group contribution	$\sum E_i$ (J/mol)	$\sum F_i$	$\sum V$ (J/cm ³)
3(-CH ₃)	3×9640	3×438	3×33.5
7(-CH ₂)	7×4190	7×272	7×16.1
1(-CH)	1×420	1×57	1×(-1)
1(-C)	1×(-5580)	1×(-190)	1×(-19.2)
1(-COO)	1×13410	1×634	1×18
Total	66500	3719	211

So, for poly-(1-MPHA), the solubility parameter calculated from the data in Table 5.3 is as follows:

$$E_{COH} = \frac{F^2}{V} = \frac{(3719)^2}{211} = 65550 \text{ J/mol} \quad (5.4)$$

$$\delta = \left(\frac{E_{COH}}{V} \right)^{0.5} \quad (5.5)$$

$$\therefore \delta = 17.6 - 17.8 \text{ J}^{1/2}/\text{cm}^{3/2}$$

E_{COH} is the cohesive energy, F is the molar attraction constant, V is the molar volume at room temperature and δ is the solubility parameter. Since E_{COH} tables are derived from experiments conducted at room temperature, the solubility parameter values are also reliable at or near room temperature^[11].

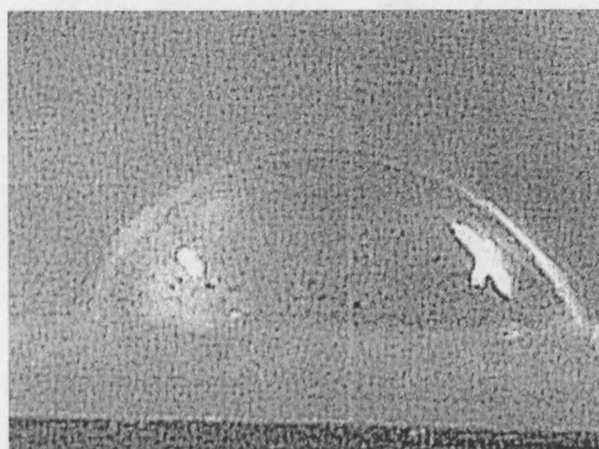
5.3.3.2 Determination of hydrophobicity

The hydrophobicity of the samples was measured by determining the contact angle of a water droplet on the copolymer sample. Images of the droplets used for the measurement of the hydrophobicity are shown in Figures 5.6 (a) and (b) for polyvinyl acetate homopolymer and the poly-(1-MPHA-co-VAc) copolymer with 8 mole% 1-MPHA incorporated. Five readings were taken and the average result is reported in Table 5.4. The contact angle was determined by measuring the width and the height of the droplet as follows in equation 5.6:

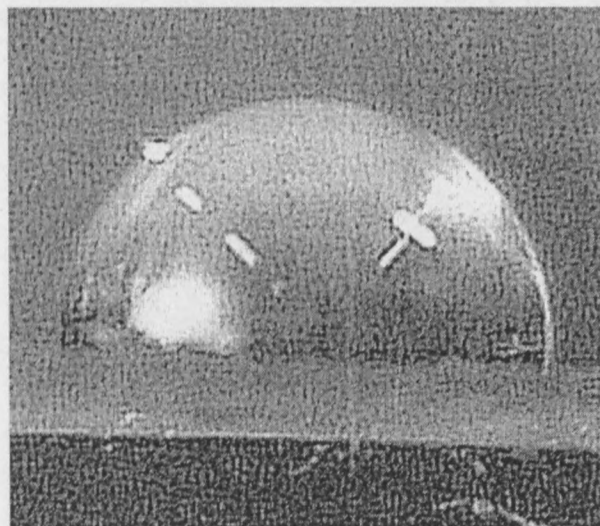
$$\tan\theta = 2 \times (H/W)$$

$$\theta = \tan^{-1}[2 \times (H/W)] \times 180/\pi \quad (5.6)$$

H is the drop height and W is the drop width.



(a)



(b)

Figure 5.6: Distilled water droplets on (a) polyvinyl acetate and (b) on a poly-(1-MPHA-co-VAc) polymer sample containing 8 mole% 1-MPHA spin-coated on a glass substrate.

The data in Table 5.4 shows a dramatic increase in the contact angle from the homopolymer of polyvinyl acetate to the copolymers of vinyl acetate and 1-MPHA, with an increase in the contact angle with increasing amounts of incorporated 1-

MPHA (F_{1-MPHA}). This trend indicates that the hydrophobicity of the copolymers increases with increasing 1-MPHA content. The initial increase in the contact angle between the homopolymer and the copolymers is rapid and then becomes gradual between the copolymer samples containing 3 and 8 mole% 1-MPHA content.

The increase in hydrophobicity with increasing weight fraction 1-MPHA in the copolymer can be attributed to the long branched hydrocarbon chain of the 1-MPHA monomer which is hydrophobic.

Table 5.4: Contact angle measurements for the poly-(1-MPHA-co-VAc) copolymers

Sample	F_{1-MPHA} (mole%)	Contact angle (°)
Polyvinyl acetate	0	70
DVAc-2	2	80
DVAc-3	3	87
DVAc-4	4	88
DVAc-8	8	93

5.3.4 Kinetics of the copolymerisation of 1-MPHA with VAc

The kinetics of the copolymerisation of 1-MPHA with vinyl acetate were studied. The monomer consumption data for both monomers is shown in Figure 5.7 as a function of time. In all the cases studied there is very little consumption of vinyl acetate. This would make the determination of the reactivity ratios inaccurate (under these feed conditions) as there is very little change in the concentration of the vinyl acetate. This behaviour suggests that in order to get a uniform copolymer microstructure, the reaction would have to be run under starve-feed conditions with 1-MPHA being introduced gradually into the reaction mixture.

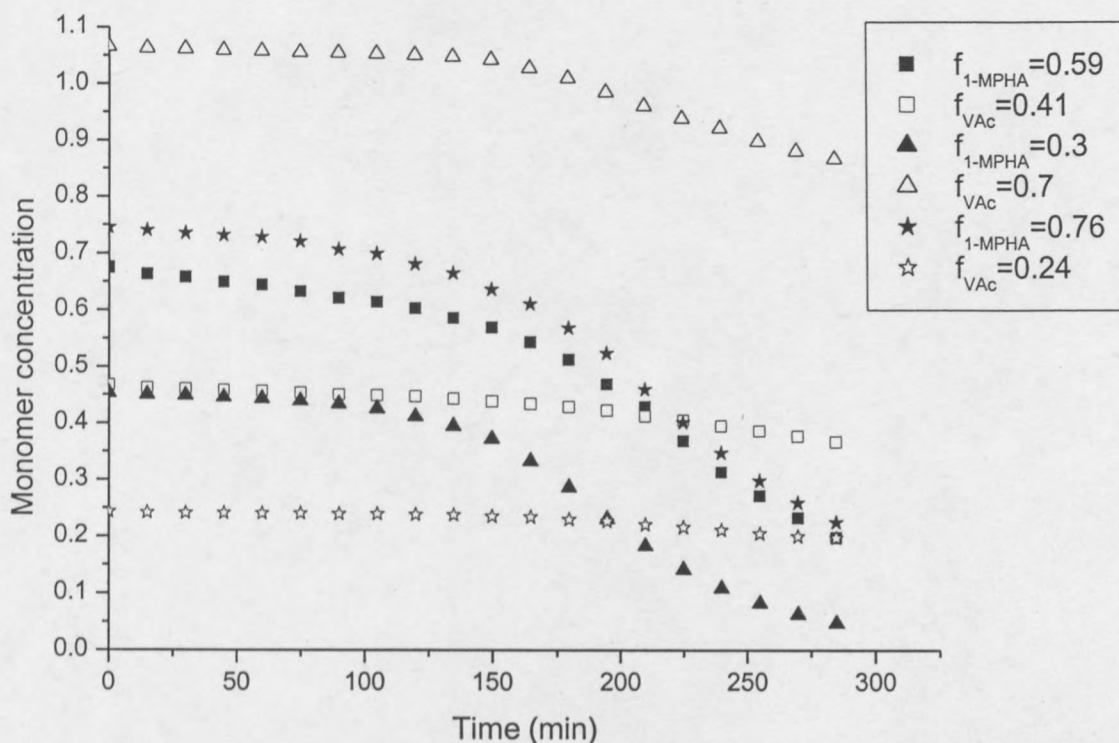


Figure 5.7: A plot of monomer consumption for both monomers as a function of time in the copolymerisation of 1-MPHA with VAc. The reactions were run at 70 °C *in situ* in an NMR instrument at 50 wt% solution in deuterated toluene with 2 wt% AIBN as initiator.

Figure 5.8 shows a plot of the rate of reaction for the three *in situ* reactions for the copolymerisation of 1-MPHA with VAc. In all three reactions there is very little change in the concentration of the vinyl acetate monomer. There is no correlation between the consumption rate of the vinyl acetate monomer and that of the 1-MPHA comonomer.

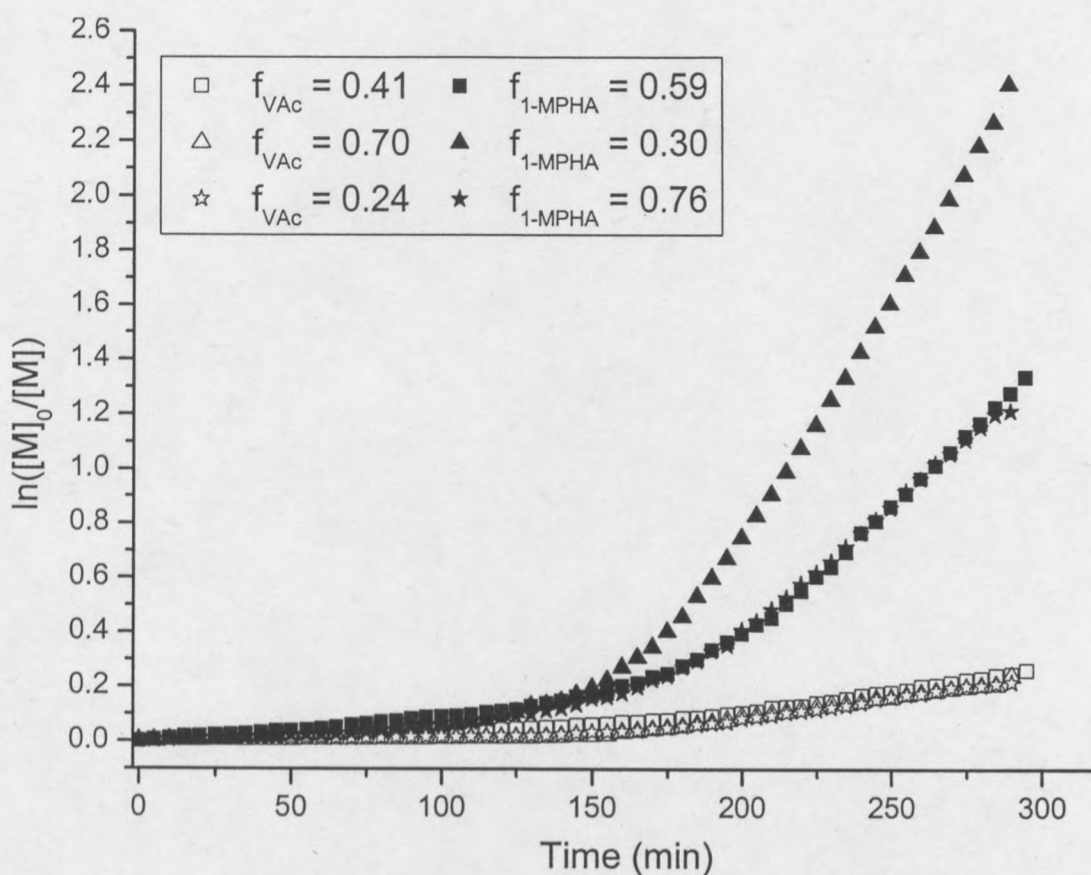


Figure 5.8: Reaction rate comparison for three 1-MPHA/VAc copolymerisation reactions carried out *in situ* an NMR instrument.

Figure 5.9 shows a plot of the 1-MPHA ratio in the monomer feed as a function of theoretical and experimental conversion which are obtained from the following equations discussed in Section 4.2.3 of Chapter 4.

$$X_{cal} = 1 - \left(\frac{f_1}{f_{10}} \right)^\alpha \left(\frac{1-f_1}{1-f_{10}} \right)^\beta \left(\frac{f_{10}-\delta}{f_1-\delta} \right)^\gamma \quad (5.7)$$

$$X_i = 1 - \frac{[M]}{[M]_0} \quad (5.8)$$

The optimum reactivity ratios are obtained by minimising the sum of squares of the residuals between the theoretical and experimental conversion, equations 5.7 and 5.8 respectively. The results for the reactivity ratio calculations are listed in Table 5.5. The theoretical and the experimental data in Figure 5.9 shows some systematic deviations which suggest that either the values of the reactivity ratios are not correct

or the model used is not appropriate. The very little change in the concentration of the vinyl acetate monomer that occurs during the reactions could be a contributing factor to the difficulty in obtaining good estimates for the reactivity ratios. The kinetic data can be best viewed as being qualitative as the low reactivity of the vinyl acetate makes it difficult to compute reliable reactivity ratios.

In general, at high initial 1-MPHA feed ratio ($f_{1-MPHA} = 0.75$ and 0.59) the numbers obtained for the reactivity ratio of the vinyl acetate comonomer are meaningless as they are negative. Sensible numbers are obtained for the reaction with the lowest initial 1-MPHA feed ratio ($f_{1-MPHA} = 0.30$) as reactivity ratios for both monomers are positive. The reactivity ratios obtained can not be used to predict reaction progress, the data at best shows that 1-MPHA is very reactive as compared to VAc. The combined reactivity ratios were obtained by combining the copolymerisation data from each of the reactions into one set of data and finding the optimum reactivity ratios by minimising the sum of squares of the residuals between the theoretical and experimental conversion. The uncertainty in the calculated reactivity ratios was determined as in Section 4.2.4 of Chapter 4 using equation 5.9^[12]:

$$S = S_r \left[1 + \frac{p}{n-p} F_{\alpha}(p, n-p) \right] \quad (5.9)$$

with S being the contour that encloses the uncertainty region, S_r is the sum of squares of the residuals, n is the number of data points, p is the number of parameters and $F_{\alpha}(p, n-p)$ is the F distribution at 95% confidence level.

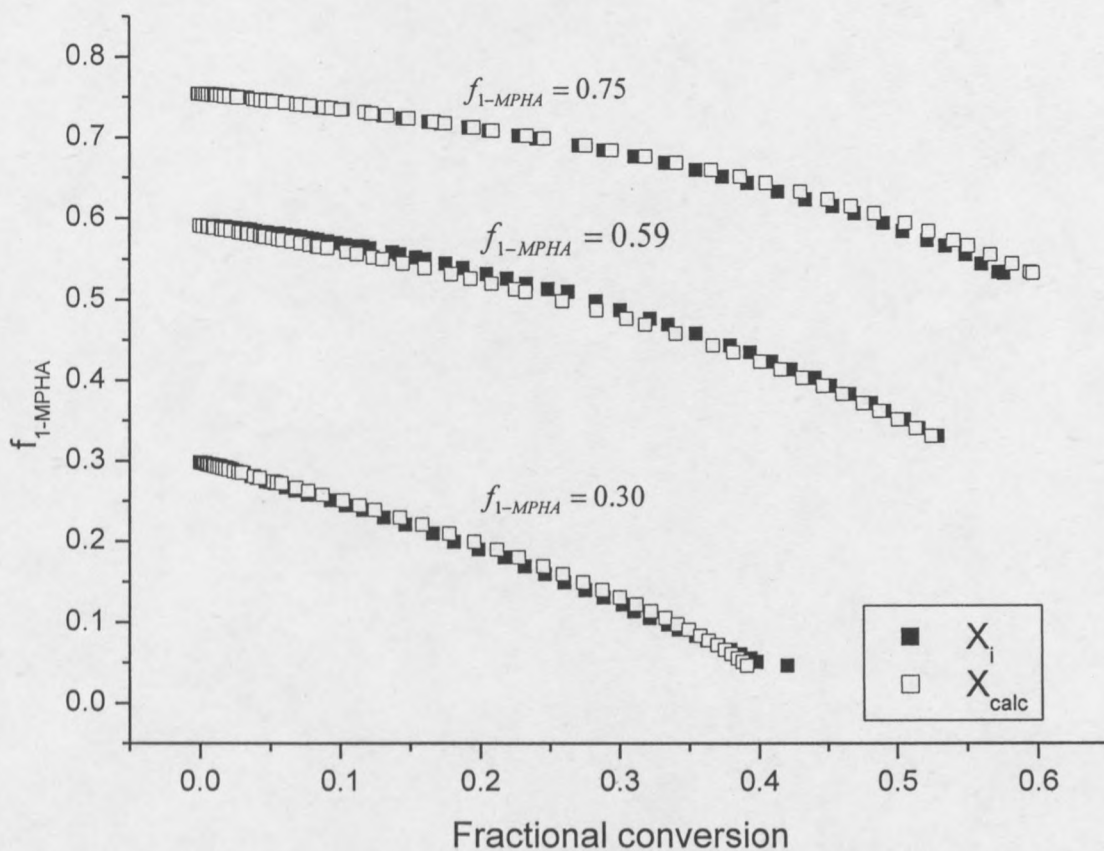


Figure 5.9: Plots of 1-MPHA ratio in the monomer feed as a function of theoretical and experimental conversion for three starting feed compositions. The data was obtained from *in situ* ^1H NMR studies of the copolymerisation of 1-MPHA with vinyl acetate. The reactions were conducted at 70 °C in deuterated toluene at 50 wt% solution with 2 wt% AIBN as initiator.

Table 5.5: Reactivity ratio results for the VAc/1-MPHA system obtained from *in situ* ^1H NMR studies at 70 °C in deuterated toluene at 50 wt% solution with 2 wt% AIBN as initiator

Experiment	n	$f_{1-MPHA,0}$	r_{1-MPHA}	r_{VAc}
1	59	0.30	7.47	0.0098
2	60	0.59	4.36	-1.37
3	59	0.75	4.37	-0.78
Combined	178		4.42	-0.07

5.4 Conclusions

1-Methyl-1-propyl-hexyl acrylate was successfully copolymerised with vinyl acetate. In the composition range that was investigated (2 – 16 wt% 1-MPHA), there was an apparent thermal stabilisation of the copolymers with increasing 1-MPHA content, as shown by the TGA results. The DMA results showed a significant drop (more than 10 °C) in T_g of the copolymers to that of the polyvinyl acetate homopolymer. The TGA and DMA results proved that the polymers that were made were true copolymers. The hydrophobicity tests show an increase in hydrophobicity with increasing 1-MPHA content. The reactivity ratios from the kinetic studies, $r_{1-MPHA} = 4.4$ and $r_{VAc} = 0.00$ were not quantitatively reliable. The data shows a rapid consumption of 1-MPHA relative to the vinyl acetate monomer.

5.5 References

1. Lazaradis, N., Alexopoulos, A. H., and Kiparissides, C., *Macromolecular Chemistry and Physics*, 2001. **202**(12): p. 2614.
2. Kong, X. Z., Pitchot, C., and Guillot, J., *Eur. Polym. J.*, 1988. **24**(5): p. 485.
3. Chen, D., Yuan, Y., Zhao, Q., Way, L., and Way, L., *J. Appl. Polym. Sci.*, 2000. **78**: p. 1057 - 1062.
4. Duquesne, S., Lefebvre, J., Delobel, R., Camino, G., LeBras, M., and Seeley, G., *Polymer Degradation and Stability*, 2004. **83**: p. 19 - 28.
5. Dube, M. A. and Penlidis, A., *Polymer*, 1995. **36**(3): p. 587.
6. *Resolution Performance Products, Product Data Sheet, VEOVA MONOMER 10*, <http://www.resins.com/resins/eu/pdf/VV 1.1>.
7. Unzue, M. J., Urretabizkaia, A., and Asua, J. M., *J. Appl. Polym. Sci.*, 2000. **78**: p. 475 - 485.
8. *Resolution Performance Products, Product Data Sheet, VEOVA MONOMER 11*, <http://www.resins.com/resins/eu/pdf/VV-1-VV 1.3>.

9. van Krevelen, D. W., *Properties of Polymers - Their correlation with chemical structure; their numerical estimation and prediction from additive group contributions*. 3rd ed. 1990: Elsevier, Amsterdam. p. 189.
10. Mathakiya, I., Rao, P. V. C., and Rakshit, A. K., *J. Appl. Polym. Sci.*, 2001. **79**: p. 1513 - 1524.
11. Bicerano, J., *Prediction of Polymer Properties*. 1993: Marcel Dekker, Inc., New York. p. 104.
12. Box, G. E. P., Hunter, W. G., and Hunter, J. S., *Statistics for Experimenters - An Introduction to Design, Data Analysis and Model Building*. 1978, New York: John Wiley & Sons, Inc. p. 485.

CHAPTER 6

CONCLUSIONS AND RECOMMENDATIONS

6.1 Conclusions

1-pentene was successfully dimerised using single site metallocene catalysis. The dimer of 1-pentene, 2-propyl-heptene, was successfully converted into the acrylic monomer, 1-methyl-1-propyl-hexyl acrylate (1-MPHA) via esterification of 4-methyl-nonan-4-ol, 4-MNOL. The structure of 1-MPHA was confirmed by NMR and FTIR data.

1-MPHA was successfully homopolymerised, as indicated by the GPC, NMR and FTIR data. ^1H NMR kinetic data revealed an extremely long induction period that was traced to the presence of a very low concentration of an impurity. Further purification of the monomer by a second pass through a silica gel column, using dichloromethane as the eluent (to remove the impurity) reduced the induction period.

Copolymerisation of 1-MPHA with a small amount of MMA (5 wt%) encouraged the homopolymerisation of 1-MPHA. Under these conditions the reaction proceeded rapidly because the MMA competes favourably with the impurity for radicals; the formed MMA-ended radicals could then add rapidly to 1-MPHA. When the impurity was completely removed from the monomer, homopolymerisation proceeded with no noticeable induction period.

TGA results for the homopolymer show thermal stability up to about 200 °C after which there is rapid degradation to about 40% of original mass at 300 °C. Poly-(1-MPHA) has a low T_g , making it attractive to use 1-MPHA as a comonomer for polymers with high T_g s or as an impact modifier to glassy polymers.

1-Methyl-propyl-hexyl acrylate (1-MPHA) was successfully copolymerised with methyl methacrylate (MMA) over a wide composition range at 70 °C. Methyl methacrylate was chosen as the comonomer because of it has been studied extensively and is very important commercially. There was a limited incorporation of 1-MPHA into the copolymer chain; about 25 mole% of 1-MPHA was incorporated when the initial feed contained about 90 wt% 1-MPHA. This limitation in incorporation is surmised to be due to the steric hindrance of the 1-MPHA monomer. Preliminary copolymerisation with other commercially available monomers such as glycidyl methacrylate and styrene was also successful. Results for these are reported in Appendices G and H.

The thermogravimetric data of all the copolymers showed an improvement in the thermal stability to that of the homopolymer of poly-(1-MPHA). The thermal stability improved with increasing MMA content towards the poly-MMA. The DMA data shows that an increase in 1-MPHA dramatically reduces the T_g onset with very little change in storage modulus below T_g . The insignificant change in storage modulus and the dramatic drop in T_g with increasing 1-MPHA content in the copolymers would give toughness at low temperature with stiffness that is comparable to PMMA.

The kinetic data at 70 °C gave a good fit between the theoretical and experimental conversion, and the reactivity ratios were estimated to be $r_{MMA} = 2.31$ [2.26-2.40] and $r_{1-MPHA} = 0.15$ [-0.05-0.2].

1-Methyl-1-propyl-hexyl acrylate was successfully copolymerised with vinyl acetate. Vinyl acetate was chosen as the comonomer because of its commercial significance. In the composition range that was investigated (2 – 16 wt% 1-MPHA), there was an apparent increase in thermal stability of the copolymers with increasing 1-MPHA content, as shown by the TGA results. The hydrophobicity tests show an increase in hydrophobicity with increasing 1-MPHA content. The reactivity ratios from the kinetic studies of the copolymerisation could not be reliably interpreted quantitatively. The data shows a rapid consumption of 1-MPHA relative to the vinyl acetate monomer.

6.2 Future work and recommendations

It has been demonstrated that the 1-methyl-1-propyl hexyl acrylate, 1-MPHA is a monomer that is capable of undergoing conventional free radical copolymerisation with comonomers such as methyl methacrylate and vinyl acetate. Glycidyl methacrylate and styrene were also successfully copolymerised with 1-MPHA. Because of the huge drop in the glass transition temperature and the increase in hydrophobicity when copolymerised (as an additive) with MMA and VAc respectively, the 1-MPHA monomer could be used (as an additive) in coatings to offer ease of application at room temperature and a good barrier to water.

A simple extension of this work could include studies where the 1-MPHA monomer could be used in an emulsion polymerisation with monomers such as MMA and VAc, and properties such as scrub resistance, pigment binding power, drying speed and ease of application could be investigated. A thorough study of the thermal decomposition and UV stability of the monomer and polymer is also necessary.

In both the copolymerisation studies there has been a significant decrease in the glass transition temperature of the copolymers with even small amounts of 1-MPHA incorporation. This decrease in the glass transition temperature is also accompanied by an improvement in the copolymer storage modulus compared to that of either homopolymer. This could indicate favourable room temperature properties under various conditions of usage and could form a part of a new structure-property study with low additions of 1-MPHA.

The work that has been done on the copolymerisation with styrene and glycidyl methacrylate can be carried out further by studied the kinetics of the copolymerisation reactions as the incorporation of 1-MPHA in those copolymers is much higher than with both MMA and VAc.

APPENDIX A

Appendix A contains additional information in the synthesis of 1-methyl-1-propylhexyl acrylate and its homopolymerisation.

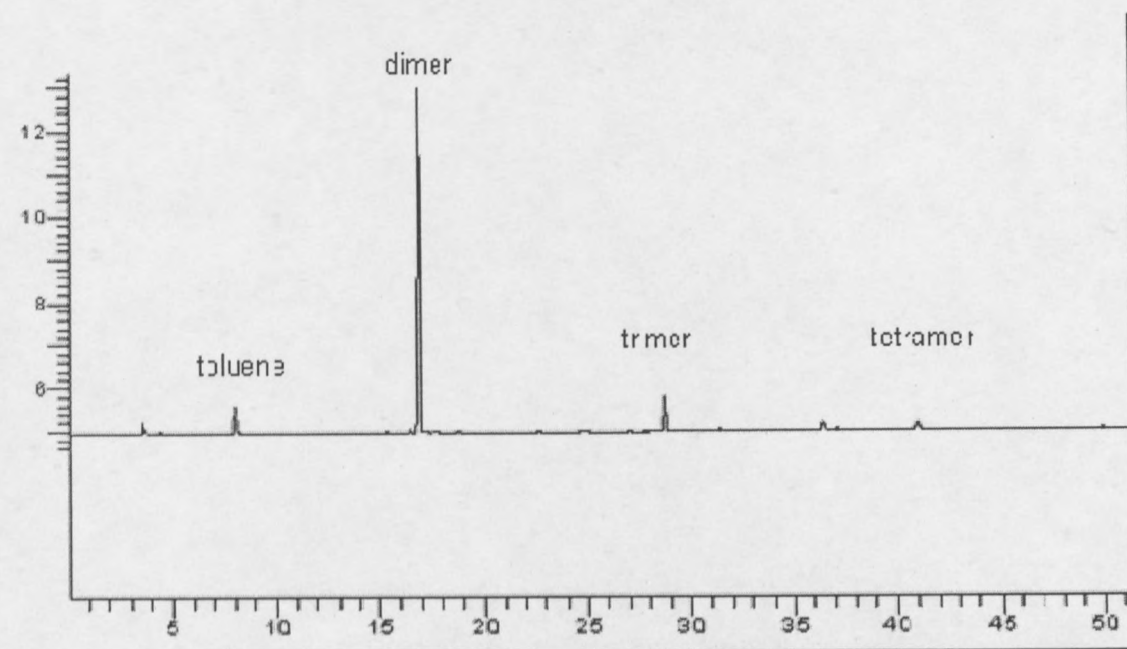


Figure A.1: A GC trace for the reaction product mixture of the oligomerisation of 1-pentene at 100:1 Al:Zr ratio.

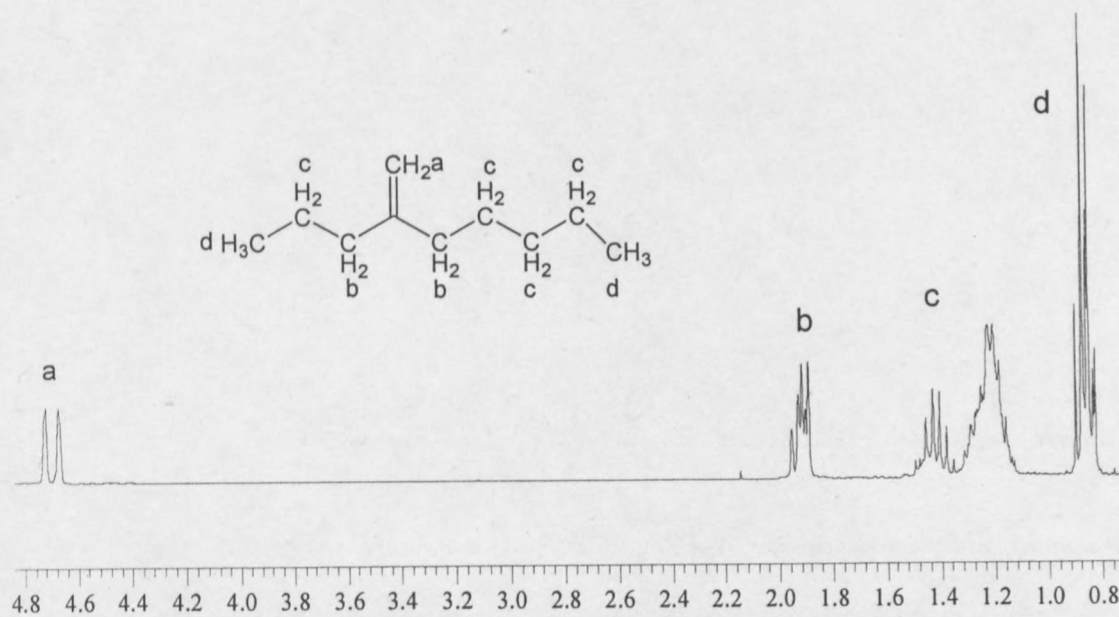


Figure A.2: ¹H NMR for the dimer oligomer of 1-pentene, 2-propyl-heptene.

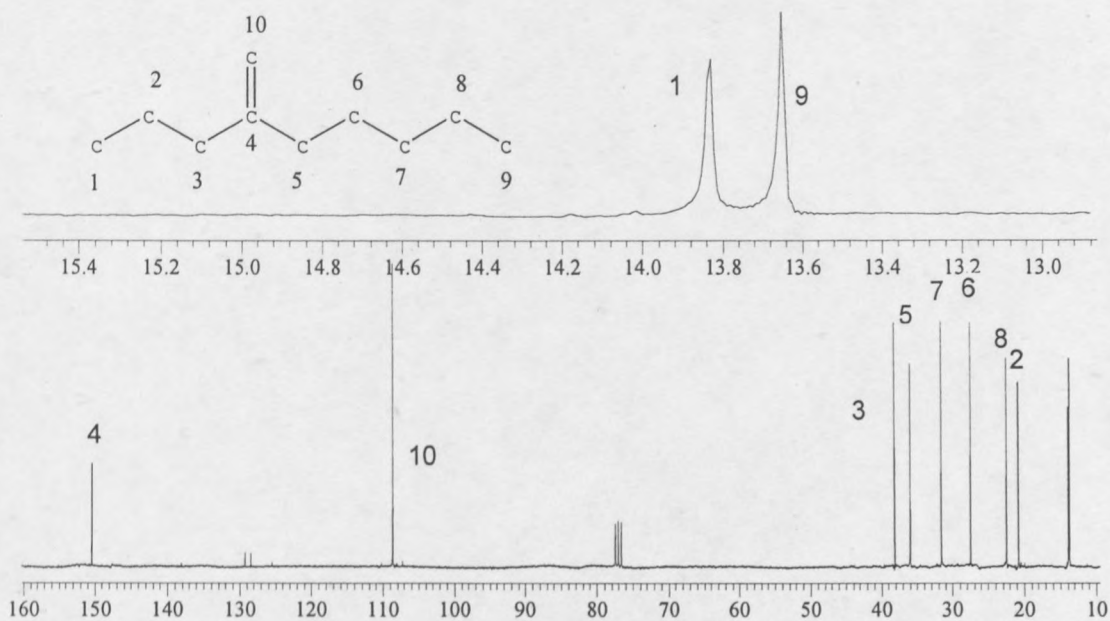


Figure A.3: ^{13}C NMR spectrum of 2-propyl-heptene with carbon atom assignment.

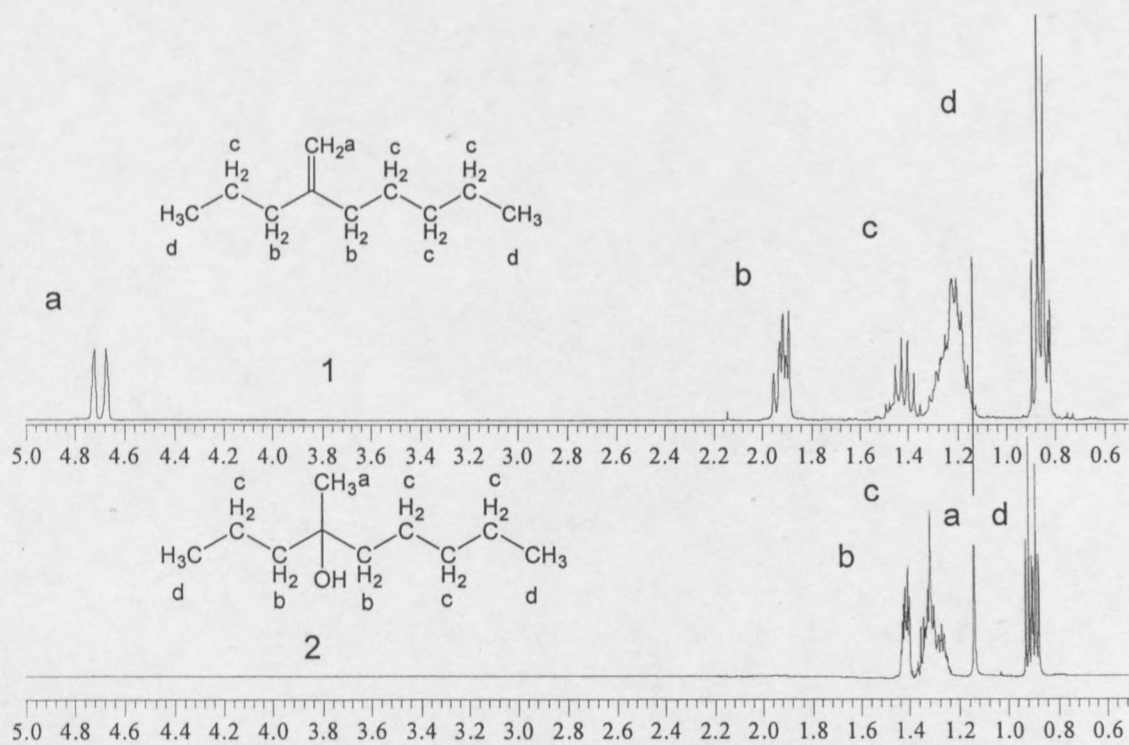


Figure A.4: ^1H NMR spectrum of 2-propyl-heptene (1) and 4-methyl-nonan-4-ol (2) showing the hydration of the oligomer.

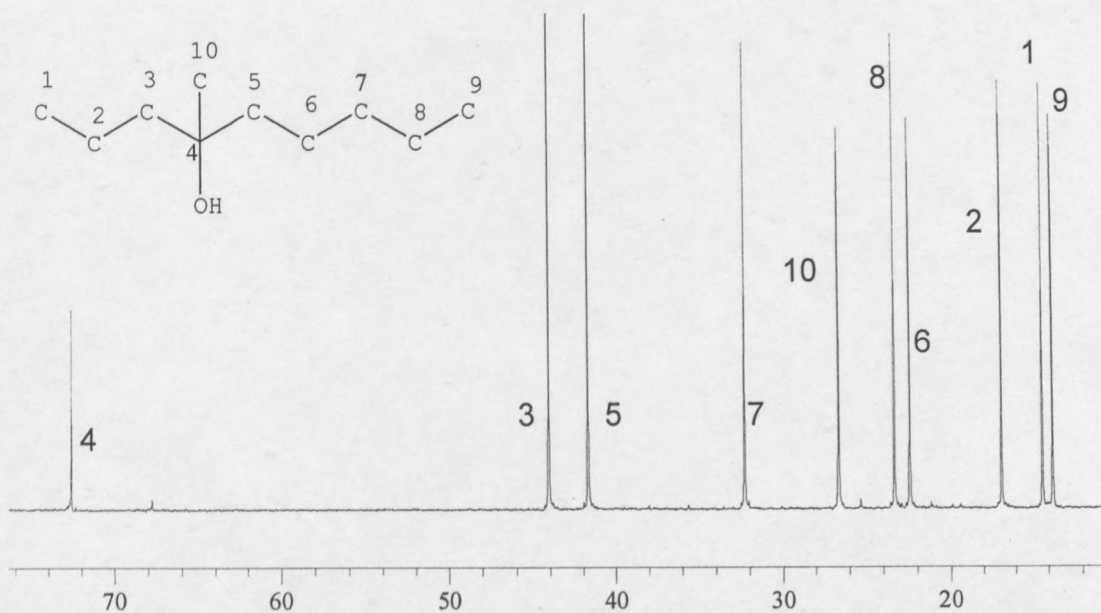


Figure A.5: ¹³C NMR spectrum of 4-methyl-nonan-4-ol with assignment of the carbon atoms.

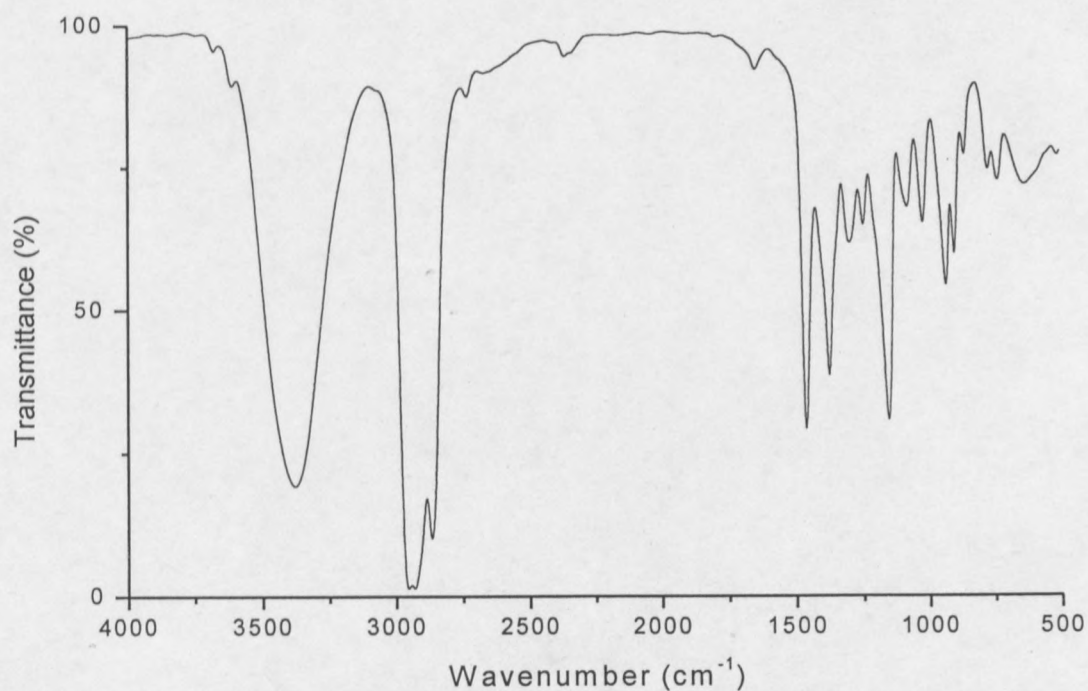


Figure A.6: FTIR spectrum of 4-methyl-nonan-4-ol showing the hydroxyl group around 3400 cm⁻¹ from the hydration of 2-propyl-heptene.

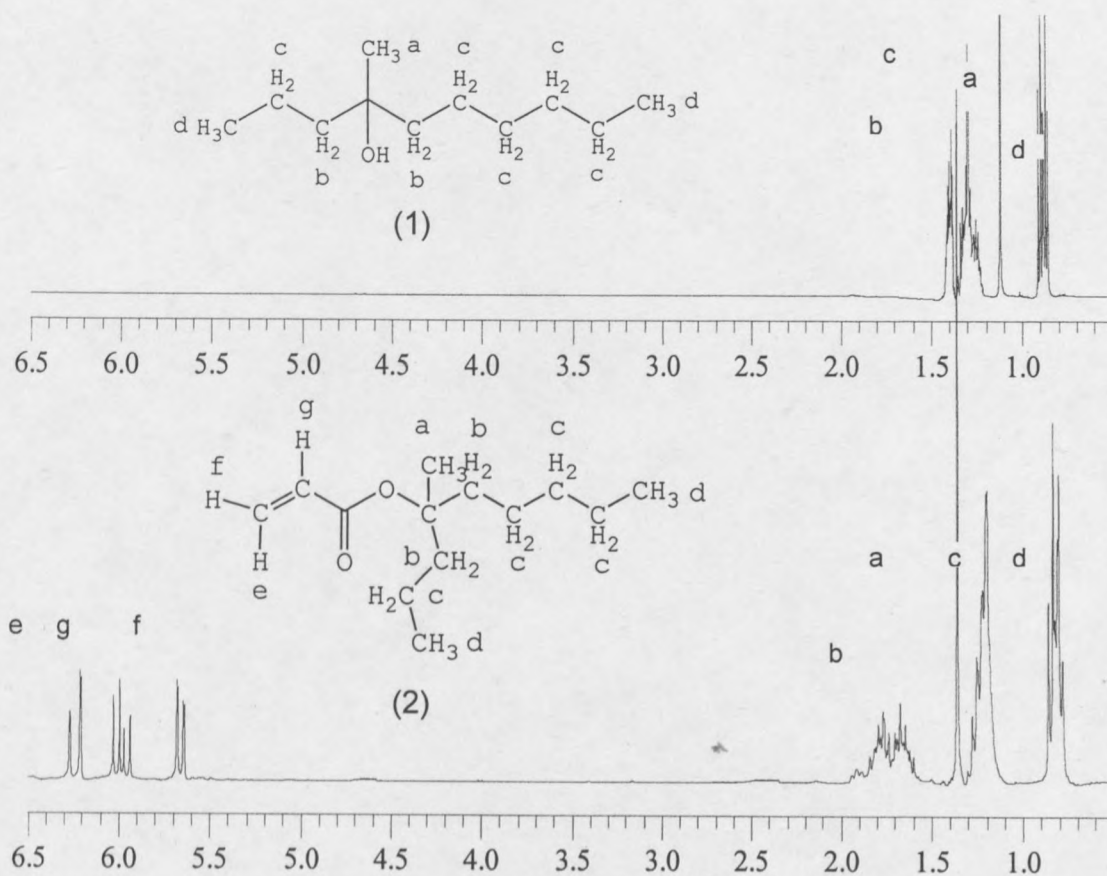


Figure A.7: ^1H NMR spectra of the reaction product of the esterification of 4-methyl-nonan-4-ol with acryloyl chloride to 1-MPHA.

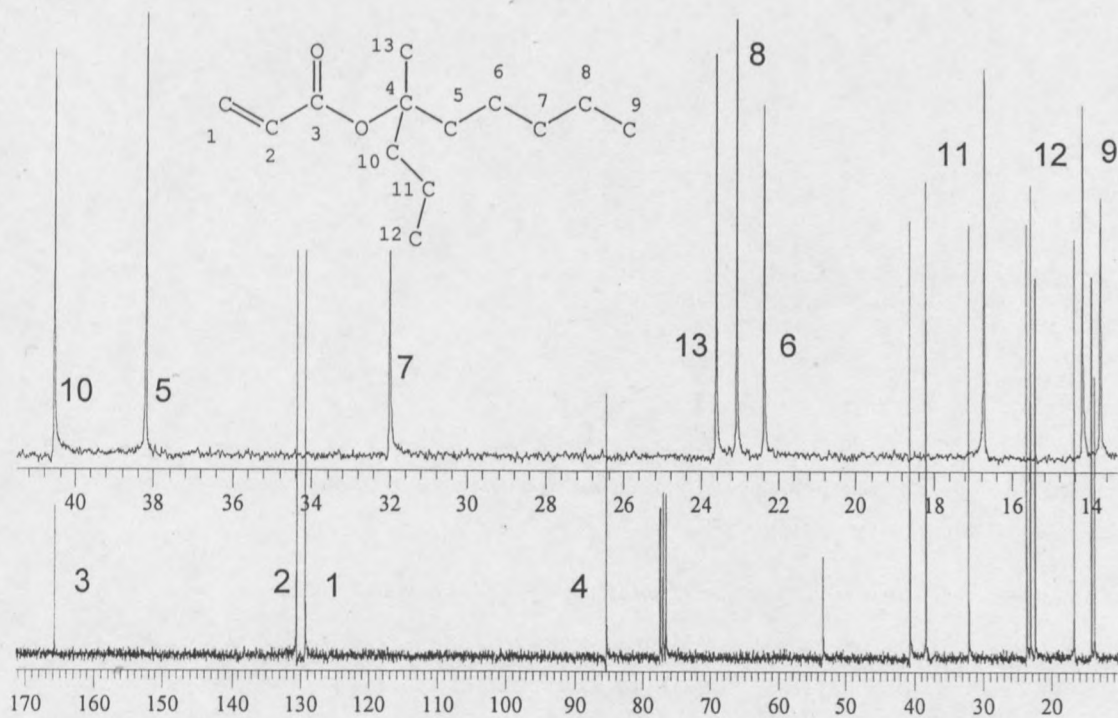


Figure A.8: ^{13}C NMR spectrum of 1-MPHA showing the assignment of the carbon atoms. The spectrum was run in CDCl_3 at 25°C .

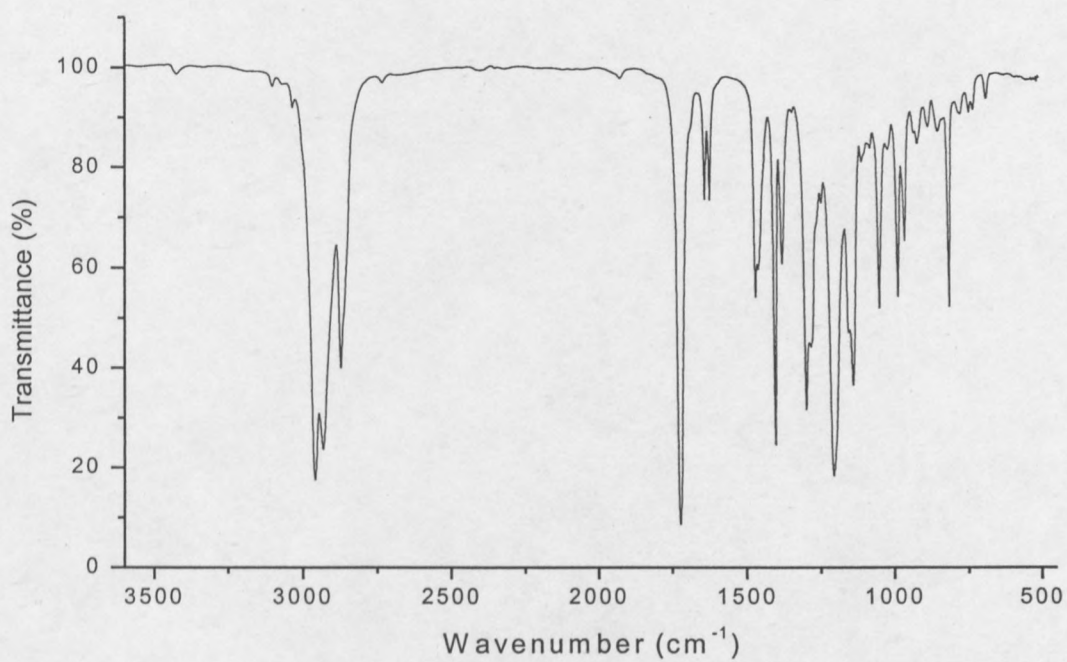


Figure A.9: FTIR spectrum of 1-MPHA showing new functional groups, -C=O at 1720 and -C=C at 1619 cm⁻¹.

APPENDIX B

Appendix B contains the raw data for the kinetics of the homopolymerisation of 1-MPHA. The data is presented in tabular form as normalised concentration as a function of time.

Table B.1: Normalised concentration as a function of time for the *in situ* homopolymerisation of 1-MPHA at different purity levels

TIME	1 column	2 columns	Pure 1-MPHA
0	1.00	1.00	1.00
5	1.00	0.99	0.98
10	0.99	0.99	0.97
15	0.99	0.98	0.95
20	0.98	0.98	0.94
25	0.97	0.97	0.93
30	0.97	0.95	0.91
35	0.97	0.94	0.88
40	0.97	0.93	0.86
45	0.96	0.92	0.84
50	0.96	0.90	0.81
55	0.95	0.89	0.79
60	0.95	0.87	0.74
65	0.94	0.85	0.73
70	0.94	0.81	0.71
75	0.93	0.79	0.68
80	0.93	0.75	0.66
85	0.92	0.71	0.64
90	0.92	0.66	0.61
95	0.91	0.63	0.59
100	0.90	0.58	0.57
105	0.89	0.54	0.55
110	0.88	0.50	0.53
115	0.87	0.46	0.52
120	0.86	0.43	0.50
125	0.84	0.39	0.49
130	0.82	0.37	0.47
135	0.79	0.35	0.46
140	0.76	0.33	0.45
145	0.72	0.31	0.43
150	0.68	0.29	0.42
155	0.64	0.27	0.41
160	0.60	0.26	0.40
165	0.56	0.24	0.39
170	0.52	0.24	0.38
175	0.49	0.22	0.37

180	0.45	0.21	0.36
185	0.43	0.20	0.35
190	0.40	0.19	0.34
195	0.38	0.19	0.33
200	0.35	0.18	0.33
205	0.34	0.17	0.32
210	0.32	0.16	0.31
215	0.30	0.16	0.30
220	0.29	0.15	0.30
225	0.27	0.15	0.29
230	0.26	0.14	0.29
235	0.25	0.13	
240	0.24	0.13	
245	0.23	0.13	
250	0.22	0.12	
255	0.21	0.12	
260	0.20	0.11	
265	0.19	0.11	
270	0.18	0.11	
275	0.18	0.10	
280	0.17	0.10	
285	0.16	0.10	
290	0.16	0.10	
295	0.16		
300	0.15		
305	0.14		
310	0.14		
315	0.14		
320	0.13		
325	0.13		
330	0.12		
335	0.12		
340	0.12		
345	0.11		
350	0.11		
355	0.11		
360	0.11		
365	0.10		

APPENDIX C

Appendix C contains the raw data for the *in situ* kinetics of the copolymerisation of 1-MPHA with MMA. The data is presented in tabular form as monomer concentration as a function of time.

Table C.1: Raw data for the *in situ* kinetics of the copolymerisation of 1-MPHA with MMA at three different initial monomer feed ratios

	MMA	1-MPHA	MMA	1-MPHA	MMA	1-MPHA
	Reaction 1		Reaction 2		Reaction 3	
Time (min)	Concentration (mol/dm ³)	Concentration (mol/dm ³)	Concentration (mol/dm ³)	Concentration (mol/dm ³)	Concentration (mol/dm ³)	Concentration (mol/dm ³)
0	2.07	1.28	1.11	1.77	0.60	1.98
5	2.06	1.27	1.10	1.76	0.59	1.98
10	2.05	1.27	1.10	1.76	0.58	1.97
15	2.04	1.27	1.10	1.76	0.58	1.97
20	2.04	1.27	1.09	1.75	0.58	1.97
25	2.03	1.26	1.08	1.75	0.57	1.97
30	2.00	1.26	1.08	1.75	0.56	1.96
35	1.98	1.25	1.07	1.75	0.56	1.96
40	1.96	1.24	1.06	1.75	0.55	1.96
45	1.93	1.24	1.06	1.75	0.54	1.95
50	1.91	1.23	1.05	1.75	0.54	1.94
55	1.89	1.23	1.04	1.74	0.53	1.94
60	1.86	1.22	1.04	1.74	0.52	1.93
65	1.83	1.22	1.02	1.74	0.51	1.92
70	1.80	1.20	1.02	1.73	0.50	1.90
75	1.76	1.19	1.01	1.73	0.50	1.89
80	1.72	1.18	1.01	1.73	0.49	1.86
85	1.68	1.17	1.00	1.72	0.48	1.86
90	1.58	1.12	0.98	1.71	0.47	1.84
95	1.53	1.11	0.96	1.71	0.46	1.82
100	1.47	1.09	0.94	1.70	0.44	1.79
105	1.42	1.08	0.94	1.67	0.43	1.78
110	1.35	1.06	0.92	1.66	0.42	1.77
115	1.28	1.01	0.91	1.66	0.40	1.74
120	1.20	0.96	0.89	1.65	0.39	1.73
125	1.14	0.94	0.87	1.63	0.37	1.67
130	1.09	0.91	0.85	1.62	0.34	1.62
135	1.01	0.85	0.84	1.61	0.34	1.60
140	0.96	0.83	0.82	1.60	0.31	1.53
145	0.90	0.79	0.79	1.57	0.29	1.47
150	0.85	0.77	0.76	1.53	0.26	1.43
155	0.80	0.75	0.73	1.52	0.24	1.34
160	0.74	0.71	0.71	1.51	0.21	1.30

165	0.69	0.67	0.67	1.47	0.19	1.23
170	0.65	0.65	0.64	1.46	0.17	1.17
175			0.61	1.41	0.15	1.13
180			0.57	1.37	0.13	1.05
185					0.11	0.95

APPENDIX D

Appendix D contains the raw data for the *in situ* kinetics of the copolymerisation of 1-MPHA with VAc. The data is presented in tabular form as monomer concentration as a function of time.

Table D.1: Raw data for the *in situ* kinetics of the copolymerisation of 1-MPHA with VAc at three different initial monomer feed ratios

	VAc	1-MPHA	VAc	1-MPHA	VAc	1-MPHA
	Reaction 1		Reaction 2		Reaction 3	
Time (min)	Concentration (mol/dm ³)	Concentration (mol/dm ³)	Concentration (mol/dm ³)	Concentration (mol/dm ³)	Concentration (mol/dm ³)	Concentration (mol/dm ³)
0	1.23	1.78	2.80	1.19	0.64	1.96
5	1.22	1.76	2.80	1.19	0.64	1.96
10	1.22	1.76	2.80	1.19	0.64	1.96
15	1.22	1.75	2.80	1.18	0.64	1.95
20	1.21	1.74	2.80	1.18	0.63	1.94
25	1.21	1.74	2.79	1.18	0.63	1.94
30	1.21	1.73	2.79	1.18	0.63	1.94
35	1.21	1.73	2.79	1.18	0.63	1.93
40	1.21	1.72	2.79	1.17	0.63	1.93
45	1.20	1.71	2.79	1.17	0.63	1.93
50	1.20	1.71	2.79	1.17	0.63	1.92
55	1.20	1.70	2.79	1.17	0.63	1.92
60	1.20	1.70	2.78	1.17	0.63	1.92
65	1.20	1.69	2.78	1.16	0.63	1.91
70	1.20	1.67	2.78	1.16	0.63	1.91
75	1.19	1.67	2.78	1.16	0.63	1.90
80	1.19	1.65	2.78	1.15	0.63	1.89
85	1.19	1.65	2.78	1.15	0.63	1.88
90	1.19	1.64	2.78	1.14	0.63	1.86
95	1.18	1.62	2.77	1.14	0.63	1.86
100	1.18	1.62	2.77	1.13	0.63	1.85
105	1.18	1.62	2.77	1.12	0.63	1.84
110	1.18	1.61	2.77	1.11	0.63	1.83
115	1.18	1.60	2.77	1.10	0.63	1.81
120	1.18	1.59	2.77	1.08	0.63	1.79
125	1.17	1.58	2.76	1.07	0.63	1.79
130	1.17	1.56	2.76	1.05	0.63	1.77
135	1.17	1.54	2.76	1.04	0.63	1.75
140	1.16	1.53	2.75	1.03	0.62	1.74
145	1.16	1.51	2.75	1.00	0.62	1.71
150	1.15	1.50	2.74	0.98	0.62	1.68
155	1.15	1.49	2.74	0.95	0.62	1.67
160	1.14	1.45	2.71	0.91	0.62	1.64

165	1.14	1.43	2.70	0.88	0.61	1.61
170	1.14	1.40	2.69	0.84	0.61	1.56
175	1.14	1.39	2.67	0.80	0.61	1.54
180	1.13	1.35	2.66	0.75	0.60	1.50
185	1.13	1.31	2.63	0.70	0.60	1.46
190	1.12	1.27	2.62	0.65	0.60	1.41
195	1.11	1.23	2.59	0.61	0.60	1.38
200	1.11	1.20	2.56	0.56	0.59	1.31
205	1.10	1.16	2.55	0.52	0.58	1.26
210	1.08	1.13	2.53	0.48	0.58	1.21
215	1.08	1.07	2.51	0.44	0.58	1.16
220	1.08	1.02	2.49	0.41	0.57	1.10
225	1.07	0.97	2.47	0.37	0.57	1.06
230	1.06	0.94	2.45	0.34	0.56	1.01
235	1.05	0.89	2.44	0.31	0.56	0.96
240	1.04	0.82	2.42	0.29	0.55	0.91
245	1.03	0.79	2.40	0.26	0.55	0.87
250	1.02	0.75	2.39	0.24	0.54	0.83
255	1.02	0.71	2.36	0.22	0.54	0.78
260	1.00	0.68	2.35	0.20	0.54	0.75
265	1.00	0.65	2.33	0.18	0.53	0.71
270	0.99	0.61	2.32	0.16	0.52	0.68
275	0.98	0.58	2.30	0.15	0.52	0.65
280	0.97	0.55	2.29	0.13	0.52	0.62
285	0.96	0.52	2.28	0.12	0.52	0.59
290	0.96	0.49	2.21	0.11	0.51	0.58
295	0.95	0.47				

APPENDIX E

Appendix E contains the results for the synthesis of the 1-pentene trimer oligomer and the corresponding alcohol.

1-Pentene trimer oligomer synthesis

The synthesis of the 1-pentene trimer oligomer 2,4-dipropyl-non-1-ene is as described in Section 3.3.1. Figure E.1 and E.2 are the ^1H and ^{13}C NMR spectra for the trimer oligomer of 1-pentene. The spectra were obtained from samples dissolved in deuterated chloroform and ran on the Varian VXR 300 dual channel broadband pulse Fourier transform NMR spectrometer. Figure E.2 (a) shows the ^{13}C NMR spectrum of the trimer showing all the carbon atoms. Figure E.2 (b) shows an expanded ^{13}C NMR spectrum of the trimer to show the carbon atoms that are close together. The carbon atoms have been assigned unambiguously.

^1H NMR

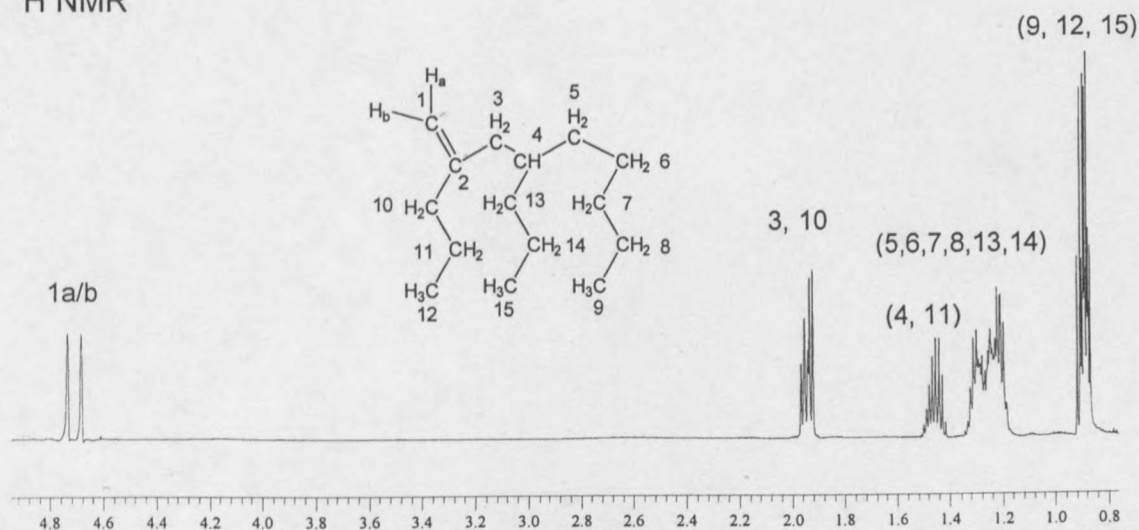


Figure E.1: ^1H NMR spectrum for the trimer oligomer of 1-pentene.

^{13}C NMR

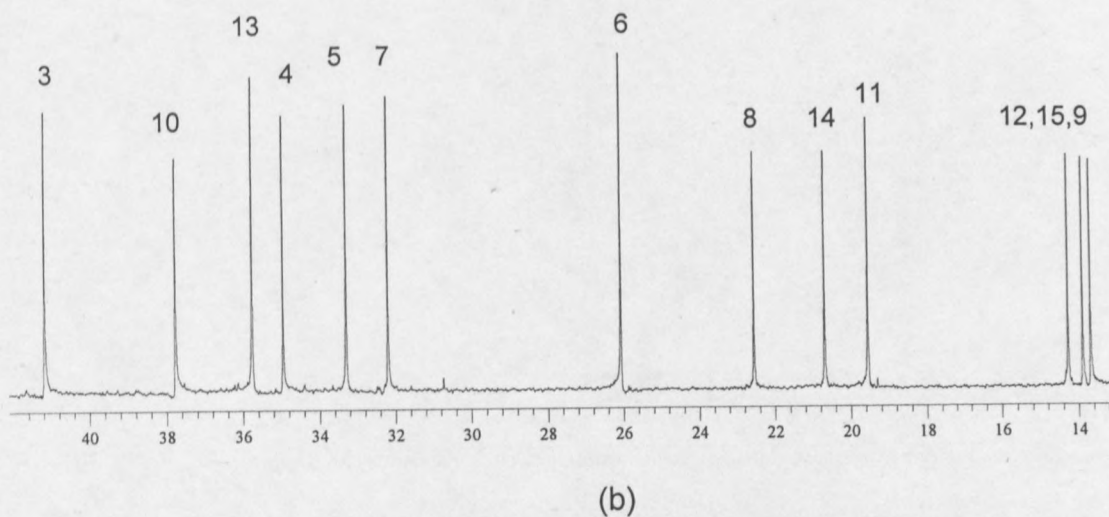
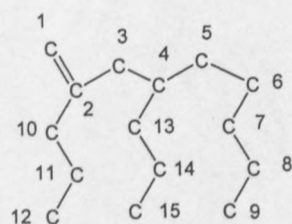
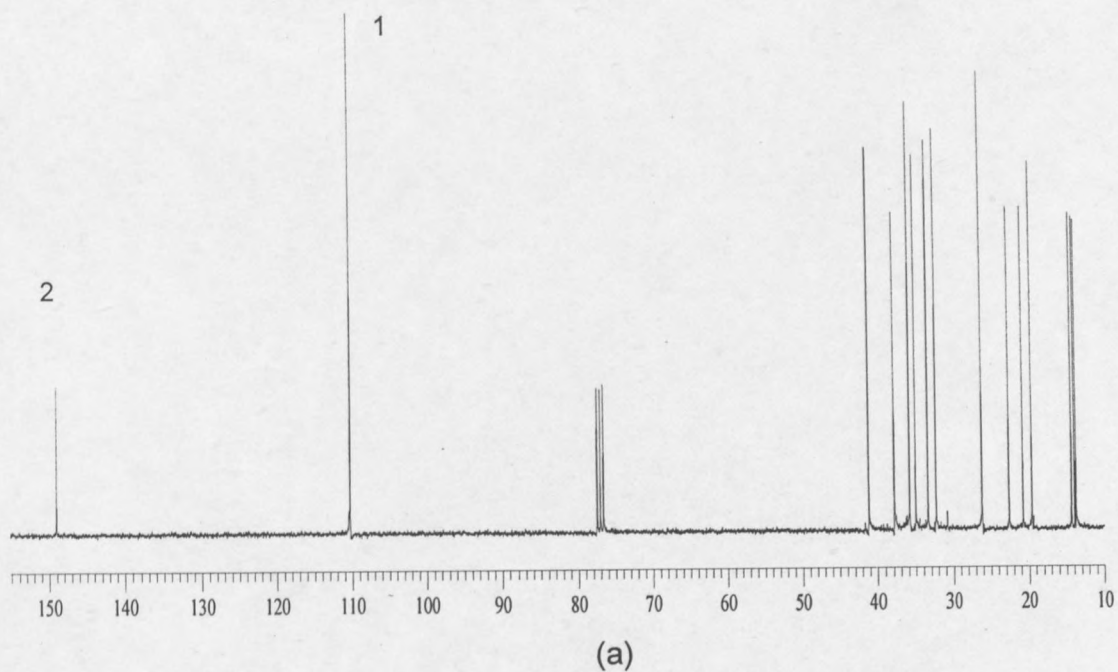


Figure E.2: ^{13}C NMR spectrum for the trimer of 1-pentene, (a) the full range of the spectrum and (b) the expanded region showing the overlapping peaks.

Hydration of the 1-pentene trimer

The procedure for the synthesis of the trimer alcohol 4-methyl-6-propyl-undecan-4-ol is similar to that of the hydration of 2-propyl-heptene described in Section 3.3.2. Figures E.3 and E.4 are the ^1H and ^{13}C NMR spectra for the trimer alcohol. The carbon atoms have been assigned unambiguously in Figure E.4. Figure E.5 is the infrared spectrum of the trimer alcohol confirming the presence of the hydroxyl group around 3400 cm^{-1} .

^1H NMR

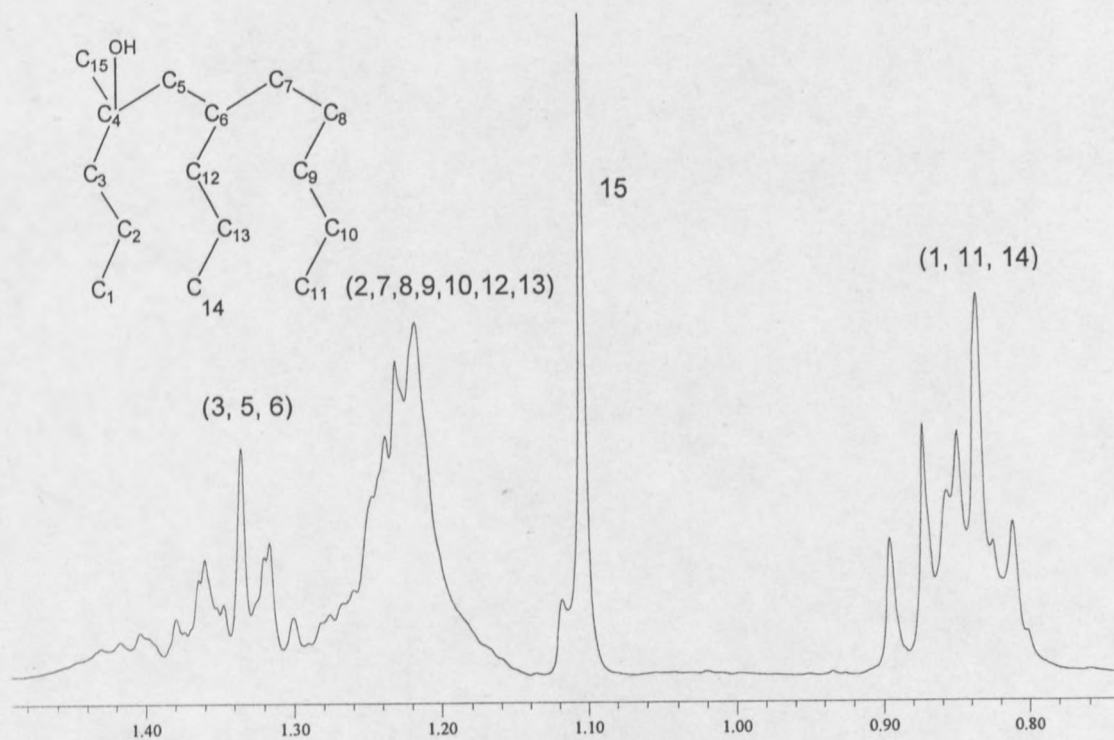


Figure E.3: ^1H NMR spectrum of the trimer alcohol.

^{13}C NMR

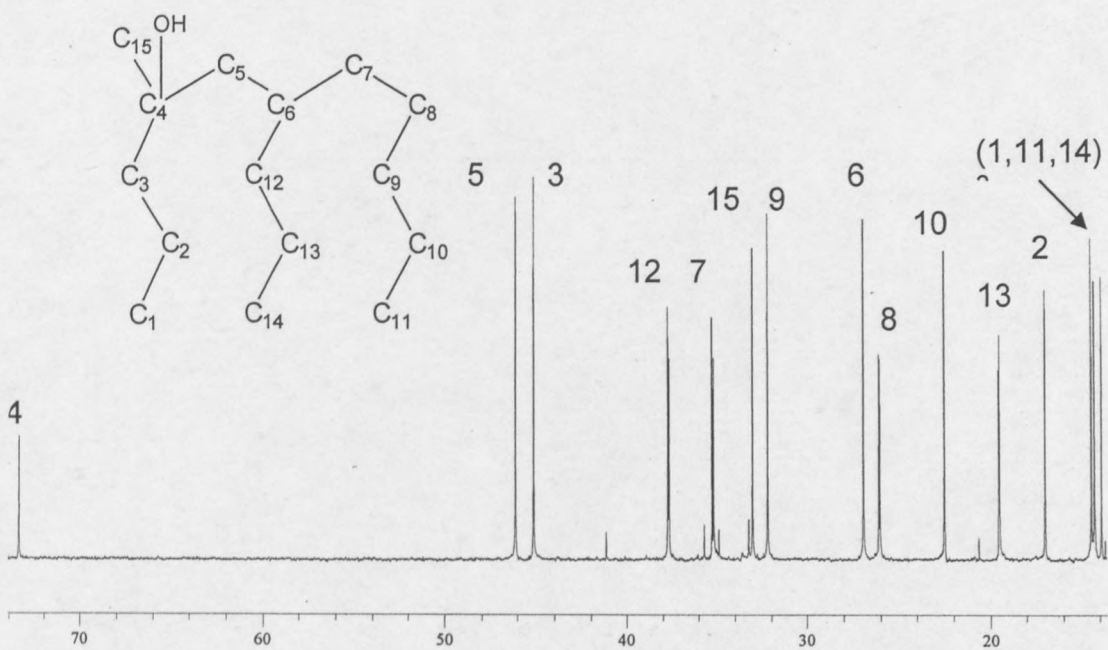


Figure E.4: ^{13}C NMR spectrum for the trimer alcohol showing the assignment of the carbon peaks.

IR

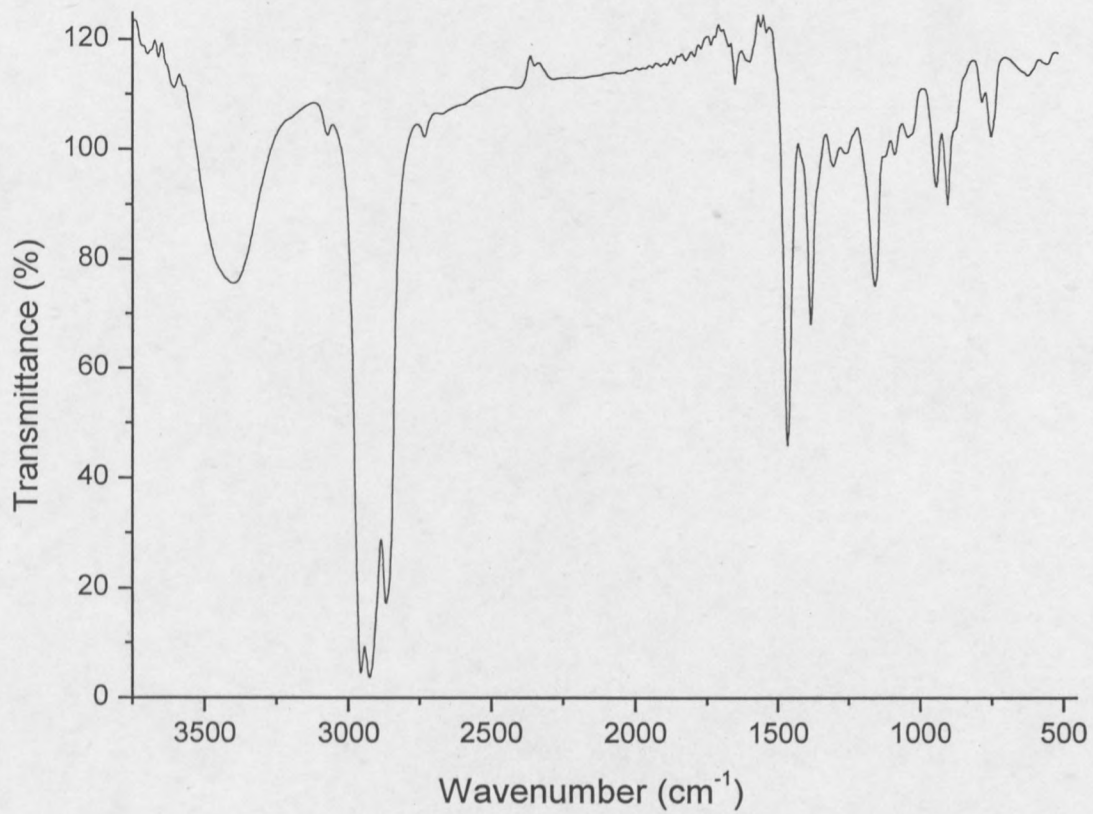


Figure E.5: FTIR spectrum for the 1-pentene trimer alcohol showing the hydroxyl group around 3400 cm⁻¹.

APPENDIX F

Appendix F contains the results for the synthesis of the tetramer of 1-pentene and the corresponding alcohol.

1-Pentene tetramer oligomer synthesis

The synthesis of the 1-pentene oligomers is as described in Section 3.3.1. Figures F.1 and F.2 are the ^1H and ^{13}C NMR spectra for the tetramer oligomer of 1-pentene, 2,4,6-tripropyl-undecen-1-ene. The spectra were obtained from samples dissolved in deuterated chloroform and ran on the Varian VXR 300 dual channel broadband pulse Fourier transform NMR spectrometer. The ^{13}C NMR spectrum in Figure F.2 shows a lot of overlap for the methylene carbon atoms but the carbon atoms of the methyl groups and the double bond carbon atoms are clearly distinguishable as assigned by the numbers on the figure.

^1H NMR

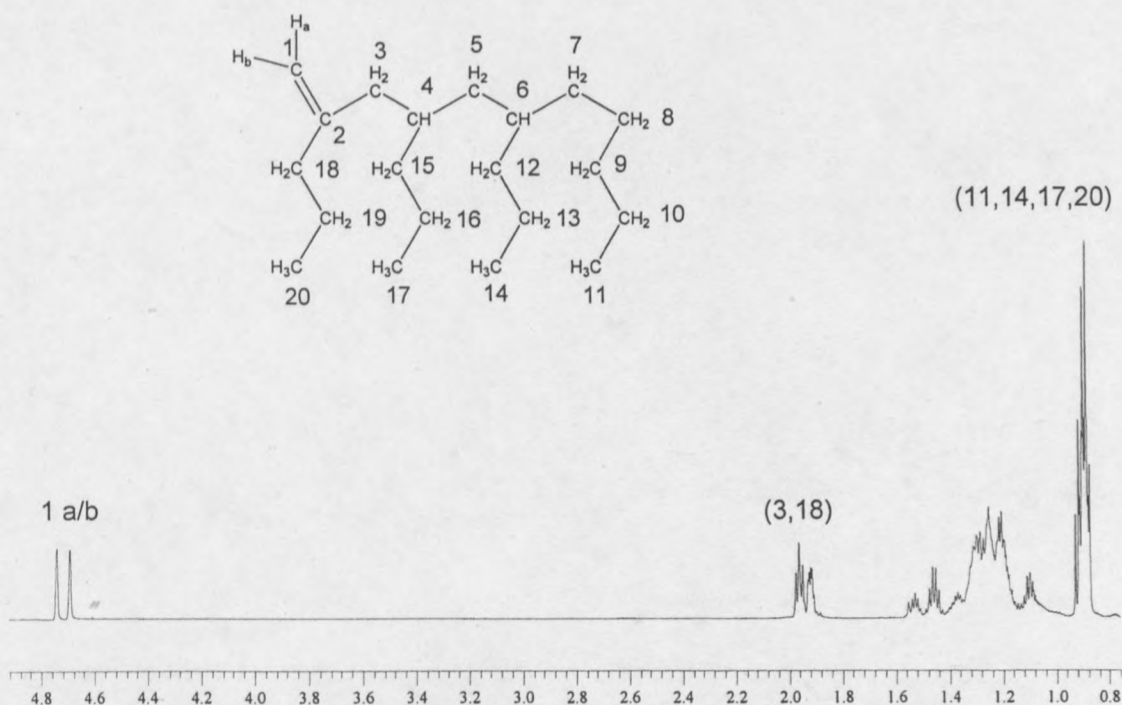


Figure F.1: ^1H NMR spectrum for the 1-pentene tetramer oligomer.

^{13}C NMR

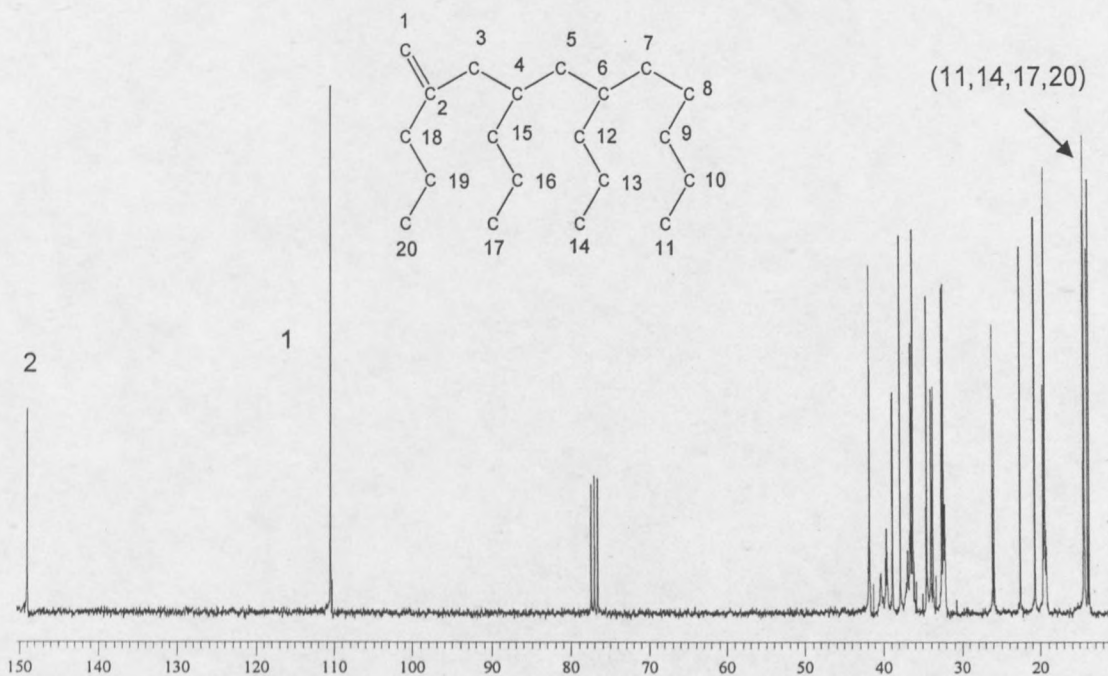


Figure F.2: ^{13}C NMR spectrum for the 1-pentene tetramer oligomer.

Hydration of the 1-pentene tetramer

The procedure for the synthesis of the tetramer alcohol 4-methyl-6,8-dipropyl-tridecan-4-ol is similar to that of the hydration of 2-propyl-heptene described in Section 3.3.2. Figures F.3 and F.4 are the ^1H and ^{13}C NMR spectra for the tetramer alcohol. Peak assignment is complicated by the overlap of the methylene carbon atoms in the carbon spectrum.

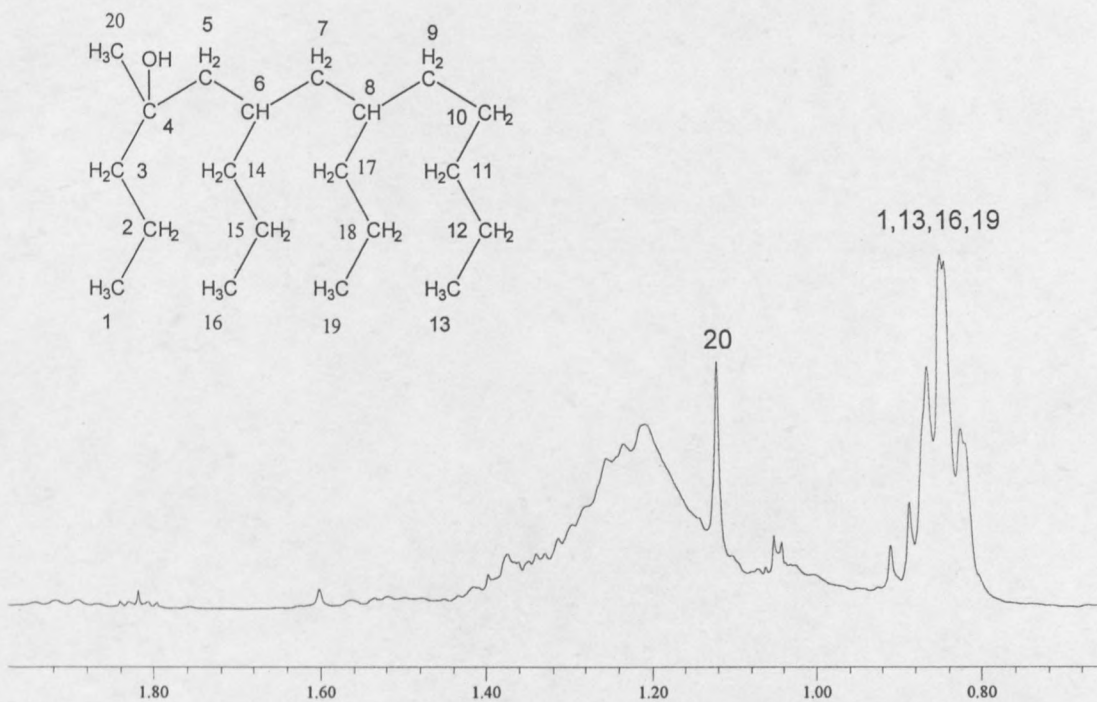


Figure F.3: ^1H NMR spectrum for the 1-pentene tetramer alcohol.

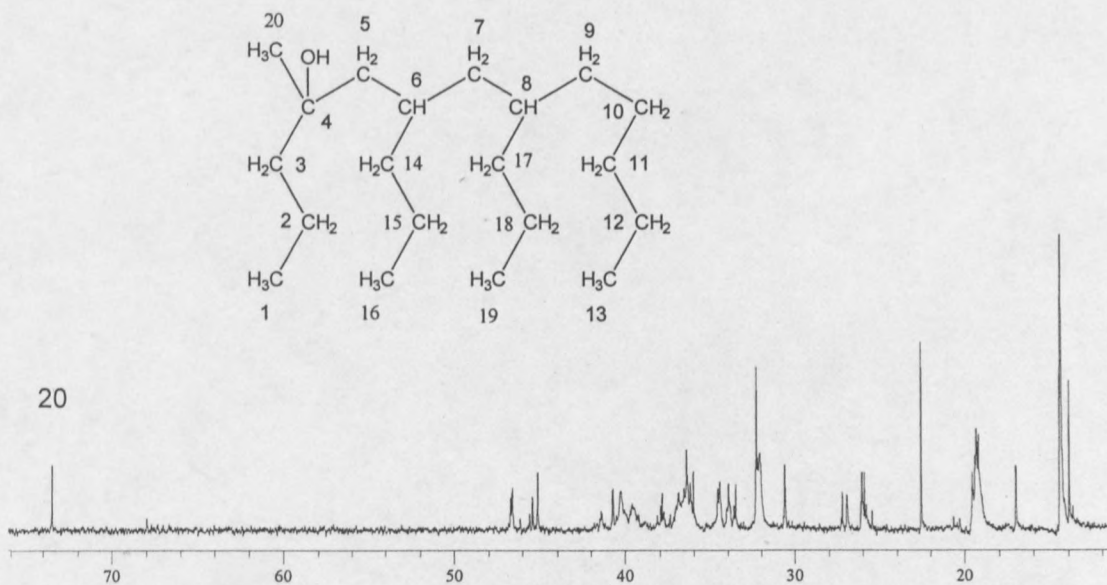


Figure F.4: ^{13}C NMR spectrum for the 1-pentene tetramer alcohol.

APPENDIX G

Appendix G contains the results for the copolymerisation of 1-methyl-propyl-hexyl acrylate with glycidyl methacrylate. The reaction conditions used and the analysis carried out were similar to those for the copolymerisation with MMA described in Section 4.2.2.

Chemical analysis

NMR

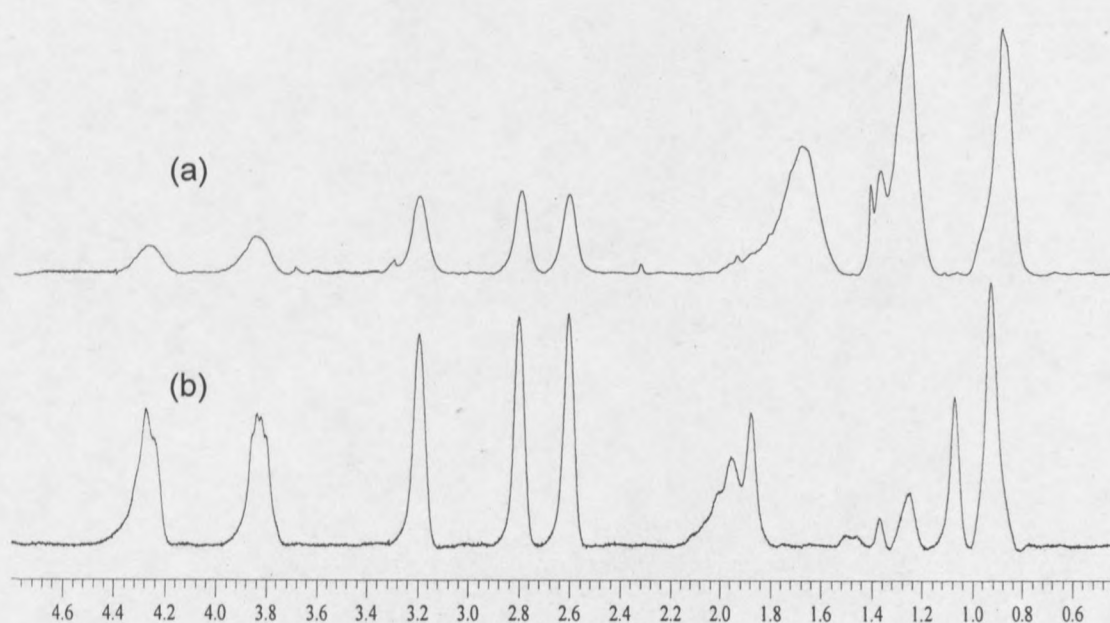


Figure G.1: ^1H NMR spectrum for the copolymers of poly-(1-MPHA-co-GMA) containing (a) 43 and (b) 5 mole% 1-MPHA.

The ^1H NMR obtained from the full conversion copolymers of poly-(1-MPHA-co-GMA) was used to determine the amount of 1-MPHA incorporated into the copolymer chain. Typical ^1H NMR scans for the copolymers are shown in Figure G.1 for two copolymers with 1-MPHA incorporation in (a) being 43 and in (b) being 5 mole%.

The mole fraction of the monomers in the copolymers was determined according to the following equation, derived by considering the intensities of the NMR peaks that

could be assigned with out ambiguity. The equation is based on the ten protons in glycidyl methacrylate and the twenty four protons in 1-MPHA, with the three epoxy ring protons of GMA being unambiguously assigned:

$$\frac{\text{Intensity of protons of the epoxy ring } (I_{ER})}{\text{Intensity of total protons } (I_T)} = \frac{3m_2}{10m_2 + 24(1 - m_2)}$$

$$3m_2(I_T) = (24 - 14m_2)I_{ER}$$

$$m_2 = \frac{24I_{ER}}{3I_T + 14I_{ER}}$$

where m_2 is the mole fraction of glycidyl methacrylate in copolymer, $m_1 = 1 - m_2$ is the mole fraction of 1-MPHA in copolymer, I_{ER} is the integrated peak intensity for the epoxy ring protons of GMA and I_T is the integrated peak intensity of total protons. The results for the incorporation calculations are listed in Table G.1.

GPC results

Table G.1: Chemical analysis data for the poly-(1-MPHA-co-GMA) copolymers

Sample	F_{I-MPHA} (mole%)	\bar{M}_n	\bar{M}_w	PDI
DG19	5	26500	128400	4.9
DG37	11	26700	61400	2.3
DG55	38	25000	54200	2.2
DG73	42	20500	31700	1.5
DG91	43	19600	39400	2

Thermal analysis

TGA

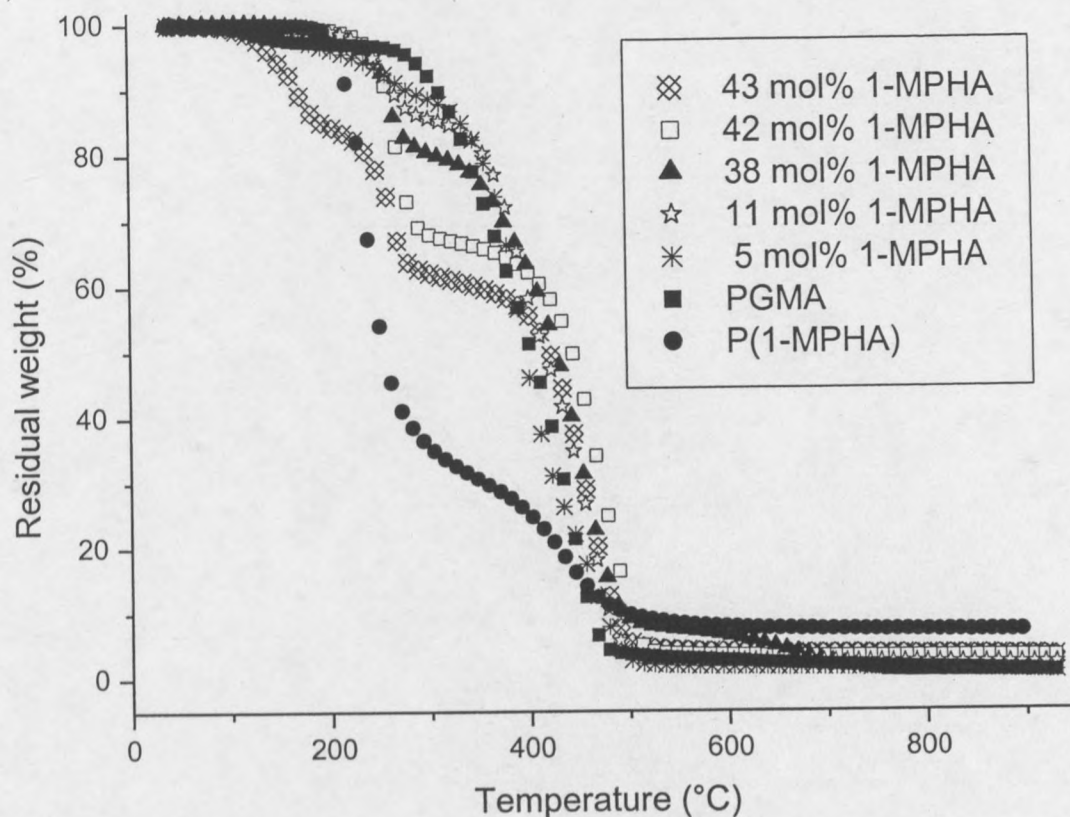


Figure G.2: TGA traces for the poly-(1-MPHA-co-GMA) copolymers.

The data in Figure G.2 is summarised in Table G.2.

Table G.2: Thermal decomposition data for the poly-(1-MPHA-co-GMA) polymers

Sample	1 st stage	2 nd stage	3 rd stage
DG91	204.0 – 297.6	373.2 – 530.5	
DG73	196.3 – 315.9	352.5 – 536.9	
DG55	193.0 – 305.1	325.1 – 530.6	
DG37	193.0 – 301.2	317.7 – 422.0	422.0 – 524.0
DG19	195.3 – 298.5	306.7 – 436.9	436.9 – 518.9
PGMA	87.9 – 163.2	259.7 – 352.0	355.8 – 496.4
P(1-MPHA)	171.7 – 322.4	364.2 – 598.6	

APPENDIX H

RESULTS FOR THE COPOLYMERISATION OF 1-METHYL-1-PROPYL-HEXYL ACRLATE WITH STYRENE

Chemical analysis

NMR

The ^1H NMR spectra obtained from the full conversion copolymers of poly-(1-MPHA-co-styrene) was used to determine the amount of 1-MPHA incorporated into the copolymer chain. Typical ^1H NMR scans for the copolymers are shown in Figure H.1 for two copolymers with 1-MPHA incorporation in (a) being 75 and in (b) being 6 mole%.

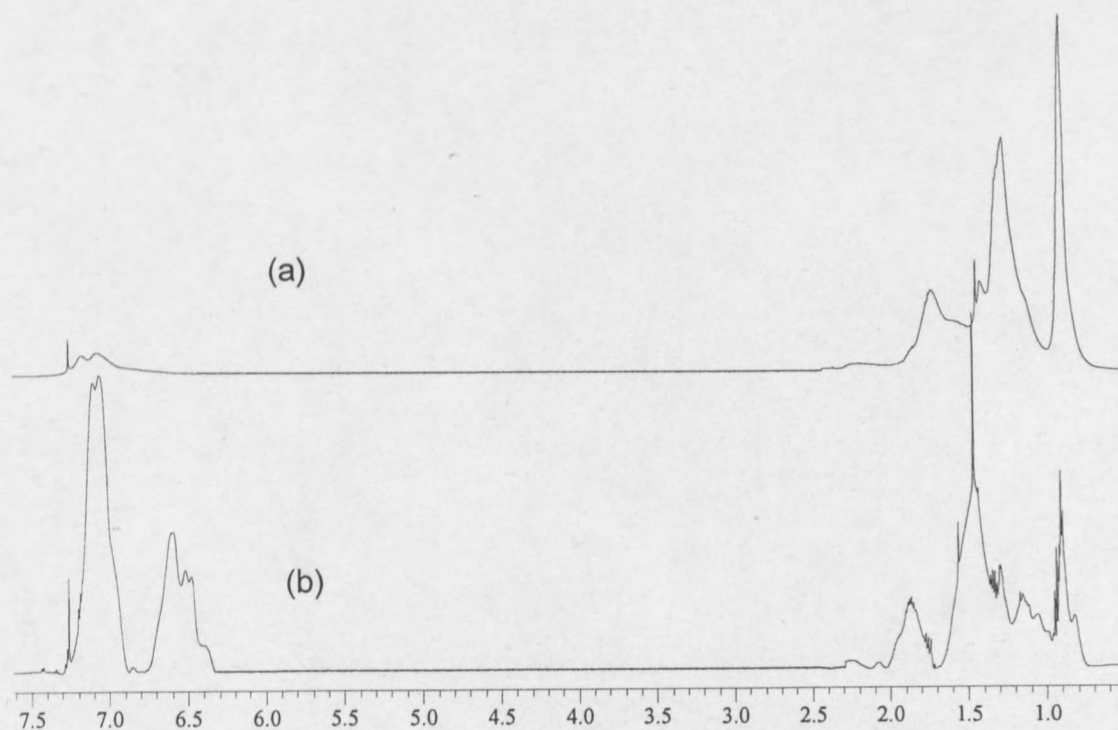


Figure H.1: ^1H NMR spectra for the poly-(1-MPHA-co-styrene) copolymers containing, (a) 75 and (b) 6 mole% 1-MPHA.

The mole fraction of the monomers in the copolymers was determined according to the following equation, derived by considering the intensities of the NMR peaks that could be assigned with out ambiguity. The equation is based on the eight protons in styrene and the twenty four protons in 1-MPHA, with the five aromatic protons of styrene being unambiguously assigned:

$$\frac{\text{Intensity of protons in the aromatic region } (I_{AR})}{\text{Intensity of total protons } (I_T)} = \frac{5m_2}{8m_2 + 24(1 - m_2)}$$

$$5m_2(I_T) = (24 - 16m_2)I_{AR}$$

$$m_2 = \frac{24I_{AR}}{5I_T + 16I_{AR}}$$

where m_2 is the mole fraction of styrene in copolymer, $m_1 = 1 - m_2$ is the mole fraction of 1-MPHA in copolymer, I_{AR} is the integrated peak intensity for the aromatic protons of styrene and I_T is the integrated peak intensity of total protons. The results for the incorporation calculations are listed in Table I.1.

Table H.1: Chemical analysis data for the poly-(1-MPHA-co-styrene) copolymers

Sample	F_{1-MPHA} (mole%)	\bar{M}_n	\bar{M}_w	PDI
DS19	6	8600	34000	3.9
DS37	26	8550	172900	20.2
DS55	51	32700	201600	6.2
DS73	63	26800	69400	2.6
DS91	75	4700	151300	32.3

Thermal analysis

TGA

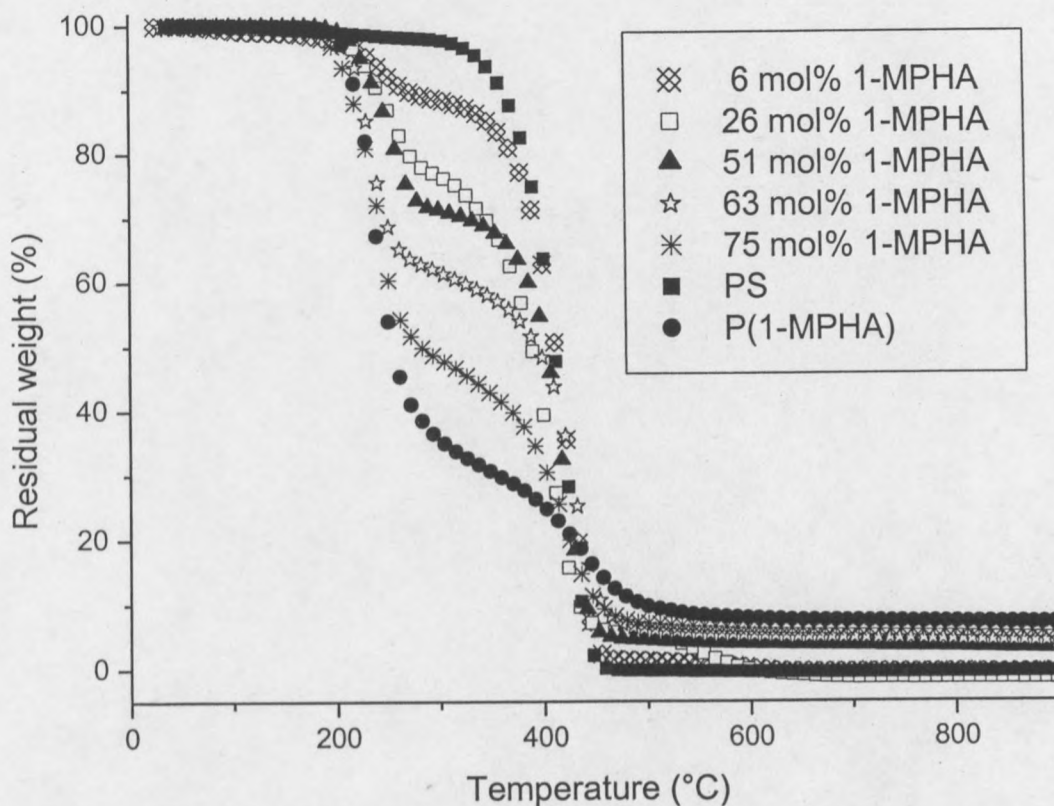


Figure H.2: TGA traces for the poly-(1-MPHA-co-styrene) copolymers.

The thermal decomposition data in Figure H.2 is summarised in Table H.2.

Table H.2: Thermal decomposition data for the poly-(1-MPHA-co-styrene) polymers

Sample	1 st stage	2 nd stage	3 rd stage
DS91	153.9 – 302.7	310.4 – 514.9	
DS73	167.9 – 293.3	319.8 – 508.8	
DS55	176.6 – 303.4	311.1 – 498.6	
DS37	156.0 – 298.5	308.5 – 475.6	508.6 – 626.5
DS19	155.0 – 294.5	312.0 – 475.8	545.5 – 640.6
PS	288.2 – 470.5		
P(1-MPHA)	171.7 – 322.4	364.2 – 598.6	